Using GIS to develop a baseline dataset for planning adaptation strategies to climate change in Central Asia and Northwest China

E. De Pauw, W. Göbel and F. Delobel

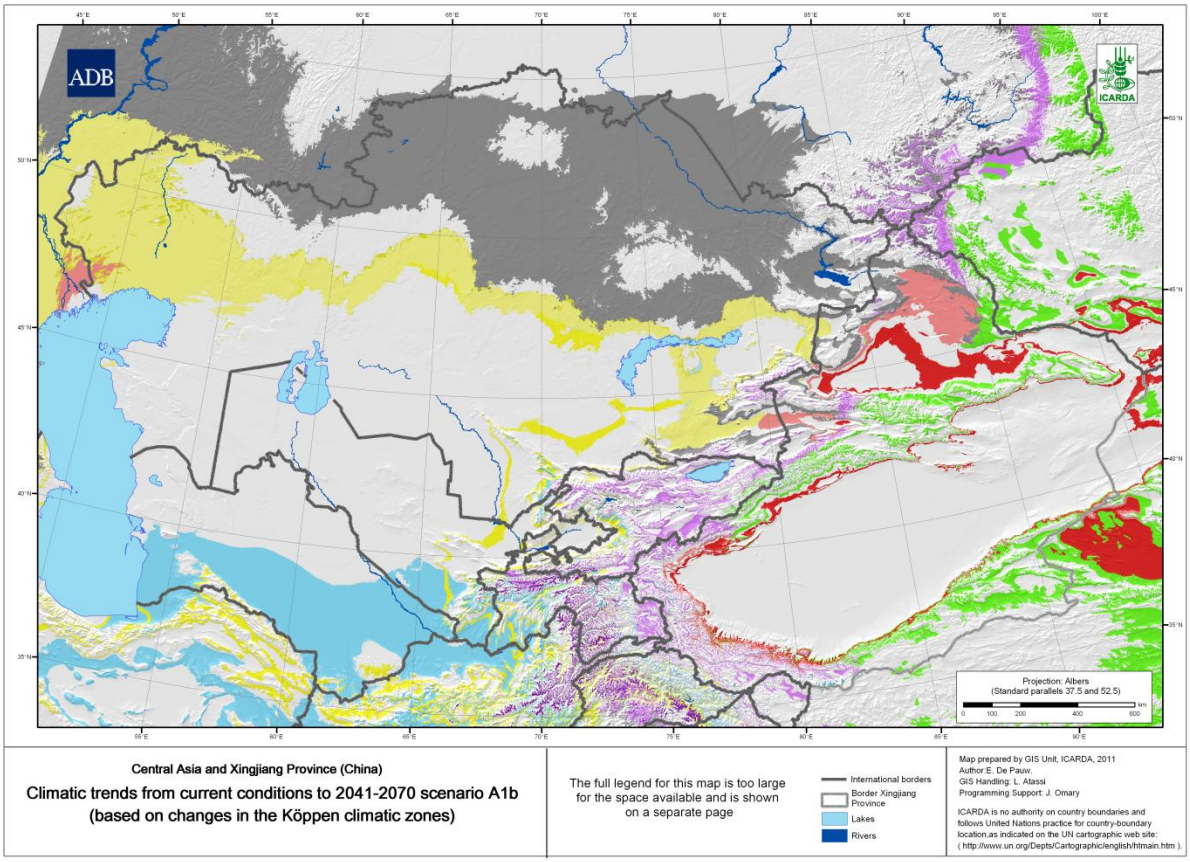

Final Report of Project "Adaptation to Climate Change in Central Asia and China"

RETA 6439: TWELFTH AGRICULTURE AND NATURAL RESOURCES RESEARCH AT INTERNATIONAL AGRICULTURAL RESEARCH CENTERS – COMPONENT 1

February 2012

TABLE OF CONTENTS

LIST OF FIGURES

LIST OF TABLES

ACKNOWLEDGEMENTS

The authors wish to thank the ICARDA GIS team who were involved in this study, particularly Ms. Layal Atassi and Mr. Fawaz Tulaymat, for preparing the numerous high-quality maps, and Mr. Jalal Omary, for the software development and process automation of map generation. Our sincere thanks are also due to our project leaders Dr.Mohamed Abdelwahad Ahmed and Dr. Aden Aw-Hassan for their good-natured support and patience for bringing this challenging study to a satisfactory conclusion.

ABSTRACT

Central Asia and the Xinjiang Province of NW China constitute a contiguous dryland area of approximately 5.6 million km^2. Despite an apparent (and misleading) monotony of the landscapes in most of the region, there is a surprising diversity in agroecologies. Moreover, it is a region that has witnessed some major environmental catastrophes and degradation of its land and water resources in its recent past, and is particularly vulnerable to the threat of climate change.

Climate change is expected to affect significantly Central Asian countries in the coming decades. According to the 2007 4^{th} Assessment Report of the Intergovernmental Panel on Climate Change (IPCC), the projected median increase in temperature is estimated to 3.7°C on average by the end of the century, with most of the increase to occur during the summer (June-July-August). Precipitation is projected to increase slightly during the winter and to decrease the rest of the year. Heavily watered winters will be more frequent, as well as drier springs, summers and autumns.
Peculiar to Central Asia and NW China are the high upstream/downstream dependencies, as the snowfall and glaciers in the mountain chains of the Tien Shan and Pamir are key to the region's hydrology and agriculture downstream. Consequences of these changes in temperature and precipitation regimes are therefore potentially harmful for the population in this vulnerable area. Food security and water availability are threatened by the increasing water scarcity and higher frequency of drought. Agriculture, which uses more than 80% of the water resources in the region and employs a large share of the population will have to adjust in order to cope with increasing stresses and to satisfy a growing population.

In this context, anticipation of climate change impacts and possible pathways for adaptation through scientific research is central for mitigating negative effects. In this perspective ICARDA initiated in 2009 a project funded by the Asian Development Bank on "Adaptation to Climate change in Central Asia and the People's Republic of China", which is aimed at increasing the knowledge about climate change in order to anticipate improved drought management and adaptation options in the existing agro-ecosystems.

The projections of the IPCC for the region come with the well-known uncertainties of climate science in its current state: uncertainty about future greenhouse gas emissions (hence the practice of working with emission scenarios), the use of Global Circulation Models (GCM) models which are often in utter disagreement, and the coarse spatial resolution of GCMs, too coarse to include small-scale processes, the ones responsible for local weather patterns (especially in mountain areas). Moreover the IPCC projections in the 4^{th} Assessment Report are for the time frame 2080-99, a time horizon too far in the future to be meaningful for planning adaptation strategies.

In order to develop climate change adaptation strategies in Central Asia that are meaningful at landscape level, there is a need for spatially '*downscaling*' climate change from the global to the regional level. This involves an increase in the spatial resolution of GCM outputs in order to simulate impact closer to the farmer environment and to anticipate changes for *nearer futures* (e.g. 2030, 2050) which are of more interest to local planners. Predictions for the near future also have the advantage that they can be verified by looking at their *continuity with trends that are already present within the current climate*. For this reason our study included a trend analysis of precipitation variability and drought in the 20^{th} century.

GIS tools have played a key role in this project through the generation of a high-resolution spatial dataset derived from publicly available low-resolution spatial data. The spatial dataset has three major components: a spatial database of downscaled high-resolution basic climatic variables (precipitation and temperature), high-resolution higher-level derived climatic variables and their changes, and a spatial dataset on drought and precipitation variability in the region. These datasets, methods used to generate them, the results and the conclusions that can be drawn from them are described in this report.

The projections of climate change provided in this study are entirely based on spatially downscaled coarse-resolution Global Circulation Models. The downscaling method is based on super-imposing coarse-resolution climate change projections on top of high-resolution current climate surfaces through spatial interpolation methods in a GIS environment. The advantages of the downscaling methodology are its ease of use, applicability to either global or regional circulation models, if available, and use of current climate as a guide for downscaling future climates.

The precipitation projections of individual GCM models show major differences whereas the projections for temperature changes are more consistent, with all models anticipating a significant warming (2-5°C) over the entire area by the end of the 21st century.

To minimize possible divergences by selecting one model or another, a multi-model ensemble approach was adopted in which the output from 7 major GCM models was averaged for two greenhouse gas emission scenarios, A1b (currently held to be an optimistic one) and A2 (a pessimistic and probably realistic one), and three time horizons, a near future (2010-2040), an intermediate future (2040-2070) and a far future (2070-2100). The multi-ensemble modeling approach has been used to assess changes in key climatic variables: precipitation, aridity, growing periods and climatic zones.

In all change themes evaluated in our study, little difference was observed between the outcomes from the A1b or A2 scenarios, making these outcomes relatively insensitive to the scenario used.

The projections based on the downscaled multi-model ensemble indicate for most of the region a modest increase in precipitation. As indicated by the study of precipitation variability during the 20th century, this trend towards increasing precipitation does not go counter with the precipitation trend of the past and grows stronger with time.
The trend towards higher precipitation could easily be countered by higher evapo-transpiration losses as a result of the increased temperatures. However, up to 2040-2070 no clear trend is anticipated, with about half of the region projected to experience a slight increase in aridity (0-10 points) and another half a slight decrease (0-10 points). For the period 2070-2100 a large increase is projected in the area affected by a slight increase in aridity (0-10 points), particularly in Kazakhstan, Uzbekistan, and Turkmenistan.

The overall effect of the changes in precipitation and temperature is expected to be positive on the growing period. Not much change is projected in the period 2010-2040 for the thermal growing period in the regions dominated by lowlands (Kazakhstan, Uzbekistan, Turkmenistan and Xingjiang). However, from 2040-2070 onward the increase in the thermal growing period is expected to be pronounced throughout the entire region. As for the moisture-limited growing period, up to 2040-2070 an increase is projected in most of Uzbekistan and Turkmenistan and a decline in the other areas. During the period 2040-2070 the moisture-limited growing period is expected to decline in most of the region.

In summary, the overall balance between changes in the thermal growing period and the moisture-limited growing period is expected to be positive by the end of the 21st century and most of the region is projected to witness an increase in the temperature- and moisture-limited growing period.

Until the end of the 21st century a gradual but significant increase is projected in the share of the region that changes from one Köppen climatic zone to another. The most significant changes are expected in mountainous areas as these are most sensitive to the impact of temperature rise. This may lead to wetter climate types in Kyrgyzstan, whereas a significant part of Kazakhstan is expected to evolve in a drier climate type with precipitation more concentrated in winter.

In our study we have focused on the application of relatively simple models on spatially downscaled climate change projections to draw conclusions about the general trends of climate change for different timelines and emission scenarios, without being crop-specific. In a companion study[1] for the same project, the potential impact of these changes on the main varieties of wheat was evaluated using the crop growth and potential yield simulation mode CROPSYST. Despite their use of different methods and focus for assessing climate change impact, the two studies complement each other and come, at their own spatial scales, to similar overall conclusions, foremost that the impact of climatic change in Central Asia is projected to be *mostly positive*. The main reason for this is that the short-duration thermal growing period, which prevails in most of the region, is projected to become longer, opening new possibilities for growing adapted and higher-yielding crop varieties, and that this thermal effect will more than compensate for any drying effect as a result of the higher temperatures.

Whereas in future studies more attention will need to be paid to the potential impact of extreme events, the results of both studies indicate that under the current projections of climate change impact, the implementation of improved land, water and crop management practices for drylands recommended for *present* climatic conditions is the most sensible way forward to adapt to climate change.

[1] R. Sommer, R., Glazirina M. and Yuldashev T. 2012. Assessing the vulnerability of selected agro-ecosystems in Central Asia to threats resulting from climate change –production and productivity of wheat. Report of sub-component 3 of the ADB funded project on "Adaptation to Climate Change in Central Asia and the People's Republic of China". ICARDA, 127 pp.

1. INTRODUCTION

Central Asia and the Xinjiang Province of NW China constitute a contiguous dryland area of approximately 5.6 million km^2. Despite an apparent (and misleading) monotony of the landscapes in most of the region, there is a surprising diversity in agroecologies. Moreover, it is a region that has witnessed some major environmental catastrophes and degradation of its land and water resources in its recent past, and is particularly vulnerable to the threat of climate change.

Climate change is expected to affect significantly Central Asian countries in the coming decades. According to the 2007 4th Assessment Report of the Intergovernmental Panel on Climate Change (IPCC), the projected median increase in temperature is estimated to 3.7°C on average by the end of the century, with most of the increase to occur during the summer (June-July-August). Precipitation is projected to increase slightly during the winter and to decrease the rest of the year, which leads to a lower amount of rainfall on annual mean. Heavily watered winters will be more frequent, as well as drier springs, summers and autumns.
Peculiar to Central Asia and NW China are the high upstream/downstream dependency, as the snowfall and glaciers in the mountain chains of the Tien Shan and Pamir are key to the region's hydrology and agriculture downstream. Consequences of these changes in temperature and precipitation regimes are therefore potentially harmful for the population in this vulnerable area. Food security and water availability are threatened by the increasing water scarcity and higher frequency of drought. Agriculture, which uses 83.6% of the water resources in the region (Abdullaev et al., 2006) and employs a large share of the population (29% according to CIA, 2009) will have to adjust in order to cope with increasing stresses and to satisfy a growing population.

In this context, anticipation of climate change impacts and possible pathways for adaptation through scientific research is central for mitigating negative effects. In this perspective ICARDA initiated a project funded by the Asian Development Bank on "Adaptation to Climate change in Central Asia and the People's Republic of China" (ICARDA, 2009), which is aimed at increasing the knowledge about climate change in order to anticipate improved drought management and adaptation options in the existing agro-ecosystems.

Within the region the projections of precipitation change by the IPCC are mixed (Fig.1). The range in precipitation change may vary indeed from -11% to +16%. Depending on the scenario and model outputs considered (see further), the expectation for Kazakhstan is a 0-5% increase in the south to a 10-16% increase in the north and east. Kyrgyzstan may expect a 0-10% increase, Turkmenistan and Uzbekistan by contrast losses of 0-11%. The picture is mixed in Tajikistan, with a range of -5 to +5% change.
These projections come with the well-known uncertainties of climate science in its current state: uncertainty about future GHG emissions (hence the practice of working with emission scenarios), the use of Global Circulation Models (GCM) models which are often in utter disagreement (see section 2.1.1.), and the coarse spatial resolution (typically 1 to 3 degrees) of GCMs, too coarse to include small-scale processes, the ones responsible for local weather patterns (especially in mountain areas). Moreover the IPCC projections in the 4th Assessment Report are for the time frame 2080-99, too far in the future to be meaningful for most of us.

Figure 1. Precipitation change projections in Central Asia and Xinjiang Province in 2080/2099, according to the average of 21 GCM models under greenhouse gas emission scenario A1b (source: IPCC, 2007)

In order to develop climate change adaptation strategies in Central Asia that are meaningful at landscape level, there is a need for spatially '*downscaling*' climate change from the global to the regional level. This involves an increase in the spatial resolution (e.g. a 10 km^2 grid cell), in order to simulate impact closer to the farmer environment. It also implies a need for higher temporal resolution in order to understand better the *seasonal distribution* of future precipitation and temperature changes. But it also means projecting changes for *nearer futures* (e.g. 2030, 2050) than those provided in the 4th IPCC Assessment Report: for the purpose of adaptation these are time horizons of more interest to local planners. Predictions for the near future also have the advantage that they can be verified by looking at their *continuity with trends that are already present within the current climate*. For this reason our study included a trend analysis of precipitation variability and drought in the 20th century.

GIS tools have played a key role in this project through the generation of a high-resolution spatial dataset derived from publicly available low-resolution spatial data. The spatial dataset has three major components: the downscaled high-resolution spatial database of basic climatic variables (precipitation and temperature), the high-resolution higher-level derived climatic variables and their changes, and the spatial dataset on drought and precipitation variability in the region. These datasets, methods used to generate them, the results and the conclusions that can be drawn from them are described in this report.

2. METHODS

2.1. CLIMATE CHANGE MAPPING: GENERAL

2.1.1. Climate change maps and planning: the limits of interpretation

Planning adaptation strategies to climate change is notoriously difficult in the light of the uncertainties of climate change science. A much asked question is, if (depending on the season) we cannot trust a weather forecast one week ahead, how can we plan for futures 25, 50 even 100 years ahead? This is certainly a valid question and there is no easy answer to it.

Global Circulation Models (GCMs), complex models that emulate the interactions between the atmosphere, land and ocean surfaces, geosphere, biosphere and human interventions, have been at the forefront in drawing the main conclusions contained in the 4th Assessment Report (AR4) of the Intergovernmental Panel on Climate Change (IPCC, 2007):
(i) that climate change is real and has started to show in the current weather;
(ii) that climate change has a discernible human signature.

Anyone familiar with AR4 knows that these conclusions are formulated, not as certainties, but in terms of 'likelihoods'. Scientifically this is a more correct formulation, but with the obvious drawback that planning for such changes requires some skilful navigation between interpretations of 'certainty' and 'likelihood'.

In this study we produce maps that provide a comprehensive picture of climatic conditions in three time intervals, 2010-2040, 2040-2070 and 2070-2100. These maps are derived from climate parameter estimates generated by the GCMs contained in AR4. In predicting these climatic variables for the future, there are two main sources of uncertainty.

The first uncertainty is that the future itself is only one possibility out of many that materializes. Given the strong linkage between greenhouse gas (GHG) emissions and global warming, the practice is therefore to 'model' first different futures, and to run the climate models under these GHG emission assumptions. The futures we worked with in this study are GHG emission scenarios A1b, A2 and B1. These are explained in section 2.1.2.

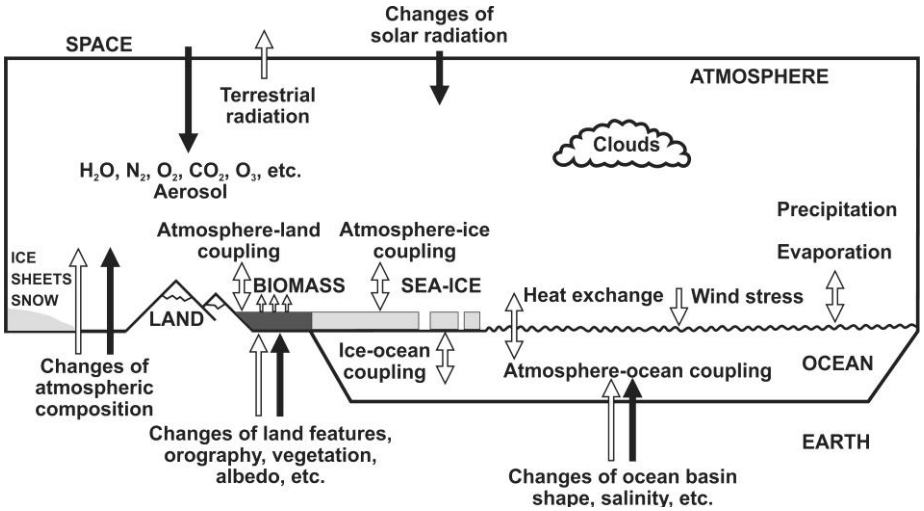

Figure 2. Schematic representation of a typical GCM

The second uncertainty is that the IPCC's 4th Assessment Report is based on simulations of 21 GCM models. Since the IPCC published its first Assessment Report in 1990, these models have grown in complexity and are now able to couple multi-layered atmospheric processes to ocean and land-surface processes (Fig. 2).

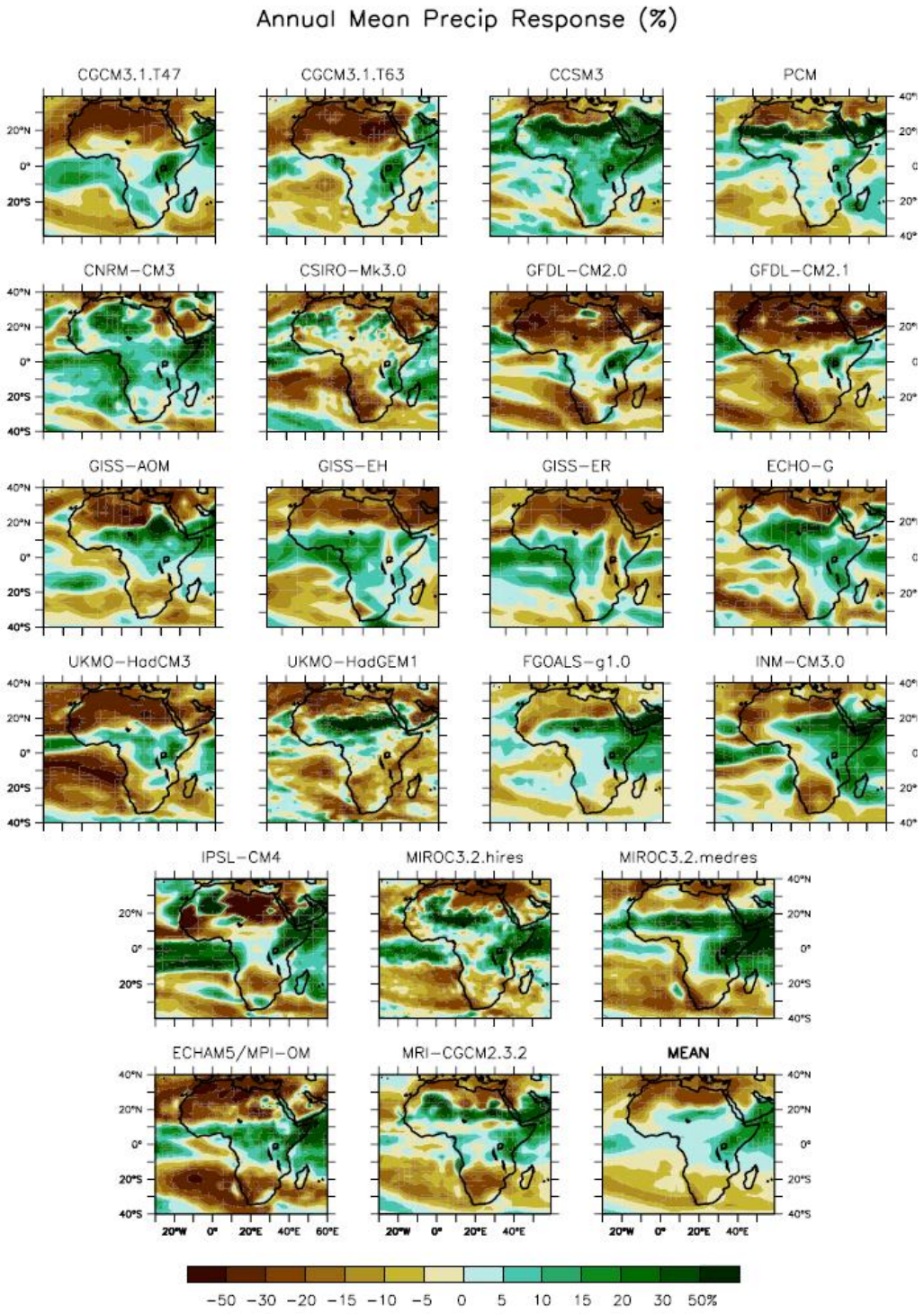

Figure 3. Relative change (%) in annual precipitation in Africa for the period 1980-1999 to 2080-2099 according to 21 GCM models (Christensen et al., 2007)

However, despite increasing sophistication, there are still considerable differences between predictions of different models originating from different research groups. This is illustrated in Figure 3, which shows a huge range in variation in the prediction of annual precipitation in Africa for the period 2080-2099, assuming GHG emission scenario A1B. For this reason it is important to select those models that are considered the most appropriate for developing adaptation strategies, or, alternatively, to apply a kind of averaging process to obtain a 'middle of the road' prediction. This step of creating a dataset from a 'multi-model ensemble' is further explained in section 2.3.1.

Typical for GCM models is that parameter estimation is at a relatively coarse spatial resolution (typically 2 to 3 degrees, corresponding to a grid cell of 10,000 – 36,000 km^2 depending on the model and geographical latitude). This scale is too coarse to include small-scale processes, the ones responsible for local weather patterns, and particularly in hilly to mountainous terrain these can be very important. Apart from these possible distortions, the coarse resolution of GCMs is perhaps the main bottleneck for planning, as it prevents linkage to features with variability at much finer spatial variability, such as arable land, water resources, human settlements, agricultural production systems, poverty hot-spots etc.
Downscaling the output of GCMs is therefore an extremely important step and is in fact the whole objective of this study. The different methods for downscaling GCMs are outlined in section 2.1.4., details on our own approach are provided in section 2.1.5.

2.1.2. Greenhouse gas emission scenarios

The three most commonly used scenarios for assessing the impact of climate change are the SRES[2] scenarios A1b, A2 and B1 (IPCC, 2007). The following description of these scenarios is taken from this summary report.

A1. The A1 storyline and scenario family describes a future world of very rapid economic growth, global population that peaks in mid-century and declines thereafter, and the rapid introduction of new and more efficient technologies. Major underlying themes are convergence among regions, capacity building and increased cultural and social interactions, with a substantial reduction in regional differences in per capita income. The A1 scenario family develops into three groups that describe alternative directions of technological change in the energy system. The A1b scenario assumes a balance between fossil-intensive and non-fossil energy sources, where balance is defined as not relying too heavily on one particular energy source, on the assumption that similar improvement rates apply to all energy supply and end use technologies.

A2. The A2 storyline and scenario family describes a very heterogeneous world. The underlying theme is self-reliance and preservation of local identities. Fertility patterns across regions converge very slowly, which results in continuously increasing population. Economic development is primarily regionally oriented and per capita economic growth and technological change more fragmented and slower than other storylines.

B1. The B1 storyline and scenario family describes a convergent world with the same global population, that peaks in mid-century and declines thereafter, as in the A1 storyline, but with rapid change in economic structures toward a service and information economy, with reductions in material intensity and the introduction of clean and resource-efficient technologies. The emphasis is on global solutions to economic, social and environmental sustainability, including improved equity, but without additional climate initiatives.

[2] SRES: Special Report on Emission Scenarios

A1b is the middle-of-the-road GHG emission scenario, A2 the more pessimistic one, and B1 the more optimistic one. With no progress on reducing GHG emissions, the A2 scenario is now being considered more realistic, whereas A1b is slowly becoming the 'optimistic' scenario, and B1 a kind of 'pie-in-the-sky' scenario.

The IPCC report is based on 23 global circulation models (GCM). As some of the necessary climatic variables were not available on-line, only 17 GCM models were selected for this study. The minimum requirement for a GCM output dataset to be selected was the availability of mean temperature and precipitation data for the three scenarios and the three time horizons.

2.1.3. Global circulation models

Among the 23 GCMs used in the IPCC report, the seven listed in Table 1 have complete publicly available datasets for precipitation, maximum, minimum and mean temperature. For the 10 GCMs listed in Table 2, full precipitation and mean temperature datasets were available.

Table 2. GCM characteristics (1) (Source: CMIP3 2007)

Name	**Institution**	**Year**	**Atmosphere Resolution**	**Parameterization over orographic features**
BCCR-BCM2.0	Bjerknes Centre for Climate Research, Norway	2005	2.8° x 2.8 x 31 levels	Subgrid scale orographic drag module to simulate the influence of small scale relief on atmospheric momentum
CSIRO-MK3.0	Commonwealth Scientific and Industrial Research Organization, Australia	2001	1.9° x 1.9° x 18 levels	Gravity wave drag (GWD) formulation of Chouinard et al. (1986). This drag is dependent on the sub-grid-scale variations in surface topography
INM-CM3.0	Institute for Numerical Mathematics, Russia	2004	4° x 5° x 21 levels	Orography gravity wave drag (Palmer et al, 1986)
MIROC3.2 (medres)	Center for Climate System Research, JAMSTEC, Japan	2004	2.8° x 2.8° x 20 levels	Internal gravity wave drag McFarlane (1987)
CGCM3.1(T47)	Canadian Centre for Climate Modelling and Analysis, Canada	2005	3.75° x 3.75° x 31 levels	Orographic drag parameterization (Scinocca and McFarlane 2000)
CGCM3.1(T63)		2005	2.8° x 2.8° x 31 levels	Orographic drag parameterization (Scinocca and McFarlane 2000)
CNRM-CM3	Meteo France, Centre de Recherches Météorolog.	2004	2.8° x 2.8° x 45 levels	No gravity drag mentioned

Data were incomplete for the following IPCC GCMs: MIROC3.2 (hires), GISS-AOM, UKMO-HadGEM1, GISS-EH, FGOALS-g1.0, BCC-CM1. These were not included in the study.

Table 3. GCM characteristics (2) (Source: CMIP3 2007)

Name	Institution	Year	Atmosphere Resolution	Parameterization over orography
ECHAM5/MPI-OM	Max Planck Institute for Meteorology, Germany	2003	1.9° x 1.9° x 31 levels	GWD according to Lott and Miller, 1997: momentum transfer from the earth to the atmosphere accomplished by orographic gravity waves, and drag exerted by the subgrid-scale mountain when the air flow is blocked at low levels
CCSM3	National Center for Atmospheric Research, USA	2005	1.4° x 1.4° x 26 levels	No gravity drag mentioned
PCM		1998	2.8° x 2.8° x 26 levels	No gravity drag mentioned
GFDL-CM2.0	Geophysical Fluid Dynamics Laboratory, USA	2005	2.0° x 2.5° x 24 levels	No gravity drag mentioned
GFDL-CM2.1		2005	2.0° x 2.5° x 24 levels	No gravity drag mentioned
IPSL_CM4	Institut Pierre-Simon Laplace, France	2005	2.5° x 3.75° x 19 levels	GWD according to Lott and Miller, 1997: momentum transfer from the earth to the atmosphere accomplished by orographic gravity waves, and drag exerted by the subgrid-scale mountain when the air flow is blocked at low levels
UKMO-HadCM3	Hadley Centre for Climate Prediction and Research, UK	1997	2.5° x 3.75° x	No gravity drag mentioned
ECHO-G	Meteorological Institute of the University of Bonn, Meteorological Research Institute of the Korea Meteorological Administration, and Model and Data Group, Germany/Korea	2005	1.9° x 1.9° x 19 levels	No gravity drag mentioned
GISS-ER	NASA – Goddard Institute for Space Studies, USA	2004	2.8° x 2.8° x ?	Physically-based estimate of gravity-wave drag detemined from the model simulation of moist convection, mountain waves, shear and deformation (Rind et al, 1988).
MRI-CGCM2.3.2	Meteorological Research Institute, Japan	2003	2.8° x 2.8° x 30 levels	No gravity drag mentioned

Tables 1 and 2 specify the methods used in the GCMs for air flow parameterizations over orographic features. Given the coarse resolutions of GCMs they use simplified representations of the earth surface. As a result GCMs underestimate greatly high altitudes in steep areas, and subsequently their influence on air flow, temperature and moisture. Our study area includes two of the highest mountain ranges of the world, the Tian Shan and the Pamir Mountains, both with peaks above 7000m. The way the atmosphere over orography is modeled might therefore affect significantly the simulation of both precipitation and temperature regimes. The most common aim of these air flow parameterizations is to transfer the momentum from the earth surface to the atmosphere by orographic waves and/or to force air flow to lift up when it is blocked at the feet of orographic features. The gravity wave drag reduces (suppresses in few cases) the cold bias at high latitudes near the tropopause (IPCC, 2007).

2.1.4. General approaches for climate change downscaling

High-resolution maps of climate change were based on a simple approach to downscaling climate change information. Generally speaking, three methods are available for downscaling GCM output to higher spatial resolutions.

- Calibration of current climate surfaces with GCM output
- Statistical downscaling with or without weather typing
- Dynamical downscaling with regional climate models (RCM)

Statistical downscaling yields good results, in terms of reproducing current climates from GCMs. They can be applied to output of different GCMs. On the down side, statistical relationships have to be established individually for each station and GCM, requiring quality data. Surfaces have to be created from point data, a problem in data scarce regions. Moreover, this method is computationally challenging.
The *dynamical downscaling* using a RCM yields the best results, even in areas with complex topography, and directly generates climate surfaces. It is the only technique able to model complex changes of topographical forcing. Different methods of dynamical downscaling are linked to specific GCMs, thus transferring inherent flaws in particular models from a lower to a higher resolution. They are also methodologically and computationally challenging.

In the absence of any downscaled data obtained from a RCM, in this study we used the *calibration method* of GCM downscaling, which involves essentially the superposition of a *low-resolution* future climate change field on top of a *high-resolution* current climate surface.
Four climatic variables were considered: precipitation, minimum, maximum and mean temperatures. Climate change as represented by these variables was assessed for three time horizons, 2011-2040, 2041-2070, 2071-2100.

2.2. Downscaling GCMs and mapping basic climate change data

2.2. 1. GCM Data sources

Three main websites are devoted to the distribution of the IPCC datasets. The first one is the IPCC data distribution portal[3], where averages over each slice of 30 years are provided for each month.

[3] http://www.ipcc-data.org/

The second one is the WCRP CMIP3Multi Model data portal[4], which gathers daily values and monthly and yearly averages for most GCMs. Most of these files can also be downloaded from the Earth System Grid (ESG) website[5].
Finally, datasets from certain GCMs, such as CNRM-CM3 and ECHAM5, can also be found at the Model and Data website[6] hosted by the Max Planck Institute for Meteorology in Hamburg.
In some cases where complete datasets could not be obtained from any of the above web sites, missing files could be found on the website of the institute which developed the GCM.

2.2. 2. GCM data processing

The transformation of GCM data into high-resolution climate maps is no trivial matter and required the following steps, which are explained in the following sections:

- Data extraction procedures
- Change mapping at coarse resolution
- Resampling
- Correcting the precipitation maps
- Generating downscaled climate surfaces
- Calculating averages
- File name coding

2.2.2. 1. Data extraction procedures

Datasets for each GCM were retrieved from the sources mentioned above in a NetCDF format (.nc), a self-describing format for weather and climate data files, developed by UCAR[7]. 'Self-describing' means that a header describes the layout of the rest of the file, in particular the data arrays, as well as arbitrary file metadata in the form of name/value attributes. This file structure is particularly suitable for creating, accessing and sharing array-oriented scientific data across networks with multiple platforms and software. The relevant data were extracted from these files using the program GrADS[8] (for Grid Analysis and Display System), which runs under Linux platforms.

The specific extraction procedure depended on the type of datasets. Data from the IPCC data portal website were merely extracted without any additional averaging. Monthly data from the ESG website were averaged over 30 years for the three periods of interest. Daily data were first averaged over the months of each year, and then averaged over each set of 30 years.

Some datasets had a calendar format incompatible with GrADS. This concerns (partly or entirely) the following GCMs: CSIRO-MK3.0, CGCM3.1 T47 and T63, PCM and GISS-ER. In order to render them compatible, the descriptor files of these datasets were modified using the programs Ncdump and Ncgen[9]. Since the data extraction was based on day numbers rather than dates, calendar options could then be simply ignored.

[4] https://esg.llnl.gov:8443/home/publicHomePage.do
[5] http://www.earthsystemgrid.org/
[6] http://www.mad.zmaw.de/projects-at-md/ensembles/experiment-list-for-stream-1/
[7] http://www.unidata.ucar.edu/software/netcdf/
[8] http://www.iges.org/grads/
[9] http://www.unidata.ucar.edu/software/netcdf/workshops/2009/utilities/NcgenNcdump.html

For datasets containing different runs without average, averaging over the different runs was done in the GIS software ArcGIS[10].

In order to save downloading time and disk space, some data were only downloaded for one quarter of the globe (0-90°N, 0-180°E), for example the daily data for the two Canadian GCMs (CGCM3.1 T47 and T63).

2.2.2.2. Change mapping at coarse resolution

After computing every monthly average for each climatic variable, GHG scenario and time horizon, the averages were subtracted by the grid of the 1961-1990 time period (also a GCM output) in the case of temperature data. In the case of precipitation data, the ratio was computed.

For mean, minimum and maximum temperature (Celsius): $\Delta T = T_{LR,21} - T_{LR,20}$

For precipitation (dimensionless): $r_{prec} = P_{LR,21} / P_{LR,20}$

with LR: low-resolution, 20: 20th century data, 21: 21st century data

The change in temperature is thus expressed in absolute terms, while the change in precipitation is relative.

Change mapping was carried out in GrADS for compatible temperature data, and in ArcGIS in the case of non-compatible temperature formats and precipitation.

2.2.2.3. Resampling

In order to refine the coarse climate change maps, a resampling was carried out down to a resolution of 0.008333 decimal degrees (about 1km). This resolution corresponds to that of the reference climate maps of the study area.

The method for resampling was the cubic convolution method. With this method, new pixel values are computed based on a weighted average of the 16 nearest pixels of the original map (4 by 4 window). This method is relatively time-consuming, but it offers a smoother appearance than other available methods (nearest neighbour or bilinear interpolation). Possible edge effects (where the 16 pixel values are not all available) were avoided by selecting an area of interest larger than the study area. In our case the resampling of the climate change maps was carried out in ArcGIS over the rectangle 32°-58°N x 44°-98.5°E. Given the large number of coarse gridded change maps, the resampling process was automated by use of a Visual Basic script.

2.2.2.4. Corrections of precipitation maps

As we used a ratio to represent the change in precipitation, corrections of the coarse-gridded change maps were needed in two cases.

GCMs regularly predicted in some areas an average of 0 mm of precipitation for both the reference period 1961-1990 and the future period under consideration. Calculating the precipitation ratio would therefore lead to indeterminate expressions. To counter this problem, precipitation was assumed not to be lower than a certain threshold value, which in our case was fixed at 0.0167 mm (or $6.43*10^{-8}$ kg m^{-2} s^{-1}), corresponding to a total amount of rainfall of 1 mm in 60 years. Values of simulations of both 20th and 21st century that were below 0.0167mm were raised to that value, so that afterwards change could be computed.

[10] http://www.esri.com/software/arcgis/index.html

A second issue is that the cubic convolution method for resampling sometimes produces negative values of relative change when the original values are close to 0 mm. The solution to obtain only positive values was to resample using the logarithm of the original values, and obtain the final change grids by exponential transformation of the latter layers.
In both cases, thresholding for no-rainfall in both time periods and resampling using logarithmic transformation, Visual Basic scripts were used to automate the process.

2.2.2.5. Generating downscaled climate surfaces of precipitation and temperature

Downscaled high-resolution (1 km) climate surfaces were obtained by adding the resampled change maps to high-resolution reference climate surfaces (De Pauw, 2008) for temperature variables, and by multiplying for precipitation. The mask for Central Asia and Xinjiang was used to restrict these computations to the study area.
The calculations were performed in ArcGIS using simple raster algebra according to the formulas:

- For mean, minimum and maximum temperature (°Celsius): $T_{HR,21} = T_{HR,20} + \Delta T_{resampled}$
- For precipitation (mm): $P_{HR,21} = P_{HR,20} * r_{resampled}$

with HR: high resolution

Also this process step was automated by means of a Visual Basic script.

2.2.2.6. Calculating averages

Finally, averages were computed for the resampled high-resolution change maps of precipitation and mean temperature. Averages were made over the year, the winter and the summer for each GCM, scenario and time horizon. The winter period covers the months December, January and February, while the summer covers June, July and August. The objective of this final operation was, given the vast amount of data generated, to synthesize the predictions of each GCM, to compare their responses and eventually to classify them accordingly.

2.2.2.7. File name coding

Given the constraints imposed by ArcGIS on the number of character for grid names (13), even such trivial matter as file naming required an informative and consistent coding system. We used the following twelve characters for file naming:

- The first two digits, from 01 to 23, referred to the GCM used;
- Characters 3 and 4 (A1, A2, B1) referred to the respective GHG scenarios;
- Characters 5 and 6 (25, 55, 85) referred to the midpoints of the future time horizons (2010-2039, 2040-2069, 2070-2099);
- Characters 7 and 8 (pr, ta, th, tl) referred to the variables: precipitation (pr), average temperature (ta), maximum temperature (th) and minimum temperature (tl);
- Characters 9 and 10 (ch, rs, ds) referred to the type of map: coarse climate change map (ch), resampled change map (rs), final downscaled map (ds).
- Characters 11 and 12 referred to the months of the year (01 to 12)

2.3. Mapping climatic change using derived climatic variables

2.3.1. Creating a multi-model ensemble basic dataset

In view of the major differences between individual model results (see section 2.1.1.), the next step towards the goals of the ICARDA-ADB project was to make a **selection** of the most appropriate GCMs.

Key criteria for selection were GCM resolution, the modeling of atmospheric processes over mountains, and their similarities in response to forcing. The models included in Table 3 were selected for further characterization and mapping of changes in more integrated attributes of the agricultural climates.

Table 3. GCM models used for synthesis mapping of attributes of the agricultural climate

No	Name	Country	Year	Resolution (degrees)+ (levels)	Source
01	BCCR-BCM2.0	Norway	2005	2.8 x 2.8 (31)	http://www.ipcc-data.org/
					https://esg.llnl.gov:8443/home/publicHomePage.do
02	CSIRO-MK3.0	Australia	2001	1.9 x 1.9 (18)	http://www.ipcc-data.org/
					https://esg.llnl.gov:8443/home/publicHomePage.do
04	MIROC3.2	Japan	2004	2.8 x 2.8 (20)	http://www.ipcc-data.org/
08	CGCM3.1(T63)	Canada	2005	2.8 x 2.8 (31)	http://www.ipcc-data.org/
					http://www.cccma.ec.gc.ca/data/cgcm3/cgcm3.shtml
09	CNRM-CM3	France	2005	2.8 x 2.8 (45)	http://www.ipcc-data.org/
					https ://esg.llnl.gov:8443/home/publicHomePage.do
					http://www.mad.zmaw.de/projects-at-md/ensembles/experiment-list-for-stream-1/cnrm-cm3/
10	ECHAM5/MPI-OM	Germany	2003	1.9 x 1.9 (31)	http://www.ipcc-data.org/
12	GFDL-CM2.0	USA	2005	2 x 2.5 (24)	http://www.ipcc-data.org/

In addition, it was decided to retain, of the 3 GHG-scenarios analyzed in the first step (A1b, A2 and B1), only scenarios A1b (a relatively mild warming scenario) and A2 (a more severe warming scenario). The three futures (2010-2040, 2040-2070, 2070-2100) were retained in this analysis.

The precipitation and temperature data obtained from the models in Table 3 were averaged for each time horizon and retained GHG-scenario and these average data formed the dataset from which new climatic variables were generated, including the potential evapo-transpiration, the agroclimatic zones, the Köppen climatic zones and the growing periods . The generation of these new climate attributes is described in the following sections.

These attributes of the agricultural climate were summarized in a series of synthesis maps and tables for the three futures and two GHG-emission scenarios:

- Future states and changes in the annual mean temperature from current conditions
- Future states and changes in the annual minimum temperature from current conditions
- Future states and changes in the annual maximum temperature from current conditions
- Future states and changes in the annual mean precipitation from current conditions
- Future states and changes in the potential evapo-transpiration from current conditions
- Future states and changes in the Köppen climatic zones from current conditions
- Future states and changes in the agroclimatic zones from current conditions
- Future states and changes in the growing periods from current conditions

The full list of synthesis maps is contained in Annex 1.

2.3.2. Mapping changes in derived climatic variables

2.3.2.1. Potential evapo-transpiration

Potential evapo-transpiration is the rate of evapo-transpiration from an extensive surface of a 8-15 cm tall, green grass cover of uniform height, actively growing, completely shading the ground and not short of water (Doorenbos and Pruitt, 1984).

The calculation of potential evapo-transpiration (PET) is a first step in the assessment of crop water requirements and irrigation needs. It is also essential for the calculation of the aridity index (see section 2.2.6.3). The recommended method for calculating PET is the Penman-Monteith method, with a calculation procedure for monthly data, as described in Allen et al. (1998). This method depends on the availability of the following meteorological data at station level: temperature, radiation, relative humidity, and windspeed.

From the GCM models we can obtain only precipitation and temperature consistently. For this reason a method was needed for approximating the results of the Penman-Monteith PET method, while requiring only temperature data. A suitable way to do this was to calculate the PET according to the Hargreaves method (PET_{Har}), and subsequently to convert these values into Penman-Monteith estimates (PET_{Pen}), using a regression equation between monthly PET_{Har} and monthly PET_{Pen}. Experience in several ICARDA projects has indicated that this method works very well in dry areas, because in dryland regions the temperature is the main contributing factor to evapo-transpiration.

From the FAOCLIM 2.0 global climate database monthly PET, calculated by the Penman-Monteith method (FAO, 2002), for 4253 stations from countries with dryland areas were extracted. For each of these stations the Köppen agroclimatic zone was calculated in accordance with the criteria in Debaveye (1985). At the same time the PET was calculated according to the Hargreaves method. This method is based on the combination of temperature data and calculated extraterrestrial radiation and has the following formula (Choisnel, 1992):

$$PET_{Har} = .0023 * Ra * (T_{mean} + 17.8) * \sqrt{(T_{max} - T_{min})}$$

with: Ra: extraterrestrial radiation ($mm.day^{-1}$), T_{mean}: mean monthly temperature, T_{max}: maximum monthly temperature, T_{min}: minimum monthly temperature

Correlations were then established between the monthly values of PET_{Pen} and PET_{Har} that referred to a Köppen climatic zone that occurs in the study area. Thus, for the climates within the Central Asia window a highly predictive statistical relationship could be established between PET-Penman/Monteith and PET-Hargreaves (Fig. 4).

Using the projected temperatures for 2010-2040 and the same relationships between monthly Tmean, Tmax, Tmin, PET_{Har} and PET_{Pen}, it was possible to map the changes in PET_{Pen} for the scenarios A1b and A2. Maps 187 and 188 show the relative changes (%) between the annual PET under current climatic conditions and the PET under respectively scenarios A1b and A2.

$$relative\ change\ (\%) = \left(\frac{PET_{cc}}{PET_{cur}} - 1\right) * 100$$

with cc: climate change
cur: current climate

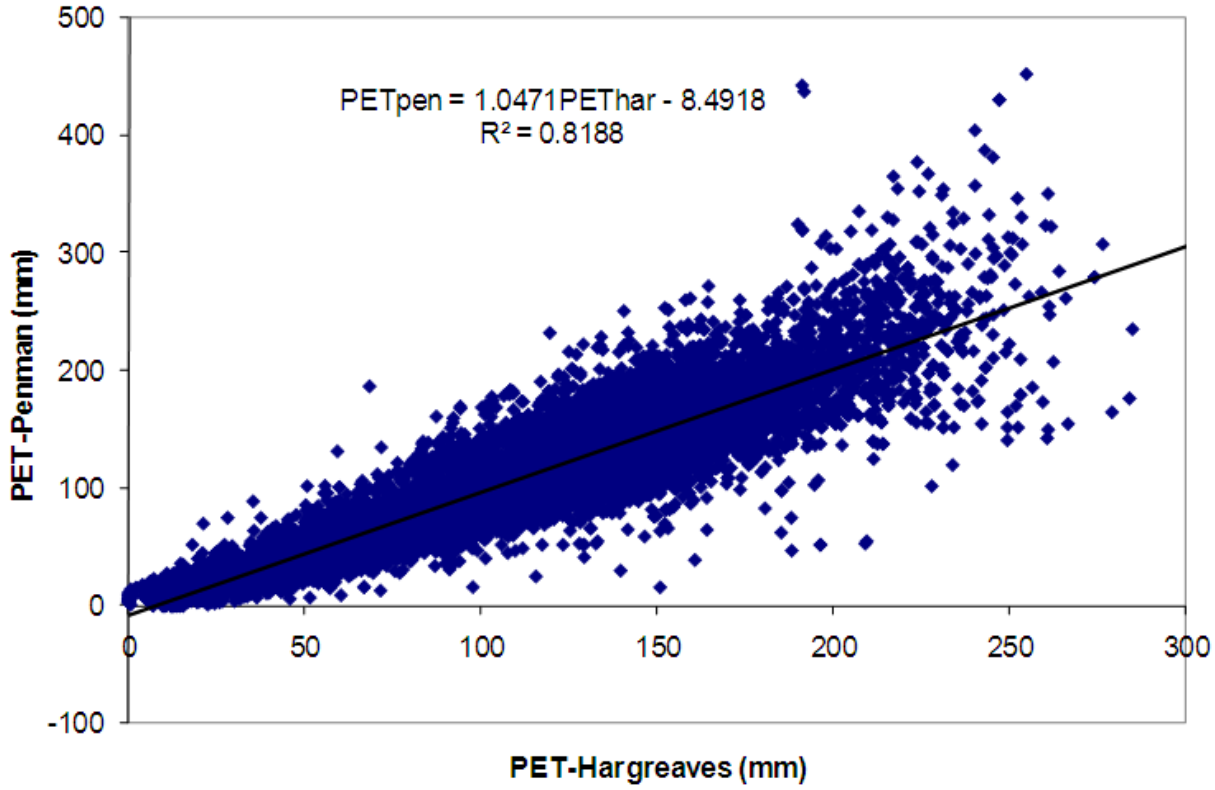

Figure 4. Correlation between monthly PET Penman-Monteith and PET Hargreaves (all climates combined except for the A, Cwc, Cfc and Dw climatic zones)

Using the projected temperatures for 2010-2040 and the same relationships between monthly Tmean, Tmax, Tmin, PET_{Har} and PET_{Pen}, it was possible to map the changes in PET_{Pen} for the scenarios A1b and A2. Maps 187 and 188 show the relative changes (%) between the annual PET under current climatic conditions and the PET under respectively scenarios A1b and A2.

$$relative\ change\ (\%) = \left(\frac{PET_{cc}}{PET_{cur}} - 1\right) * 100$$

with cc: climate change
cur: current climate

2.3.2.2. Aridity index

The aridity index is the ratio of the annual precipitation over the annual potential evapo-transpiration (UNESCO, 1979). By taking the ratio of the projected annual precipitation and projected annual PET-Penman/Monteith, calculated for each time frame according to the approach of section 2.3.2.1., the aridity index was mapped for scenario A1b and A2.

2.3.2.3. Growing periods

The climatic growing period is a concept developed to estimate the duration of the period during the year in which neither moisture nor temperature are limiting to plants. It is calculated by means of a model developed by the Food and Agriculture Organization of the United Nations (FAO, 1978). Under

rainfed conditions, both moisture and temperature can be limited. Under irrigated conditions, only temperature is to be considered a limiting factor. Thus the calculation of the growing period has two components, the calculation of the moisture-limiting and temperature-limiting growing periods separately, and their combination into a moisture-temperature-limited growing period.

The criterion used for the definition of a *moisture-limited growing period* is the ratio of actual evapo-transpiration (AET) to potential evapo-transpiration (PET). If this ratio for any particular month is higher than a user-defined threshold (in this study 0.5), that month is part of a growing period. If it is not, that month is not part of the growing period. The start date of the growing period is obtained from linear interpolation of the AET/PET ratios between the last month that is part of the growing period, and the first month that is not part of the growing period. The end date, inversely, is obtained by linear interpolation of the AET/PET ratios between the last month that is part of the growing period, and the first one that is not part of the growing period.

The following equations were used for estimating the length, onset and end of the moisture-limited growing period:

$$GP\_ON = M\_Start + NDays\frac{Thre - R_0}{R_1 - R_0}$$

$$GP\_END = M\_End + NDays2\frac{Thre - R_{n-1}}{R_n - R_{n-1}}$$

$LGP = GP\_END - GP\_ON$

with: GP_ON: growing period onset date
GP_END: growing period end date
LGP: length of growing period (days)
M_Start: the number of days from 1 January up to the end of the last month that is not part of the growing period
M_End: the number of days from 1 January up to the end of the month preceding the last month of the growing period
NDays: number of days in the first month of the growing period
NDays2: number of days in the last month of the growing period
Thre: AET/PET threshold for defining a growing period (user-defined; for this study set to 0 .5)
R_0: AET/PET ratio for the month preceding the first month of the growing period;
R_1: AET/PET ratio for the first month of the growing period;
R_{n-1}: AET/PET ratio for the month preceding the last month of the growing period;
R_n: AET/PET ratio for the last month of the growing period.

Similarly the temperature-limited growing period was calculated with reference to a temperature threshold, below which there is no growing period:

$$GP_{t,on} = M_{t,on} + NDays_t\frac{Thre_t - Temp_0}{Temp_1 - Temp_0}$$

$$GP_{t,end} = M_{t,end} + NDays2_t\frac{Thre_t - Temp_{n-1}}{Temp_n - Temp_{n-1}}$$

$LGP_t = GP_{t,end} - GP_{t,on}$

with: $GP_{t,on}$: onset date of the temperature-limited growing period
$GP_{t,end}$: end date of the temperature -limited growing period
LGP_m: length of temperature-limited growing period
$M_{t,on}$: the number of days from 1 January up to the end of the last month that is not part of the temperature-limited growing period
$M_{t,end}$: the number of days from 1 January up to the end of the month preceding the last month of the temperature -limited growing period
$NDays_t$: number of days in the first month of the temperature-limited growing period
$NDays2_t$: number of days in the last month of the temperature-limited growing period
$Thre_t$: temperature threshold for defining a temperature-limited growing period (user-defined; for this study set to 5°C)
$Temp_0$: Mean temperature for the month preceding the first month of the temperature-limited growing period;
$Temp_1$: mean temperature for the first month of the moisture-limited growing period;

By combining the moisture-limited growing period with a temperature-limited growing period, length, onset and end of the growing period, limited by both moisture and temperature, can be calculated.

The growing periods under current climatic conditions were mapped in three aspects: moisture-limited growing period (Map 196a), temperature-limited growing period (Map 196b), and moisture-temperature-limited growing period (Map 196c).

The changes in these three growing period components were obtained by subtraction of the growing periods lengths in the current climate from those in the three time frames and two scenarios.

2.3.2.4. Climatic zones according to the Köppen classification system

The Köppen climate classification system, devised by Waldimir Köppen (1846-1940), is based on the annual and monthly averages of precipitation and temperature. Initially published in 1918, the original Köppen classification system has been revised several times, especially by Geiger and Köppen himself (Köppen and Geiger, 1928). Despite its venerable age, the Köppen climate classification is still the most widely used to date. The system has 6 major subdivisions, designated by a capital letter:

A-climates: tropical moist climates

These climates have year-round temperatures above 18°C and abundant rainfall. Their general extent is north and south of the equator to about latitudes 15°- 25°. On the basis of seasonal distribution of the precipitation, they can be subdivided into Af-climates (tropical wet), Am-climates (tropical monsoon, with moderate dry season), Aw-climates (tropical wet and dry, with winter drought) and As-climates (tropical wet and dry, with summer drought).

B-climates: dry climates

These climates are characterized by precipitation that is deficient in comparison to the water requirements of plants. Generally speaking, their occurrence is related to one of three situations: (i) the subtropical deserts, between roughly 20° and 30° latitude, (ii) continental areas of mid-latitudes, far away from a moisture source, (iii) rainshadow effects caused by high mountains.
Depending on their degree of dryness Köppen subdivided dry climates into BS-climates (semi-arid or steppe climates) and BW (arid or desert climates). Further differentiation of the BS or BW climates is done on the basis of the temperature regime and the seasonal characteristics of the dry period.

C-climates: moist climates with mild winters

These temperate and mild climates are characterized by adequate precipitation and distinct summer and winter seasons. Winters may be cold but are not severe. The C-climates occur mostly along both the eastern and western edges of continents, between roughly 20° and 40° latitude. Depending on the presence and timing of the dry season they are subdivided into Cw-climates (with dry period in winter), Cs-climates (with dry period in summer), and Cf-climates (without pronounced dry period). Köppen made a further differentiation on the basis of the summer temperature regime.

D-climates: moist climates with cold winters

These climates have warm to cool summers and cold winters, with persistent snow cover. They occur between latitudes 40° and 70° and as they are linked to the presence of large continental landmasses do only occur in the northern hemisphere. As for the C-climates, they are further subdivided in the Köppen classification according to the seasonality and occurrence of a dry period, and on the basis of the temperature regime of summer.

E-climates: arctic climates

These climates are characterized by year-round low temperatures and include the polar tundra (ET) and ice sheets (EF), as well as locations in high mountain ranges.

F-climates: polar climates

Table 4 provides a listing and short description of all subdivisions of the Köppen system that occur within the area covered by the study for the considered time horizons and emission scenarios. Using monthly precipitation and temperature, the Köppen zones were calculated in accordance with the criteria in Debaveye (1985). For the detailed calculation and definition of the Köppen climatic zones in terms of annual and monthly precipitation and temperature variables is referred to Annex 2.

Table 4. Köppen climatic zones inside the study area

Code	Symbol	Description
7	BS0h	Hot semi-arid (steppe) climate, neither winter nor summer drought
8	BS0k	Cool semi-arid (steppe) climate, neither winter nor summer drought
9	BS0k’	Cold semi-arid (steppe) climate, neither winter nor summer drought
11	BSwh	Hot semi-arid (steppe) climate, winter precipitation
12	BSwk	Cool semi-arid (steppe) climate, winter precipitation
13	BSwk’	Cold semi-arid (steppe) climate, winter precipitation
15	BSsh	Hot semi-arid (steppe) climate, summer precipitation
16	BSsk	Cool semi-arid (steppe) climate, summer precipitation
17	BSsk’	Cold semi-arid (steppe) climate, summer precipitation
20	BW0h	Hot arid (desert) climate, neither winter nor summer drought
21	BW0k	Cool arid (desert) climate, neither winter nor summer drought
22	BW0k’	Cold arid (desert) climate, neither winter nor summer drought
24	BWwh	Hot arid (desert) climate, winter precipitation
25	BWwk	Cool arid (desert) climate, winter precipitation
26	BWwk’	Cold arid (desert) climate, winter precipitation
28	BWsh	Hot arid (desert) climate, summer precipitation
29	BWsk	Cool arid (desert) climate, summer precipitation

30	BWsk'	Cold arid (desert) climate, summer precipitation
32	Cwa	Warm temperate rainy climate with dry winter and hot summers
33	Cwb	Warm temperate rainy climate with dry winter and warm summers
36	Csa	Warm temperate rainy climate with dry and hot summers
37	Csb	Warm temperate rainy climate with dry and warm summers
40	Cfa	Warm temperate rainy climate without dry season and hot summers
41	Cfb	Warm temperate rainy climate without dry season and warm summers
45	Dfa	Continuously humid subarctic climate with hot summer
46	Dfb	Continuously humid subarctic climate with warm summer
47	Dfc	Continuously humid subarctic climate with cool summer
49	Dwa	Subarctic climate with cold, dry winter and hot summer
50	Dwb	Subarctic climate with cold, dry winter and warm summer
51	Dwc	Subarctic climate with cold, dry winter and cool summer
53	Dsa	Subarctic climate with humid winter and hot summer
54	Dsb	Subarctic climate with humid winter and warm summer
56	E	Arctic climate
57	F	Polar climate

Using the projected precipitation and temperature values for 2010-2040, 2040-2070, 2070-2100 under scenarios A1b and A2, it was possible to map the Köppen zones for these futures. Stability or changes in the Köppen zones compared to current conditions are shown in Figures 37-42.

2.4. MAPPING HISTORICAL PRECIPITATION AND DROUGHT

2.4.1. The data set

All maps are based on the Full Data Reanalysis Product Version 4 of the Global Precipitation Climatology Centre (GPCC).[11] It is a gridded monthly data set that is available at spatial resolutions of 2.5, 1.0, and 0.5 degrees. The spatial extent is the entire world with the exception of Antarctica. The grids for each month from January 1901 to December 2007 have been constructed as deviations from average monthly precipitation during the period 1951 to 2000.

For this study, the 0.5-degree version of the data set has been used. The advantages of using the GPCC Full Data Reanalysis Product are:

- It is one of the data sets with the highest spatial resolution available.
- Of all the gridded precipitation data sets, it is the one that is based on the largest number of stations (between around 8,000 and 45,000 globally, depending on which year).
- It covers the longest period (from January 1901 to December 2007) of all gridded precipitation data sets.
- It does not contain gaps in the time series; for each month from 1901 to 2007, an estimate of monthly precipitation for each grid cell is provided.

[11] U. Schneider, T. Fuchs, A. Meyer-Christoffer and B. Rudolf (2008): Global Precipitation Analysis Products of the GPCC. Global Precipitation Climatology Centre (GPCC), DWD, Internet publication, 1-12. Data and description can be downloaded from http://gpcc.dwd.de.

- All station data used have been thoroughly quality controlled.

When interpreting the results obtained through analysis of this data set, it should to be taken into consideration that the data have not been corrected for systematic gauge measurement errors. These are mainly due to losses from evaporation or wind drift and can reach up to about 30% in tropical and subtropical areas, much more at higher latitudes. However, it is also to be understood that practically all precipitation data from meteorological stations are subject to this error and that it is not particular to gridded data. In practical applications of meteorological data this error is frequently ignored.

The time-series grids have been constructed as deviations from average monthly precipitation during the period 1951 to 2000. Although GPCC used more stations to construct these grids than have been used for any of the other gridded data sets available, the number of stations is still quite small in the more sparsely populated parts of the world, especially in desert regions. Moreover the number and spatial distribution of stations used for the construction of the surfaces varies over time, which may cause some local distortions in the time series which have not been adjusted. Over larger areas, the general trends should, however, always stand out clearly.

Because of the relatively small number of stations in desert regions, the limits of areas without any or with very little rainfall during any particular month or year can be only approximate and are also affected by rounding errors. In areas with less than about 1 mm precipitation per month this can cause spatial patterns and artefacts to become visible on maps of precipitation-derived indices which magnify such subtle differences .This is, however, without any real meaning or consequence.

2.4.2. Data Processing

GPCC supplies the data set as 1,284 compressed text files, one file for each month from January 1901 to December 2007. Each file contains the average precipitation values for the land areas of all 0.5x0.5-degree grid cells of the world with the exception of Antarctica and islands with sizes less than about 1-degree square. In order to facilitate the calculation of various statistics and indices across time, the data have been rearranged by grid cell into 67,368 text files, each containing the 107-year data series for one cell. The subsequent analyses, computation of precipitation totals and statistics, computation of the Standardized Precipitation Index (SPI) for drought mapping, and regression analysis of precipitation and SPI, have been undertaken for each grid cell in turn and the results rearranged in the form of map layers that have been downscaled to grids with a resolution of 30x30 arc-seconds (roughly 1x1 km).

2.4.2.1 Computation of the Standardized Precipitation Index (SPI)

The Standardized Precipitation Index (SPI)[12] is a tool designed to make the relative intensities of droughts and wet periods comparable across different climates. A drought condition identified by a certain value of the SPI is expected to happen anywhere with comparable frequency. The SPI can be determined relatively easily as it is based on precipitation totals alone but this is also its main weakness; the index does not take into account differences in evaporative demand or soil moisture storage.

The SPI is used for periods with lengths of between one month and several years. For the current study, the annual SPI has been mapped for each year from 1901 to 2007. To compute the index, a Gamma

[12] The first publication on the SPI is: McKee, Thomas B., Nolan J. Doesken, and J. Kleist, 1993: The relationship of drought frequency and duration of time scales. Eighth Conference on Applied Climatology, 17-22 January 1993,

distribution is fitted to the non-zero precipitation totals of all the years falling into a reference period. In the present case, the entire period 1901/2007 for which data are available has been chosen as reference period. The fitted distribution, together with the probability of precipitation being greater than zero, permits to calculate the probability that a certain precipitation total is exceeded. This probability is then interpreted as applying to a standard normal distribution and converted into a deviation from the mean in multiples of the standard deviation: the SPI.

If the combined model – probability of precipitation greater than zero and Gamma distribution fitted to non-zero values – is a perfect fit for precipitation at a site, the standard normal distribution provides direct information on the expected frequencies of drought or high-rainfall events associated with a certain SPI value (see Table 5).

Table 5. Expected frequencies of SPI values

SPI value	Theoretical frequency from standard normal distribution	Event expected to happen approximately every ... years	Description
> +4.0	$3.1671243*10^{-5}$	31574	Extremely wet
> +3.0	0.001349898	741	
> +2.0	0.022750132	44	
> +1.5	0.0668072	15	Very wet
> +1.0	0.15865526	6	Moderately wet
+1.0 to -1.0	0.6826895	2 out of 3	Near normal
< -1.0	0.15865526	6	Moderately dry
< -1.5	0.0668072	15	Very dry
< -2.0	0.022750132	44	Extremely dry
< -3.0	0.001349898	741	
< -4.0	$3.1671243*10^{-5}$	31574	

2.4.2.2 Time-trend analysis

Simple linear regression models were fitted to the 107-year time series of annual precipitation of each 0.5x0.5 degree grid cell by the least-squares method. From these models, the following trend surfaces have been derived and mapped:

- average absolute change of annual precipitation in mm per decade,
- average relative change of annual precipitation in % per decade,
- correlation between annual precipitation and time,
- fraction of the change of precipitation explained by the linear time trend (coefficient of determination adjusted for the number of years in the series),
- t-significance level of the linear time trend of precipitation (two-sided t-test).

The annual SPI-values were subjected to a similar regression analysis in order to prepare a set of maps that shows the trends of drought in the region.

2.4.2.3. Downscaling of results

The values in the GPCC data set stand for the spatial averages across each of the 0.5x0.5 degree wide grid cells. Similarly, the results of the various calculations undertaken on these data result in surfaces with the same 0.5x0.5-degree resolution whose grid cells, again, contain values representing spatially average conditions. These surfaces can, therefore, not be simply resampled to a higher resolution by a smoothing interpolation process as this would distort the area averages.

For downscaling the initial low-resolution result surfaces to a resolution of 30x30 arcseconds (approximately 1x1 km), an iterative procedure has, therefore, been used that conserves area averages:

- Surfaces of variables that are not strongly influenced by terrain, such as SPI or time-trend variables, are, in a first step, resampled to high resolution by a straightforward interpolation process (bilinear interpolation or cubic convolution): the first provisional downscaled result.
- In the second step, this high-resolution grid is then aggregated again to the original resolution by computing the mean values for each low-resolution grid cell.
- Through subtraction of or division by the original low-resolution surface, a grid of resampling errors is generated. Division is used for zero-bounded variables, such as precipitation, subtraction in other cases, such as SPI which can be negative (drought) or positive (wet conditions). If the error is below an acceptable threshold for each grid cell (1% has generally been used in the present study), the resampled high-resolution grid is the final, downscaled result.

3. RESULTS

3.1. Downscaling basic climatic variables

3.1.1. Precipitation and temperature changes using all GCM models

Using the methods and processing steps outlined in section 2.2, the following grid maps were generated:

- Resampled change maps (5184 maps)
    - 7 GCMs x 4 variables x 3 scenarios x 3 time horizons x 12 months (= 3024)
    - 10 GCMs x 2 variables x 3 scenarios x 3 time horizons x 12 months (= 2160)
    - Unit: °C for temperatures, dimensionless for precipitation (ratio)
    - Spatial extent: rectangle 32° to 58°N, 44° to 98.5°E
- Future climate maps (5184 maps)
    - 7 GCMs x 4 variables x 3 scenarios x 3 time horizons x 12 months (= 3024)
    - 10 GCMs x 2 variables x 3 scenarios x 3 time horizons x 12 months (= 2160)
    - Unit: °C for temperatures, mm for precipitation
    - Spatial extent: Central Asian countries plus the Chinese province of Xinjiang.
- Averaged change maps (918 maps)
    - Yearly: 17 GCMs x 2 variables x 3 scenarios x 3 time horizons (= 306)
    - Summer and winter: 17 GCMs x 2 variables x 3 scenarios x 3 time horizons (= 612)
    - Unit: °C for temperatures, dimensionless for precipitation (ratio)
    - Spatial extent: rectangle 32° to 58°N, 44° to 98.5°E

As mentioned earlier, the averaged change maps were produced in order to classify the different GCMs according to the magnitude and the patterns of the changes in temperature and in precipitation.
Differences between GCM responses are logically expected to be the most marked under the scenario A2, with the most pessimistic GHG emission trend. Annual averages of precipitation and mean temperature change for the third time horizon (2070-2100) under this scenario are visualized in respectively Figure 5 and Figure 6.

As for the precipitation change, GCMs generally predict a reduction in the west of the study area, as an extension of the precipitation decrease in the Mediterranean basin, and a slight increase in the East. Some GCMs (GFDL-CM2.0 and 2.1, IPSL-CM4, ECHO-G, UKMO-HadCM3 and GISS-ER) predict this reduction to happen in about half of the study area, with a more or less pronounced decrease over Turkmenistan, where precipitation is already very low. On the other hand GCM CCSM3 shows a completely opposite trend of increasing precipitation over the entire study area. Others (BCCR-BCM2, CSIRO-MK3, MIROC3.2, CGCM3.1 T47 and T63, CNRM-CM3, and even INM-CM3.0) predict a relative status quo in most of the study area with a significant increase in the Xinjiang province, although in absolute terms the change is relatively small.

Concerning the temperature change, all GCMs agree on a significant warming (roughly from +2°C to +5°C) over the whole area, with for most of them predicting a slighter temperature increase in the west, around the Caspian Sea. MIROC3.2, ISPL-CM4, UKMO-HadCM3 and ECHO-G predict a more intense warming towards the north, reaching tremendous levels of +7, +8°C. On the other hand, PCM and MRI-CGCM2.3.2 show a relatively limited increase (+2°C to +4°C) of temperature with very little spatial variations.

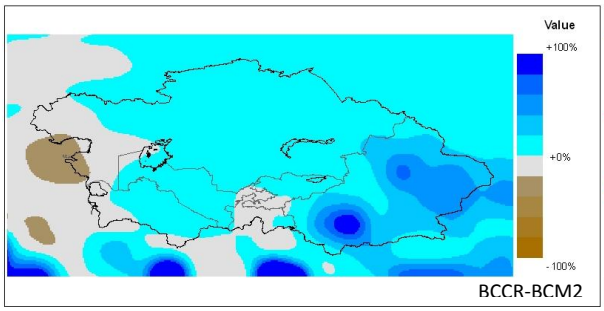
Value
+100%
+0%
-100%
BCCR-BCM2

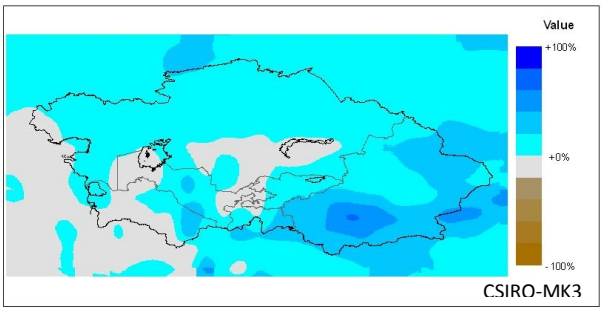
Value
+100%
+0%
-100%
CSIRO-MK3

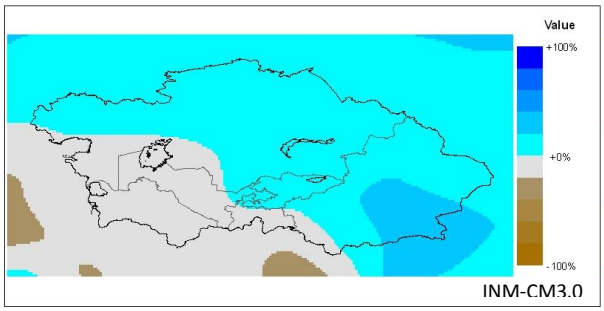
Value
+100%
+0%
-100%
INM-CM3.0

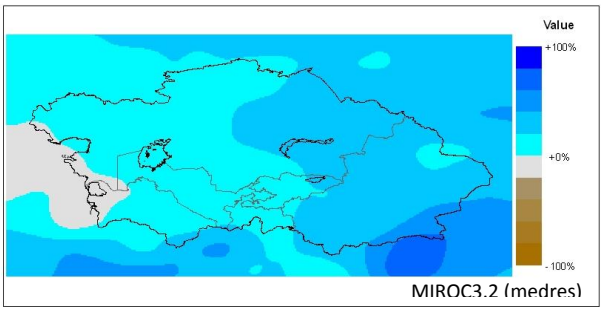
Value
+100%
+0%
-100%
MIROC3.2 (medres)

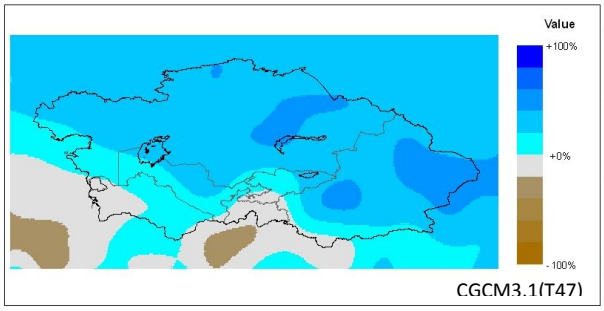
Value
+100%
+0%
-100%
CGCM3.1(T47)

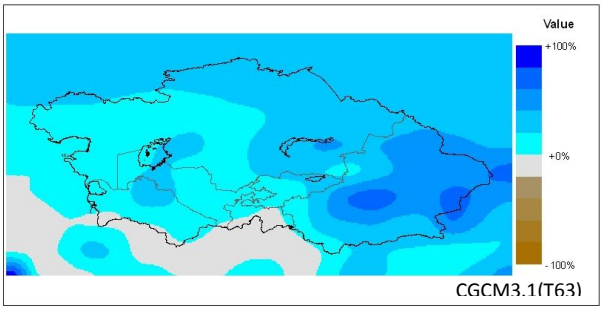
Value
+100%
+0%
-100%
CGCM3.1(T63)

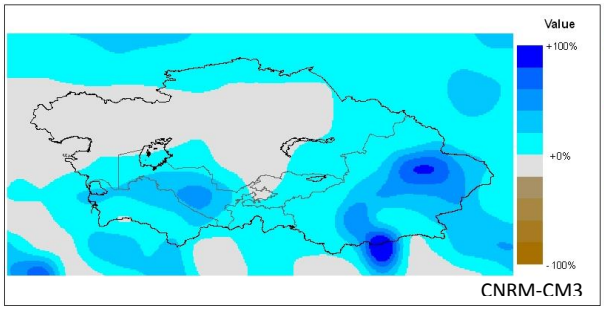
Value
+100%
+0%
-100%
CNRM-CM3

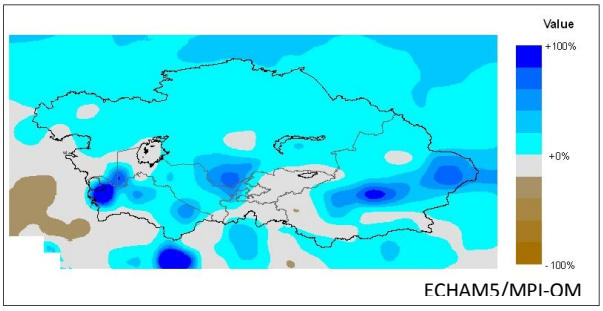
Value
+100%
+0%
-100%
ECHAM5/MPI-OM

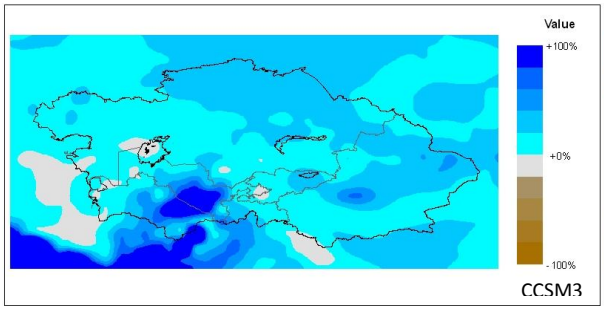
Value
+100%
+0%
-100%
CCSM3

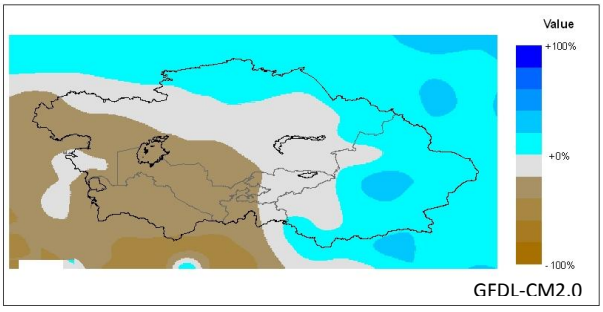
Value
+100%
+0%
-100%
GFDL-CM2.0

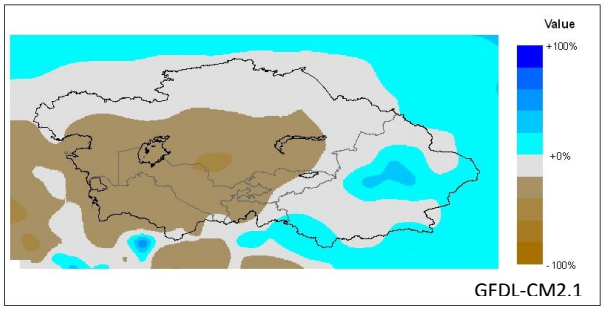
Value
+100%
+0%
-100%
GFDL-CM2.1

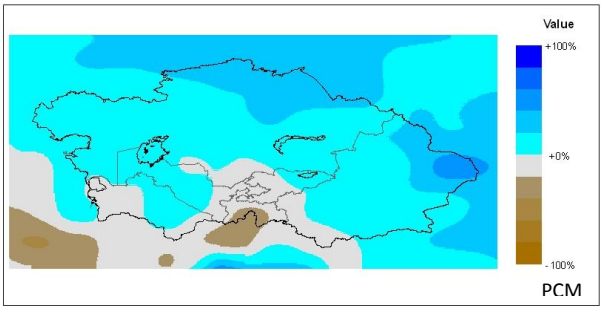
Value
+100%
+0%
-100%
PCM

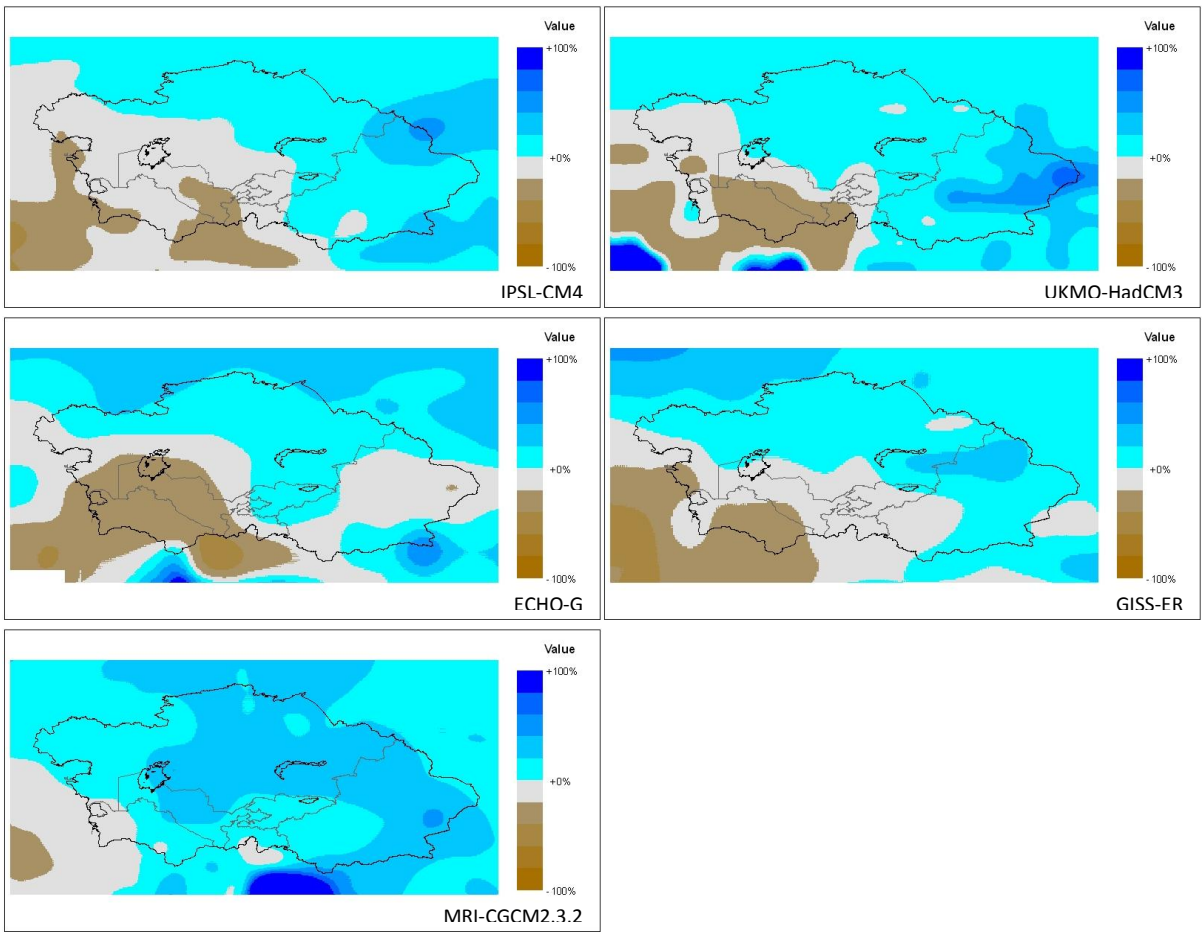

Figure 5. Comparison between 17 GCM models of average annual change (%) in precipitation for the A2 scenario in 2070-2100

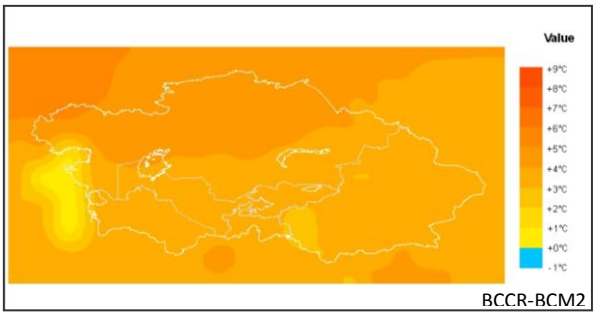
Value
+9°C
+8°C
+7°C
+6°C
+5°C
+4°C
+3°C
+2°C
+1°C
+0°C
-1°C
BCCR-BCM2

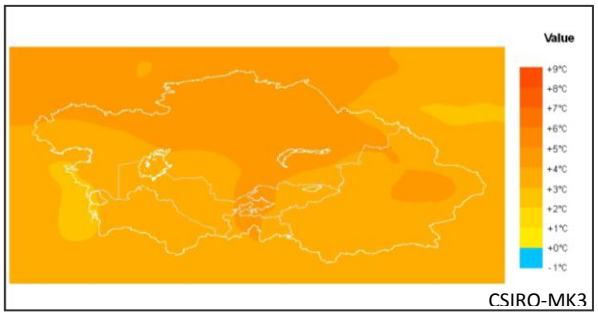
Value
+9°C
+8°C
+7°C
+6°C
+5°C
+4°C
+3°C
+2°C
+1°C
+0°C
-1°C
CSIRO-MK3

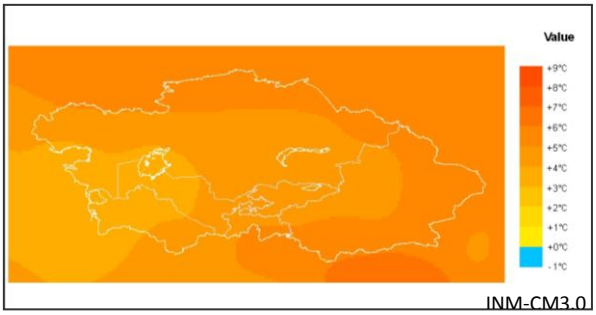
Value
+9°C
+8°C
+7°C
+6°C
+5°C
+4°C
+3°C
+2°C
+1°C
+0°C
-1°C
INM-CM3.0

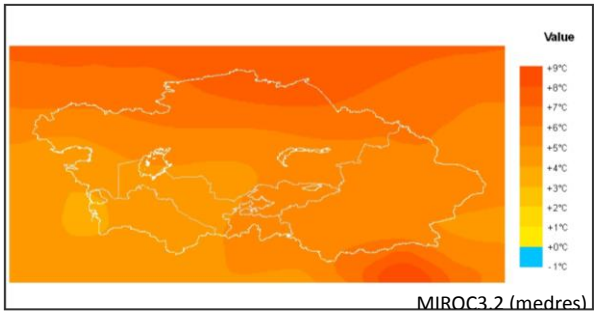
Value
+9°C
+8°C
+7°C
+6°C
+5°C
+4°C
+3°C
+2°C
+1°C
+0°C
-1°C
MIROC3.2 (medres)

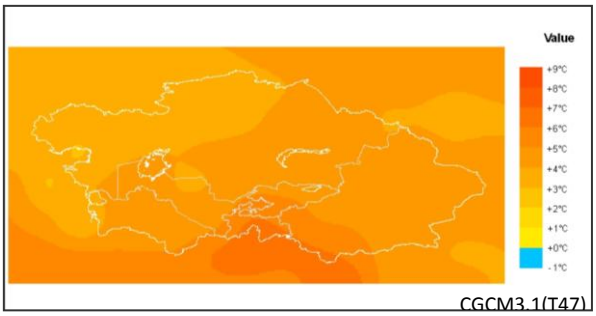
Value
+9°C
+8°C
+7°C
+6°C
+5°C
+4°C
+3°C
+2°C
+1°C
+0°C
-1°C
CGCM3.1(T47)

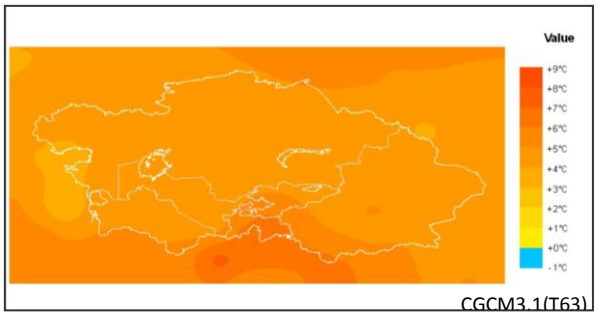
Value
+9°C
+8°C
+7°C
+6°C
+5°C
+4°C
+3°C
+2°C
+1°C
+0°C
-1°C
CGCM3.1(T63)

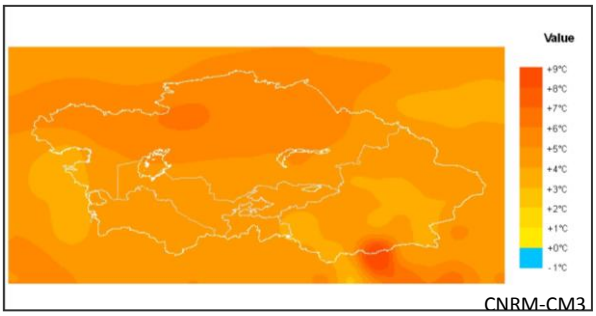
Value
+9°C
+8°C
+7°C
+6°C
+5°C
+4°C
+3°C
+2°C
+1°C
+0°C
-1°C
CNRM-CM3

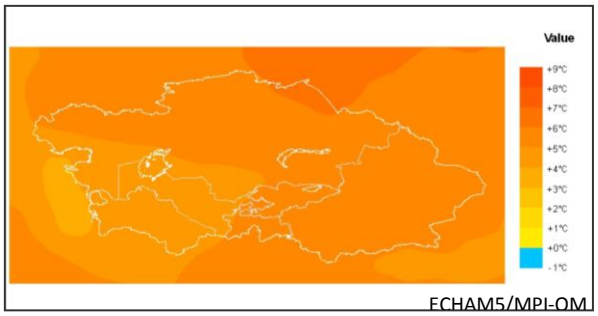
Value
+9°C
+8°C
+7°C
+6°C
+5°C
+4°C
+3°C
+2°C
+1°C
+0°C
-1°C
ECHAM5/MPI-OM

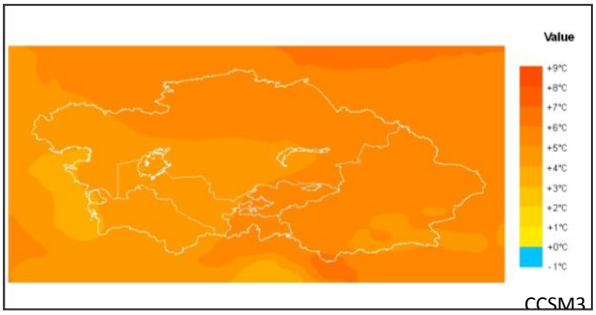
Value
+9°C
+8°C
+7°C
+6°C
+5°C
+4°C
+3°C
+2°C
+1°C
+0°C
-1°C
CCSM3

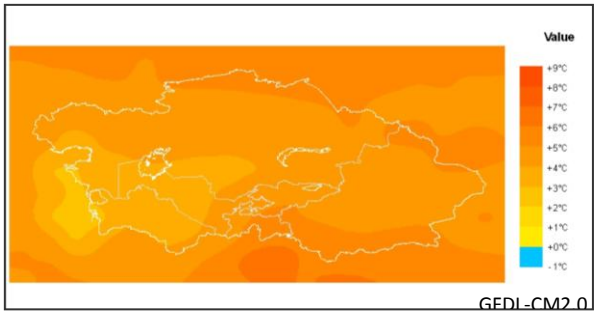
Value
+9°C
+8°C
+7°C
+6°C
+5°C
+4°C
+3°C
+2°C
+1°C
+0°C
-1°C
GFDL-CM2.0

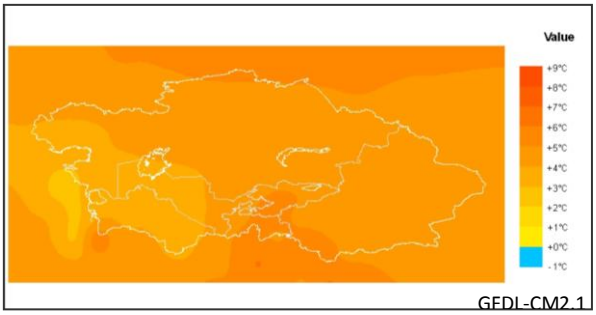
Value
+9°C
+8°C
+7°C
+6°C
+5°C
+4°C
+3°C
+2°C
+1°C
+0°C
-1°C
GFDL-CM2.1

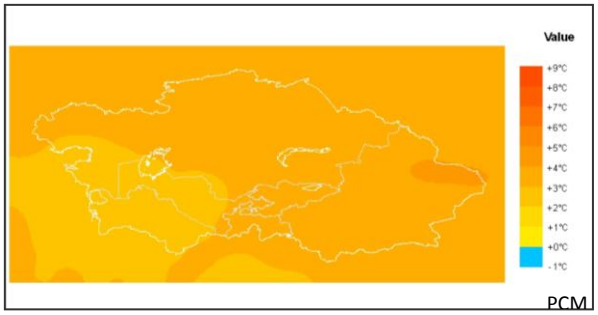
Value
+9°C
+8°C
+7°C
+6°C
+5°C
+4°C
+3°C
+2°C
+1°C
+0°C
-1°C
PCM

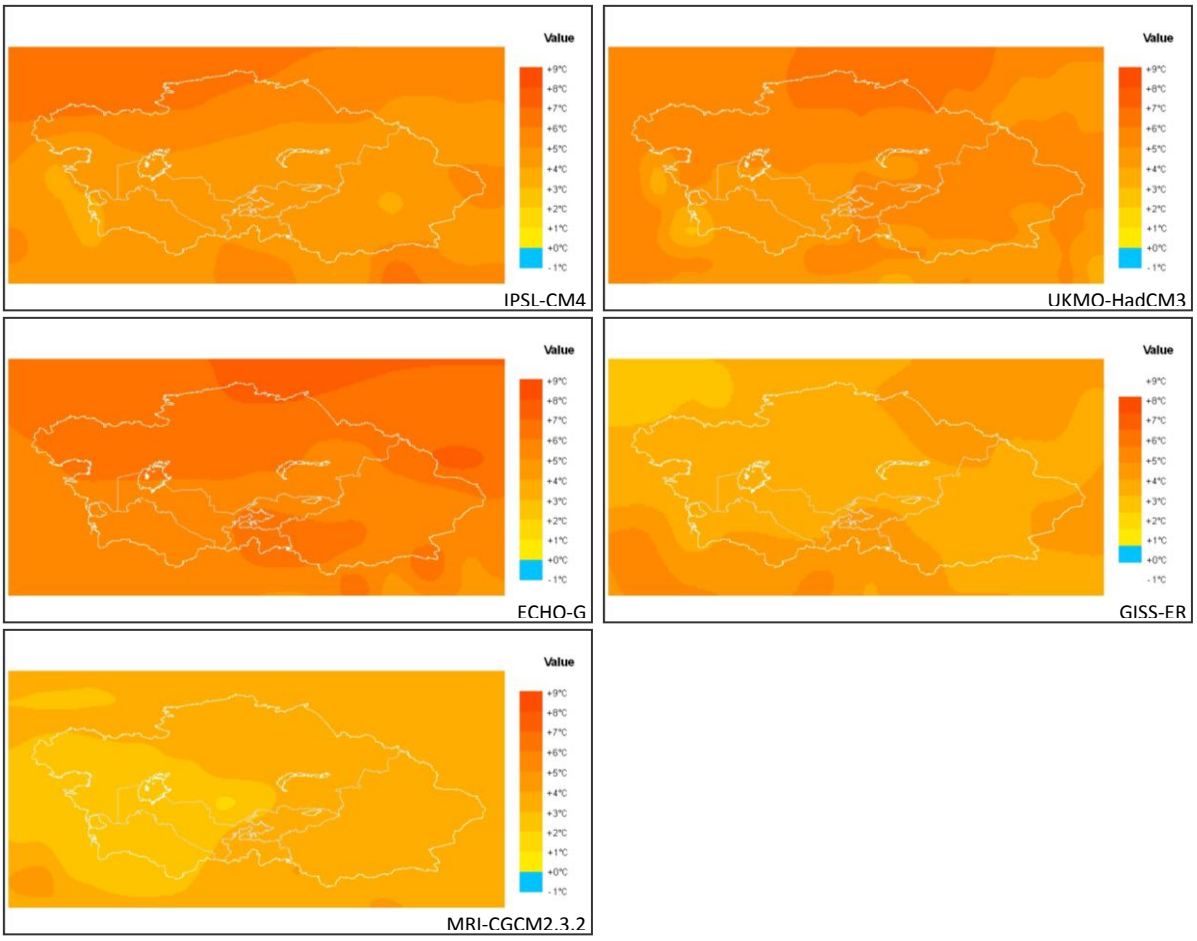

Figure 6. Comparison between 17 GCM models of average annual change (°C) in temperature for the A2 scenario in 2070-2100

3.1.2. Mapping precipitation changes using the multi-model ensemble dataset

The precipitation change maps (Figures 7-12) presented in this section and summary table 6 refer to projected changes in the annual precipitation during three time horizons (2010-2040, 2040-2070, 2070-2100) under two GHG emission scenarios (A1b, A2), with current climate (1960-1990).

In summary these projections based on downscaled multi-model ensemble annual precipitation indicate for most of the region a modest increase in precipitation (0-30 mm/year), with a tendency to grow stronger with time. The trend is most pronounced in the mountainous countries Kyrgyzstan and Tajikistan, where by the end of the 21st century the projection is for a increase of the annual precipitation in the range 30-60 mm/year in 15-30% of these countries. In this respect the differences in the projections between the two scenarios A1b and A2 are not pronounced.

It is also noteworthy that the overall trend towards increasing precipitation in the region as projected by the GCM-model ensemble *does not go counter the precipitation trend of the 20th century and grows stronger with time*.

Table 6. Projected changes in annual precipitation for different time horizons and scenarios

Current to A1b-2010-2040						
Change (mm	Kazakhstan	Uzbekistan	Turkmenist	Kyrgyzstan	Tajikistan	Xingjiang
-30 - 0	1	1	67	13	0	2
0 - 30	98	99	33	86	91	98
30 - 60	1	0	0	1	9	0
Current to A2-2010-2040						
Change (mm	Kazakhstan	Uzbekistan	Turkmenist	Kyrgyzstan	Tajikistan	Xingjiang
-30 - 0	2	0	3	4	0	2
0 - 30	98	98	97	90	72	98
30 - 60	0	2	0	6	25	1
60 - 90	0	0	0	0	3	0
Current to A1b-2040-2070						
Change (mm	Kazakhstan	Uzbekistan	Turkmenist	Kyrgyzstan	Tajikistan	Xingjiang
-30 - 0	10	1	20	3	24	1
0 - 30	90	99	80	97	74	97
30 - 60	0	0	0	1	1	2
Current to A2-2040-2070						
Change (mm	Kazakhstan	Uzbekistan	Turkmenist	Kyrgyzstan	Tajikistan	Xingjiang
-30 - 0	2	0	22	1	2	0
0 - 30	92	100	78	92	84	96
30 - 60	6	0	0	8	11	4
60 - 90	0	0	0	0	3	0
Current to A1b-2070-2100						
Change (mm	Kazakhstan	Uzbekistan	Turkmenist	Kyrgyzstan	Tajikistan	Xingjiang
-30 - 0	6	0	31	1	1	0
0 - 30	80	98	69	70	80	86
30 - 60	14	2	0	29	13	12
60 - 90	1	0	0	0	6	2
90 - 120	0	0	0	0	1	0
Current to A2-2070-2100						
Change (mm	Kazakhstan	Uzbekistan	Turkmenist	Kyrgyzstan	Tajikistan	Xingjiang
-30 - 0	18	6	29	8	11	0
0 - 30	71	94	71	63	69	83
30 - 60	9	0	0	29	15	15
60 - 90	2	0	0	0	5	2

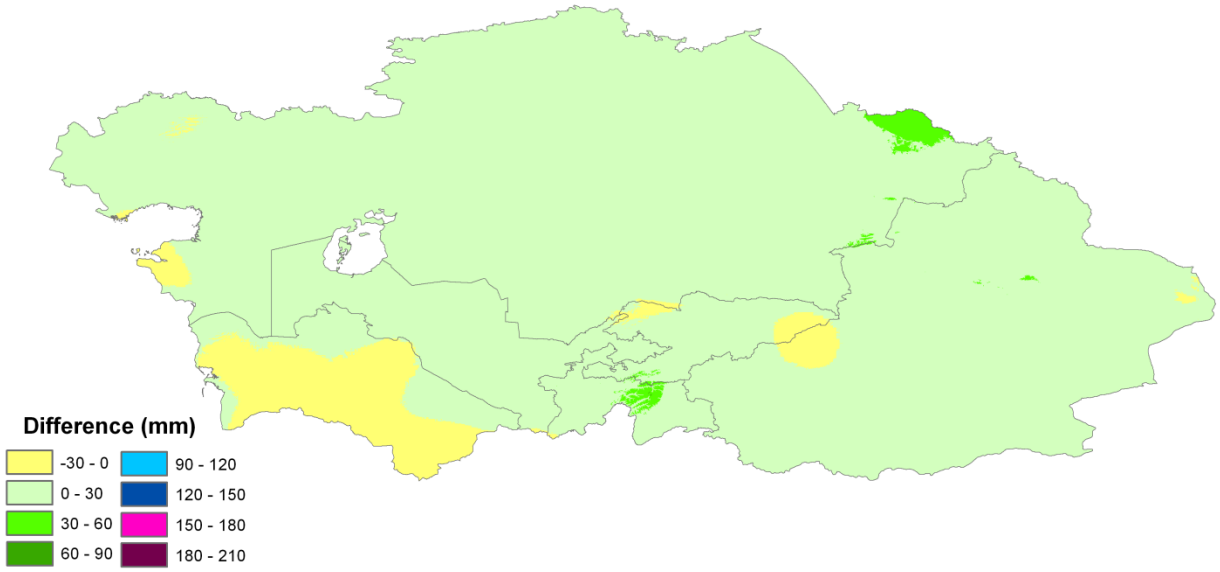

Figure 7. Projections of absolute changes in annual precipitation 2010-2040 scenario A1b compared to 1960-1990

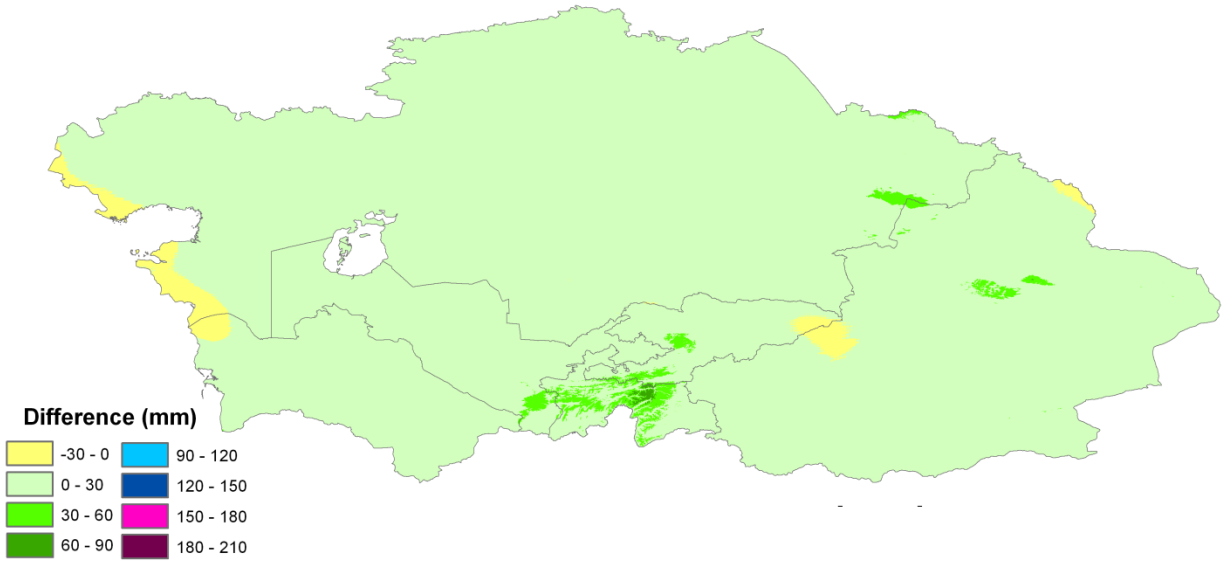

Figure 8. Projections of absolute changes in annual precipitation 2010-2040 scenario A2 compared to 1960-1990

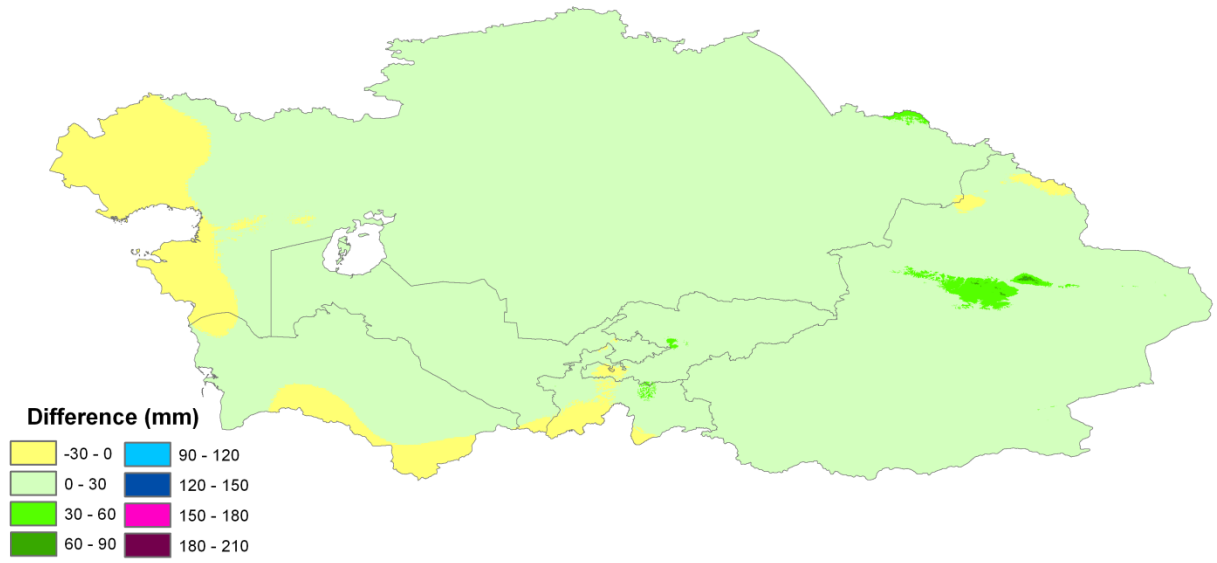

Figure 9. Projections of absolute changes in annual precipitation 2040-2070 scenario A1b compared to 1960-1990

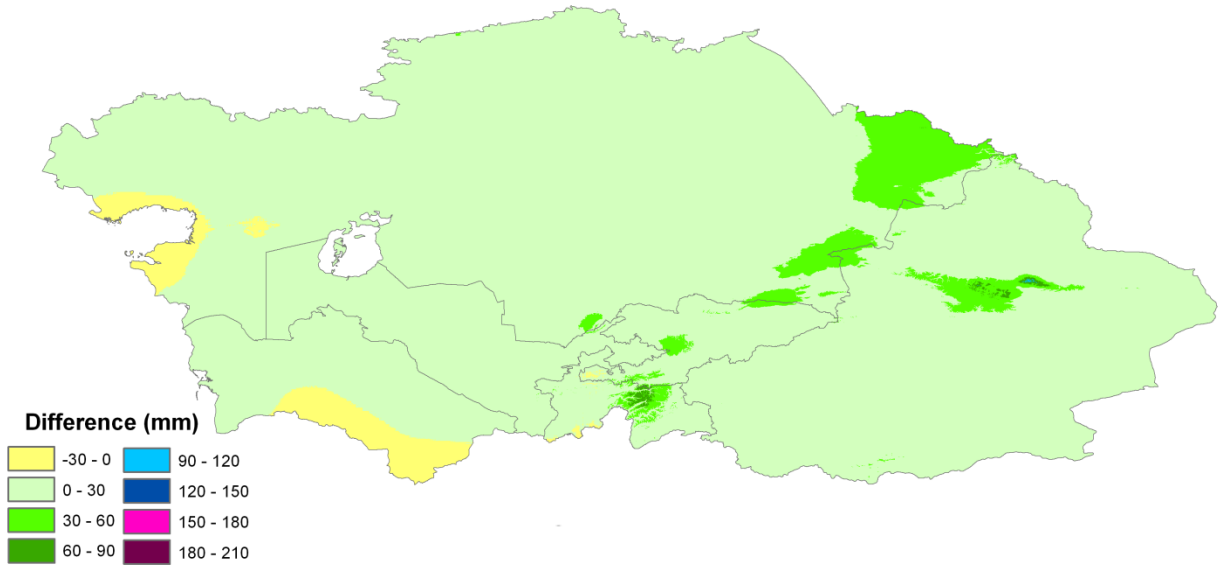

Figure 10. Projections of absolute changes in annual precipitation 2040-2070 scenario A2 compared to 1960-1990

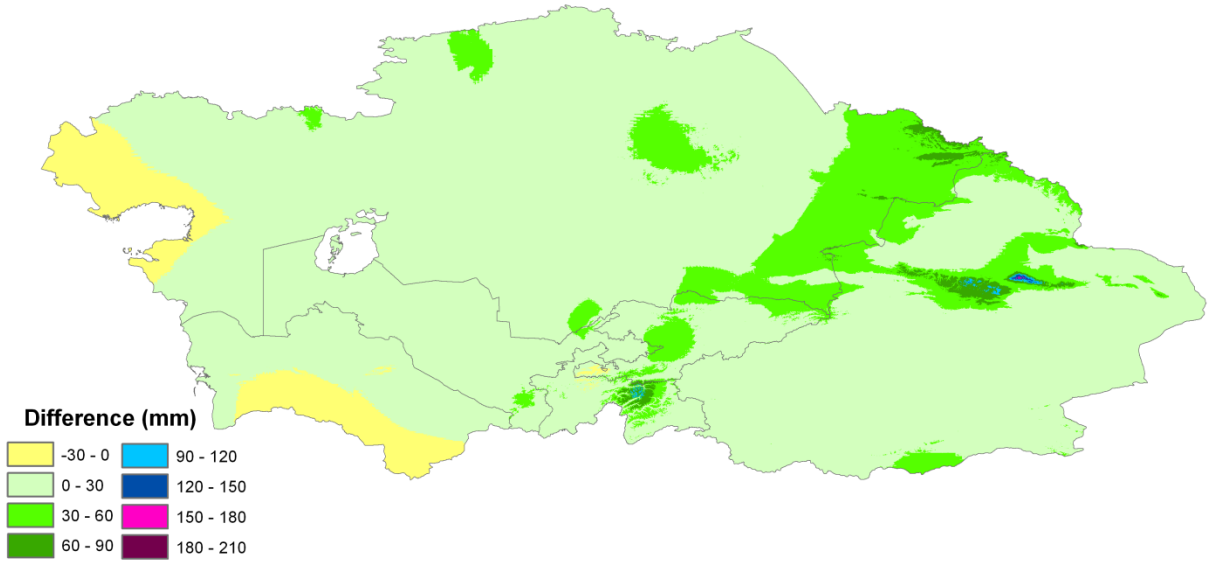

Figure 11. Projections of absolute changes in annual precipitation 2070-2100 scenario A1b compared to 1960-1990

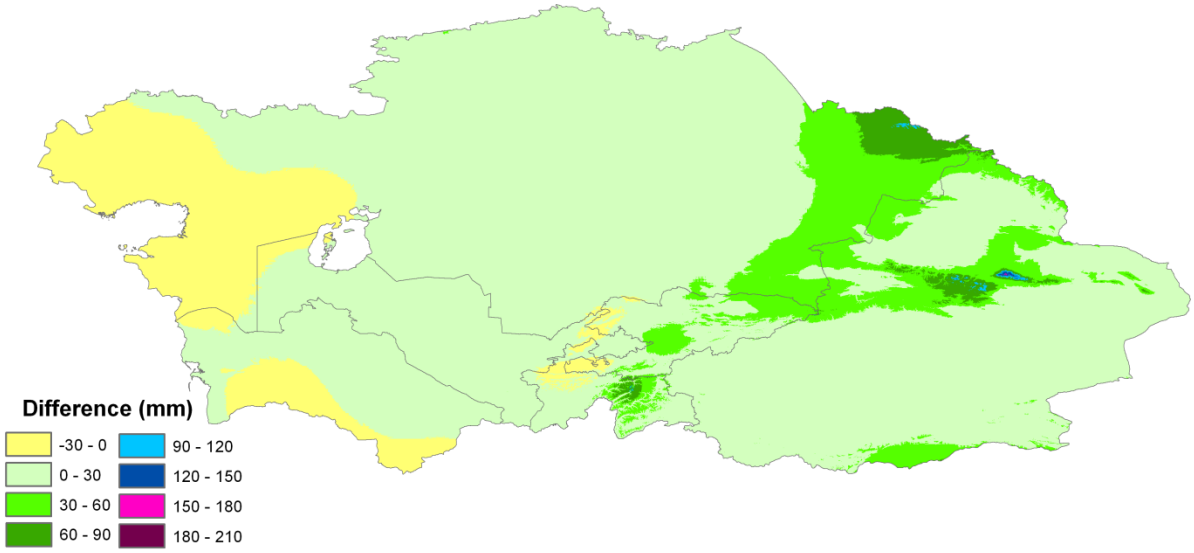

Figure 12. Projections of absolute changes in annual precipitation 2070-2100 scenario A2 compared to 1960-1990

3.2. Mapping changes in derived climate variables

3.2.1. Changes in aridity

The spatial changes in aridity are visualized for the three time horizons 2010-2040, 2040-2070 and 2070-2100 and the two selected emission scenarios A1b and A2 in Figures 13-18 and summarized in Tables 11-16. The indicator used for projecting changes is the percentage change in the annual aridity index (also called aridity index points).

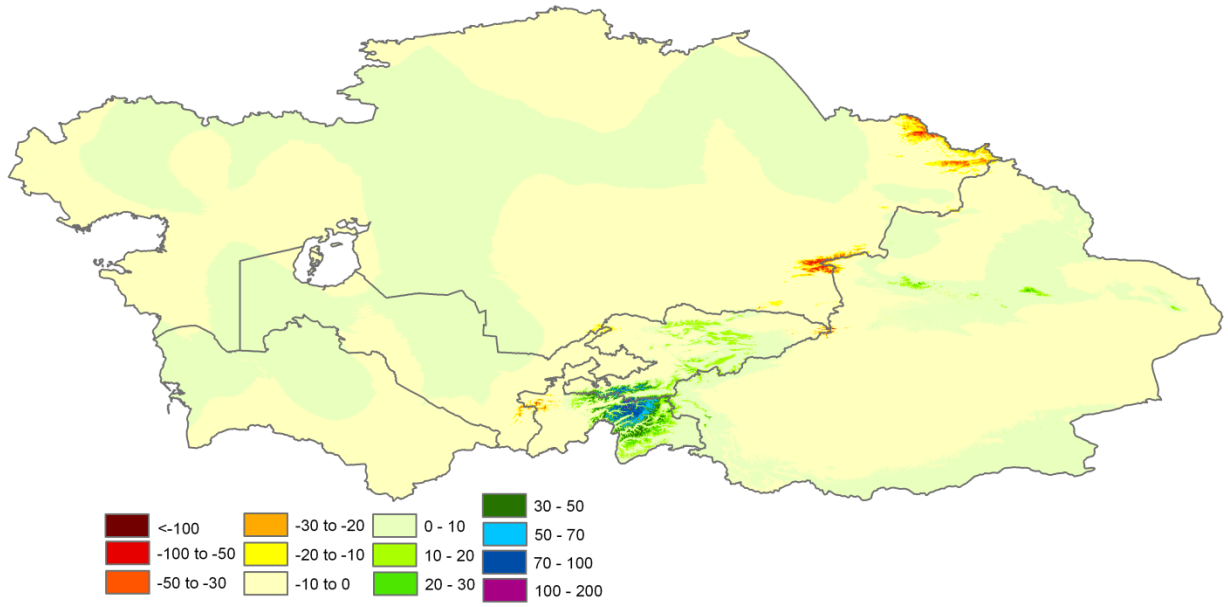

Figure 13. Projections of changes in aridity index points for the period 2010-2040 scenario A1b compared to 1960-1990

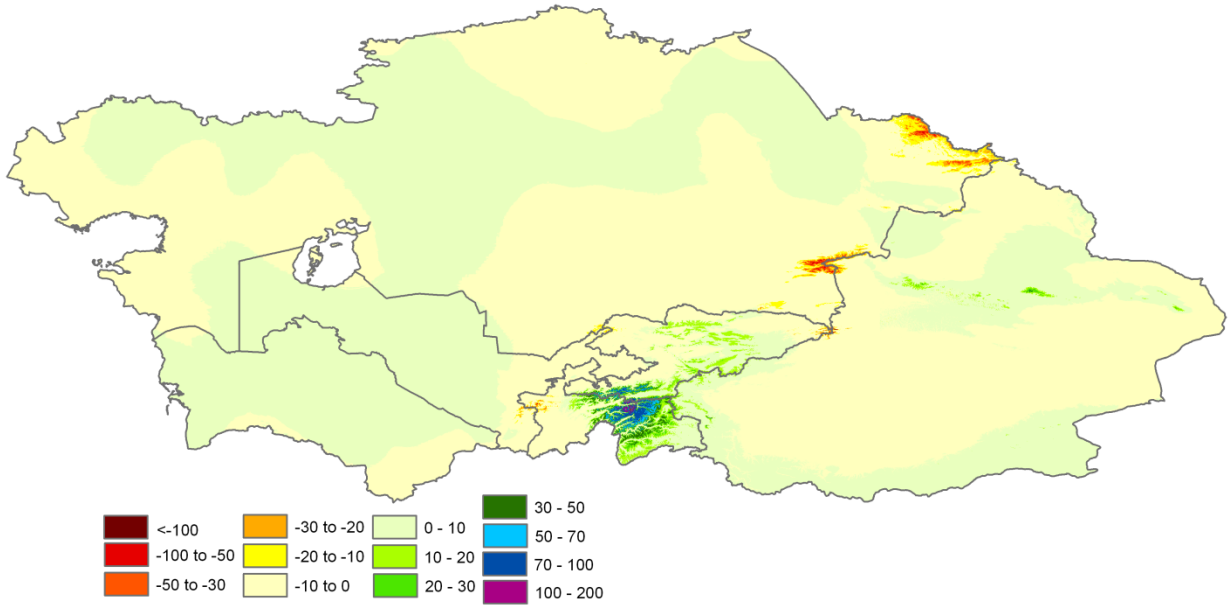

Figure 14. Projections of changes in aridity index points for the period 2010-2040 scenario A2 compared to 1960-1990

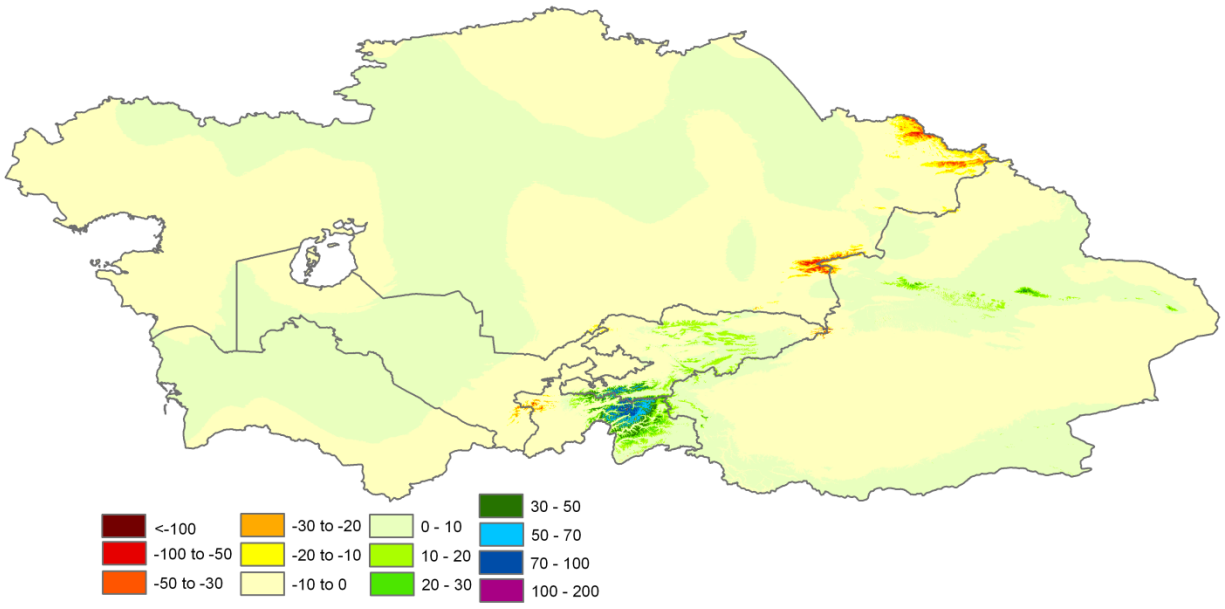

Figure 15. Projections of changes in aridity index points for the period 2040-2070 scenario A1b compared to 1960-1990

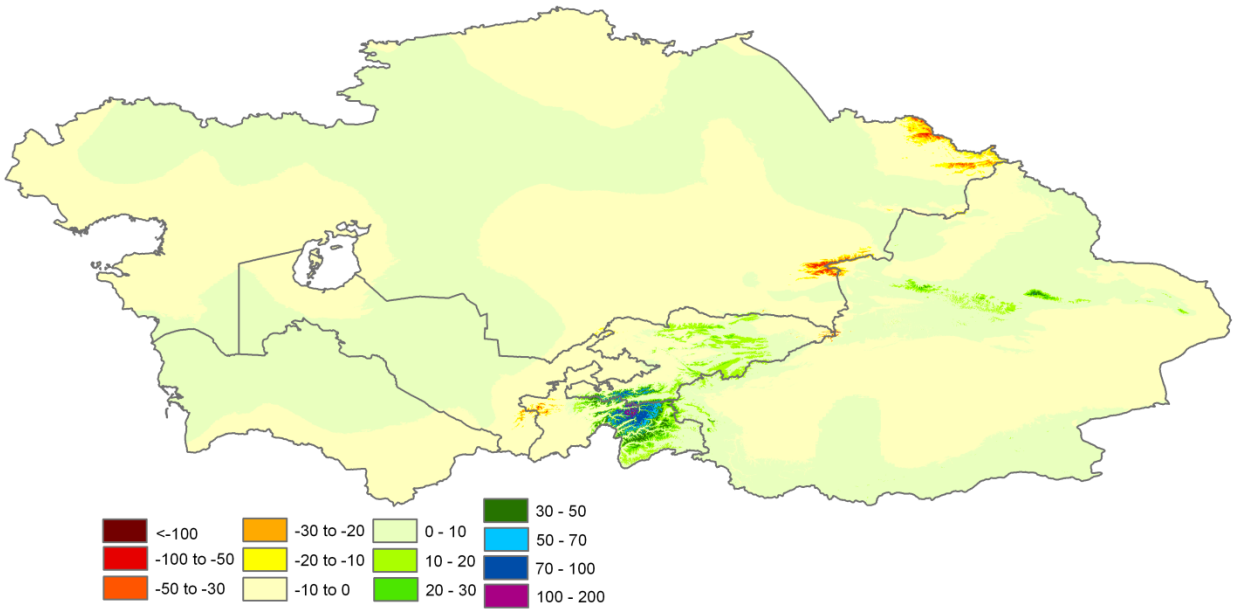

Figure 16. Projections of changes in aridity index points for the period 2040-2070 scenario A2 compared to 1960-1990

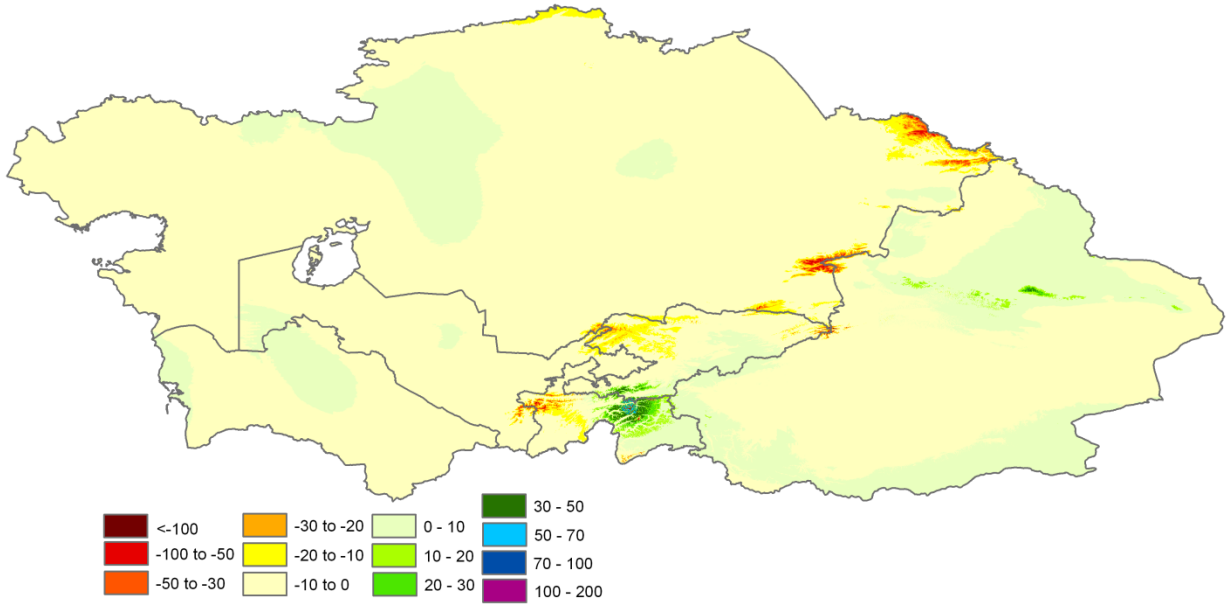

Figure 17. Projections of changes in aridity index points for the period 2070-2100 scenario A1b compared to 1960-1990

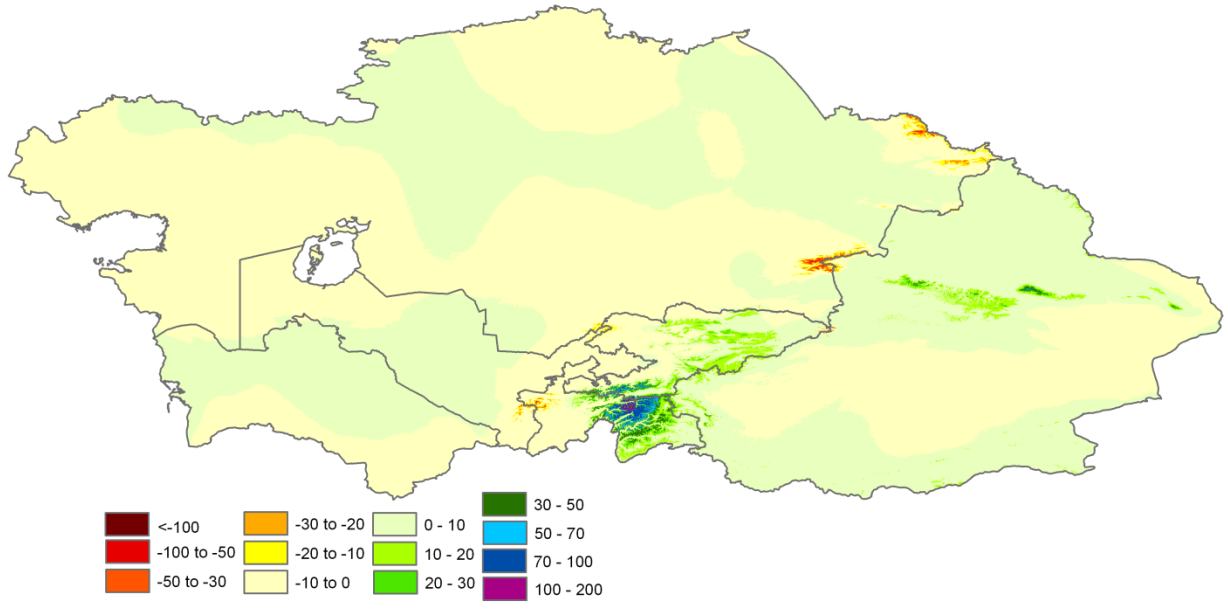

Figure 18. Projections of changes in aridity index points for the period 2070-2100 scenario A2 compared to 1960-1990

Up to 2040-2070 no clear trend can be discerned, as the projections indicate for about half of the region a slight increase in aridity (0-10 points) and roughly another half a slight decrease (0-10 points). As tables 11-16 indicate, there are of course greater disparities within individual countries. Particularly noticeable in this respect is a very pronounced decrease of aridity in the Pamir Mountains of Tajikistan and parts of Kyrgyzstan, which aligns very well with the projected precipitation increases in these high mountain areas.
During the period 2070-2100 a large increase is projected in the area affected by a mild increase in aridity (0-10 points), particularly in Kazakhstan, Uzbekistan, and Turkmenistan.
As in the case of precipitation change, little difference is observed in the projection results between the A1b and A2 scenarios, except for the period 2070-2100 where the A2 scenario results in a *more pronounced decrease of aridity* than A1b.

3.2.2. Changes in growing periods

The spatial changes in the growing periods are visualized for the three time horizons 2010-2040, 2040-2070 and 2070-2100 and the two selected emission scenarios A1b and A2 in Figures 19-36 and are summarized in Tables 17-34 of Annex 3. Three indicators are used for projecting changes:

- the total moisture-limited growing period
- the total temperature-limited growing period
- the total moisture- and temperature-limited growing period

These indicators refer to the cumulated periods in which respectively moisture, temperature or both are assumed to be non-limiting to plants, in accordance with the model explained in section 2.3.2.3.

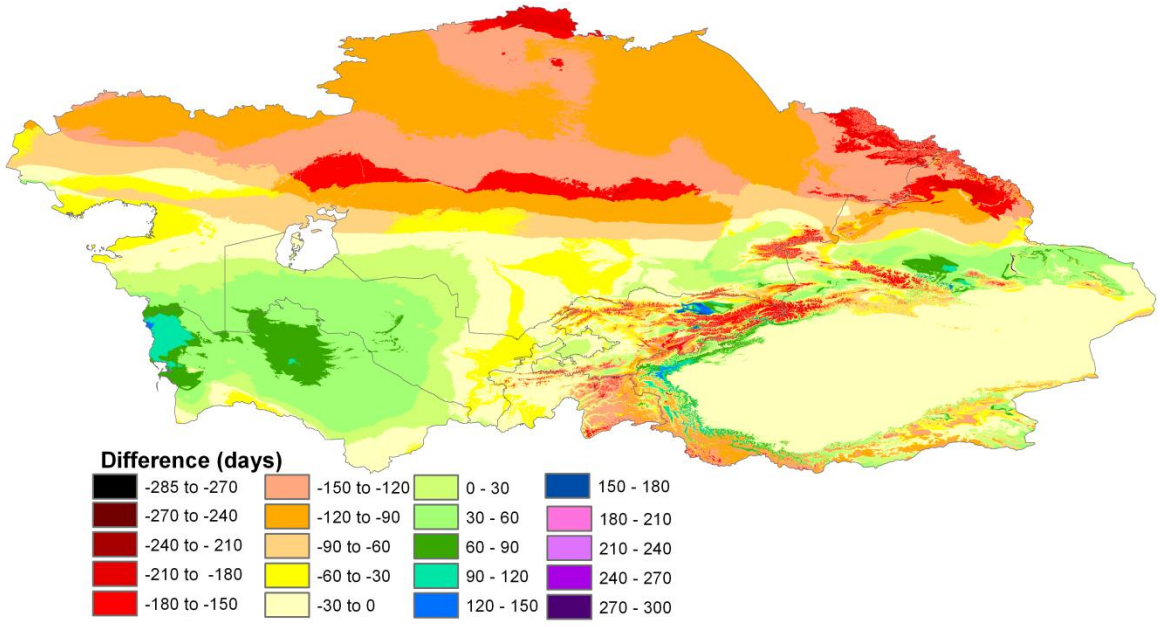

Figure 19. Projections of changes in the total moisture-limited growing period for the period 2010-2040 scenario A1b compared to 1960-1990

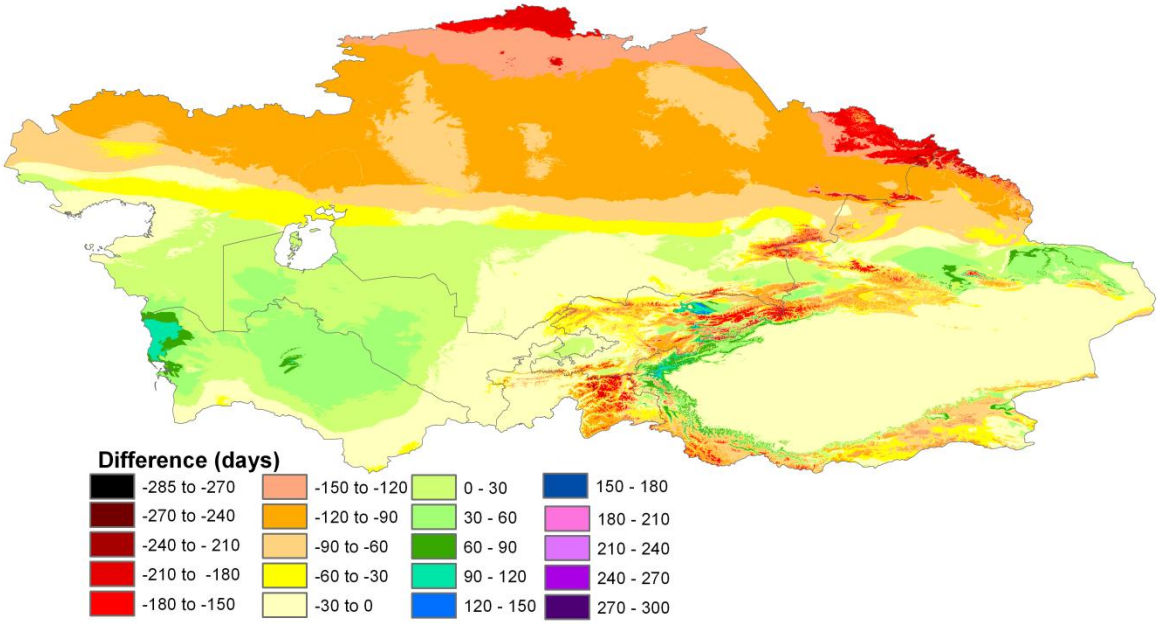

Figure 20. Projections of changes in the total moisture-limited growing period for the period 2010-2040 scenario A2 compared to 1960-1990

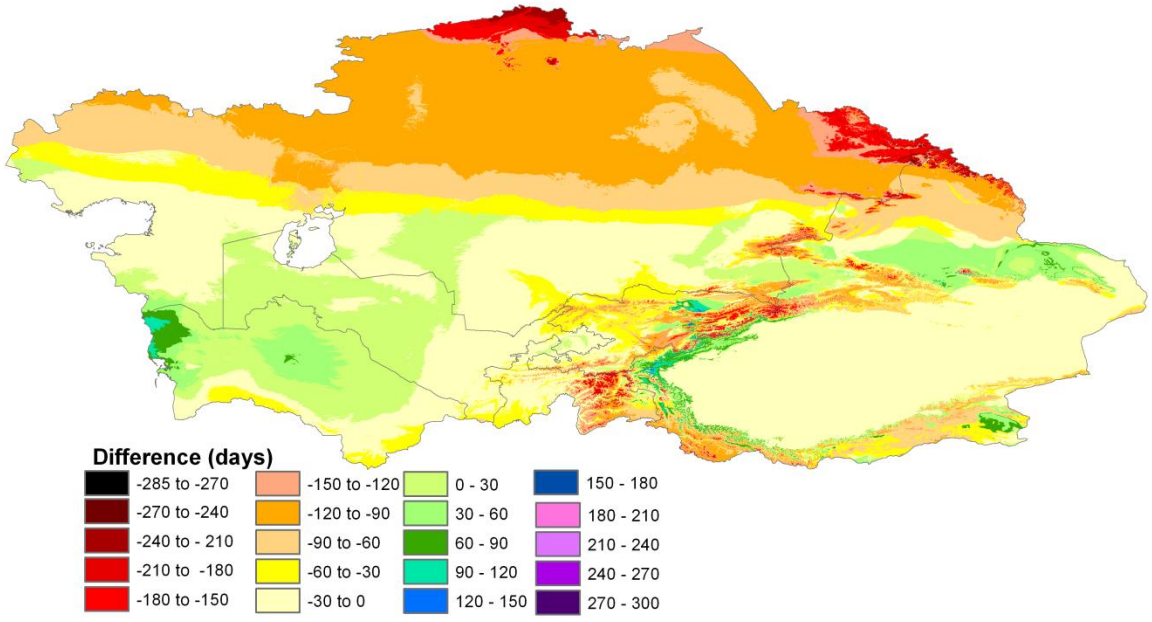

Figure 21. Projections of changes in the total moisture-limited growing period for the period 2040-2070 scenario A1b compared to 1960-1990

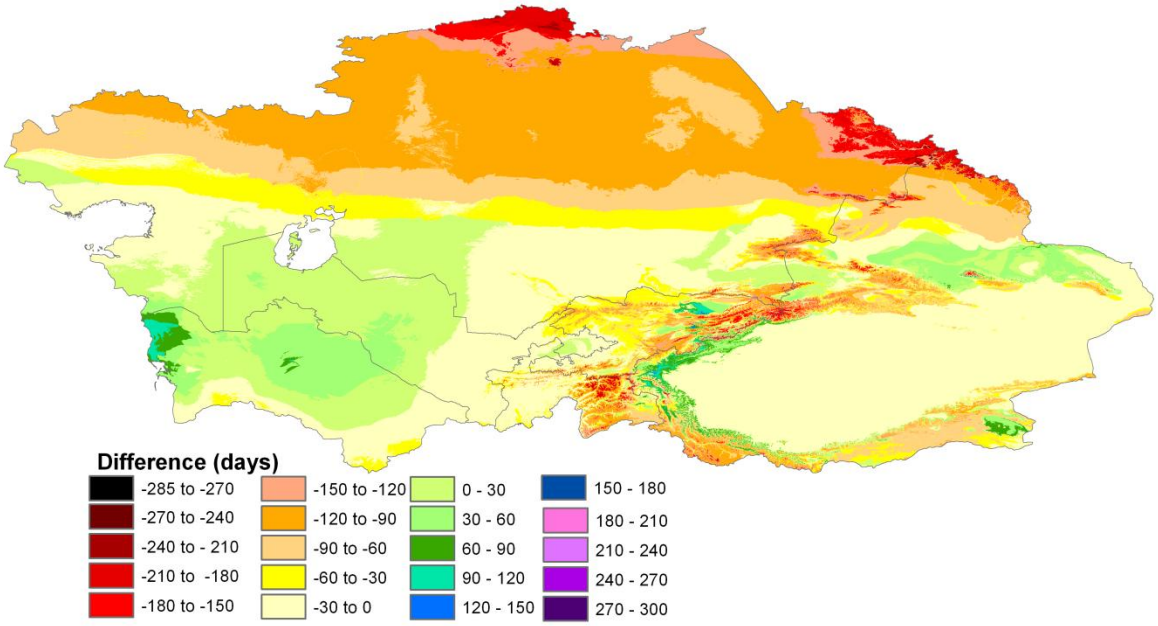

Figure 22. Projections of changes in the total moisture-limited growing period for the period 2040-2070 scenario A2 compared to 1960-1990

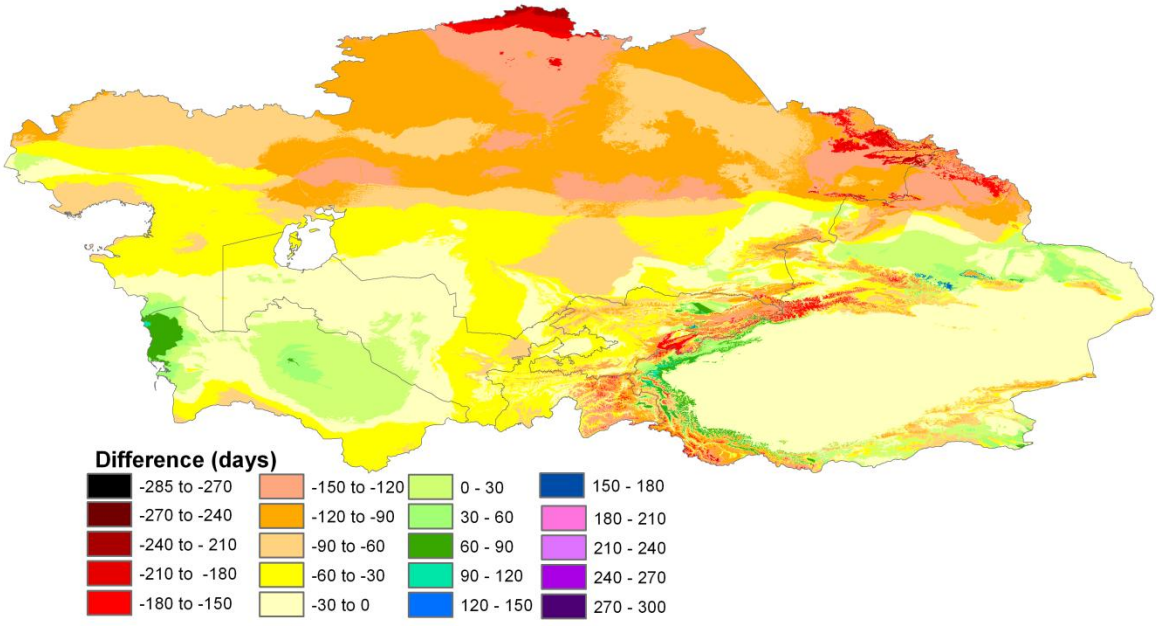

Figure 23. Projections of changes in the total moisture-limited growing period for the period 2070-2100 scenario A1b compared to 1960-1990

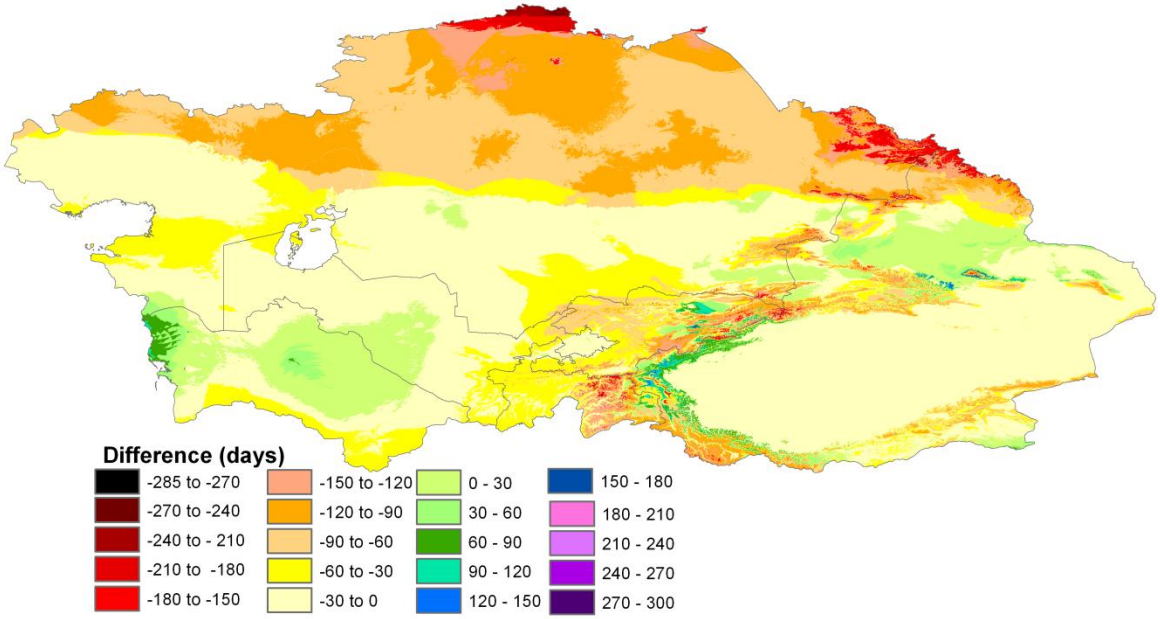

Figure 24. Projections of changes in the total moisture-limited growing period for the period 2070-2100 scenario A1b compared to 1960-1990

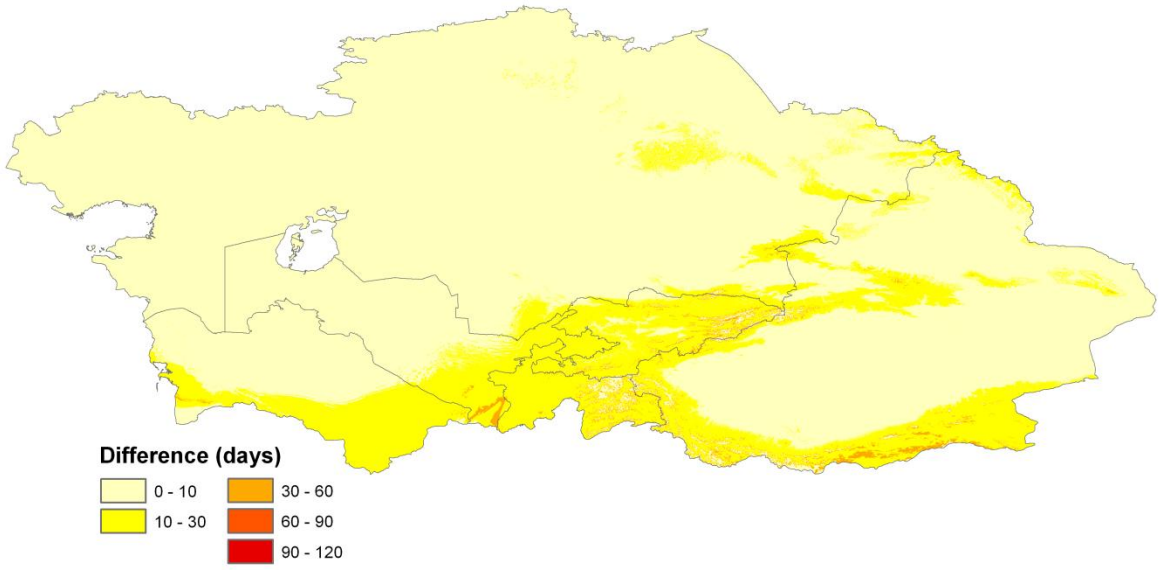

Figure 25. Projections of changes in the total temperature-limited growing period for the period 2010-2040 scenario A1b compared to 1960-1990

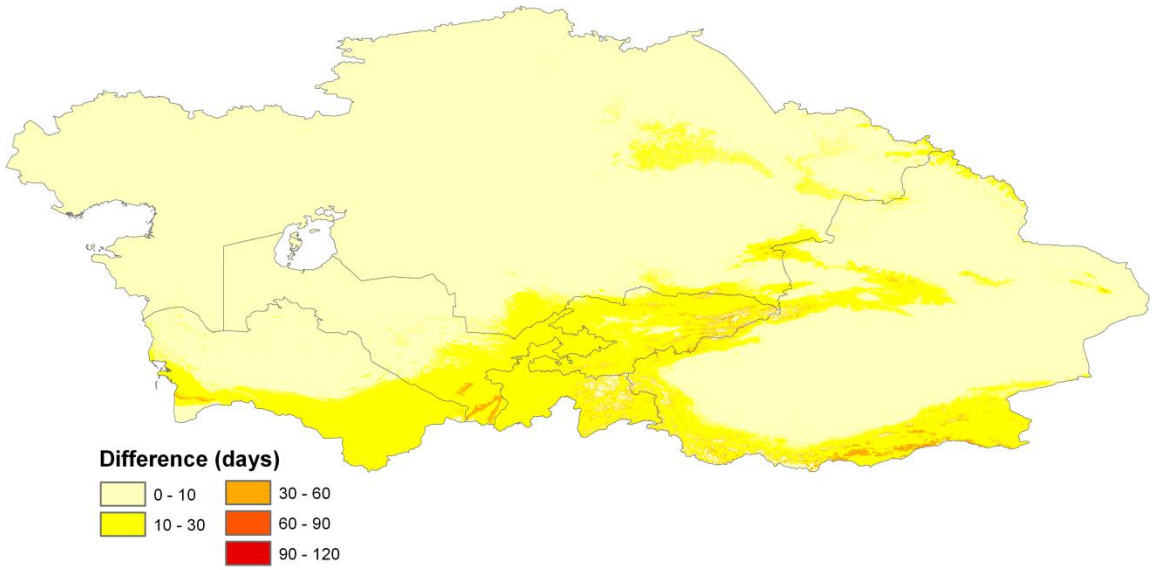

Figure 26. Projections of changes in the total temperature-limited growing period for the period 2010-2040 scenario A2 compared to 1960-1990

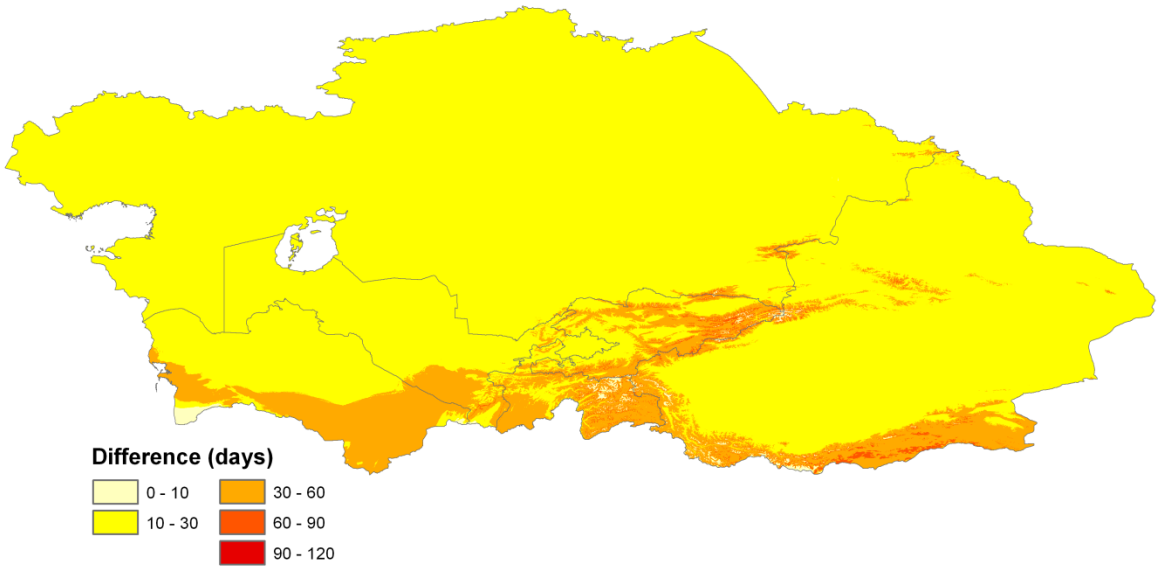

Figure 27. Projections of changes in the total temperature-limited growing period for the period 2040-2070 scenario A1b compared to 1960-1990

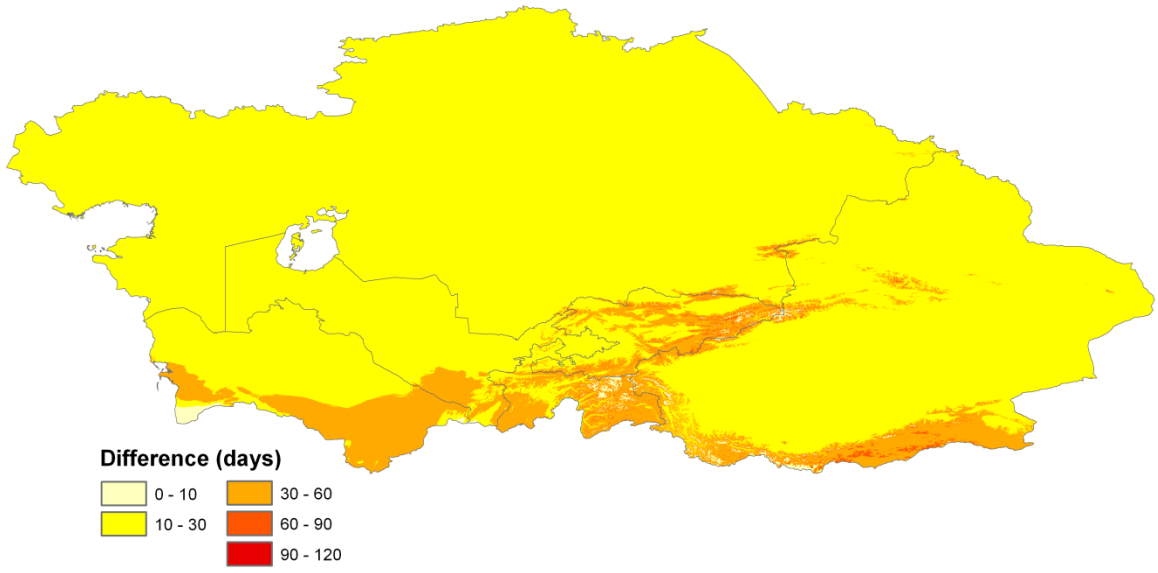

Figure 28. Projections of changes in the total temperature-limited growing period for the period 2040-2070 scenario A2 compared to 1960-1990

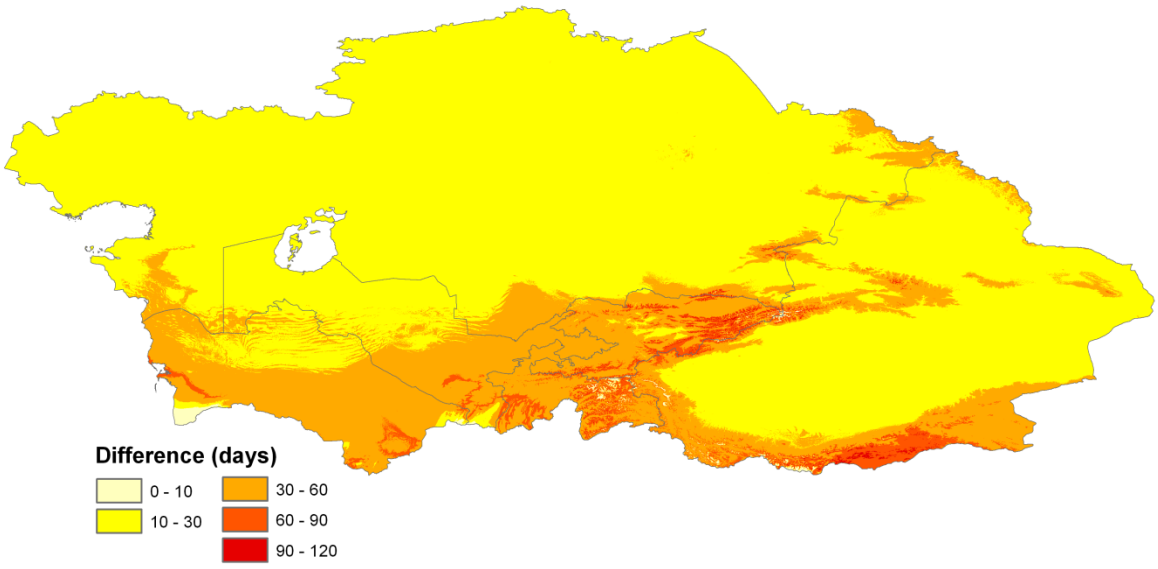

Figure 29. Projections of changes in the total temperature-limited growing period for the period 2070-2100 scenario A1b compared to 1960-1990

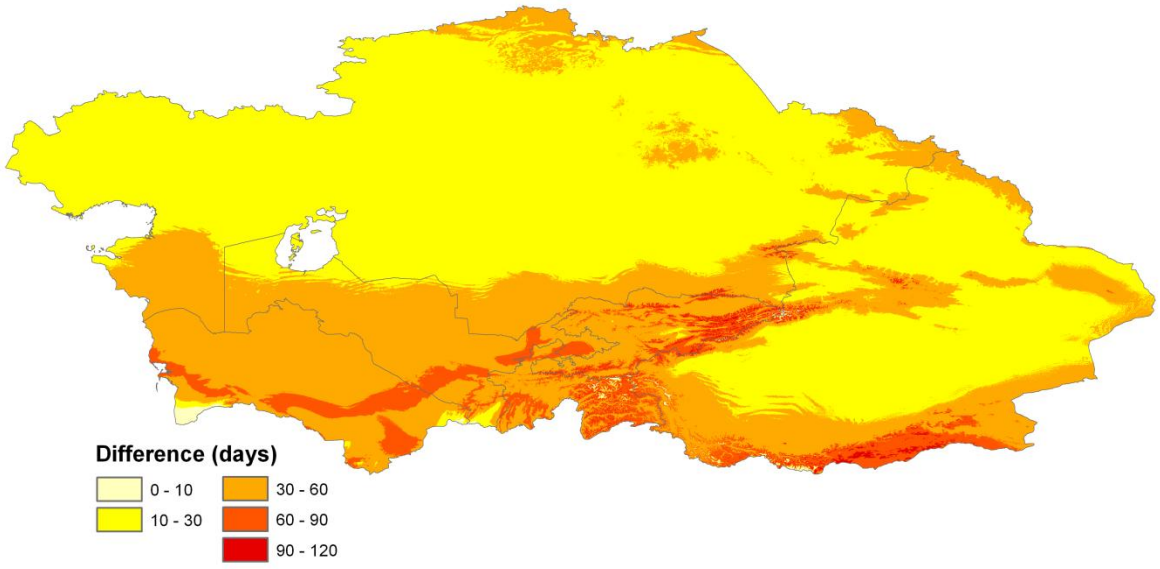

Figure 30. Projections of changes in the total temperature-limited growing period for the period 2070-2100 scenario A2 compared to 1960-1990

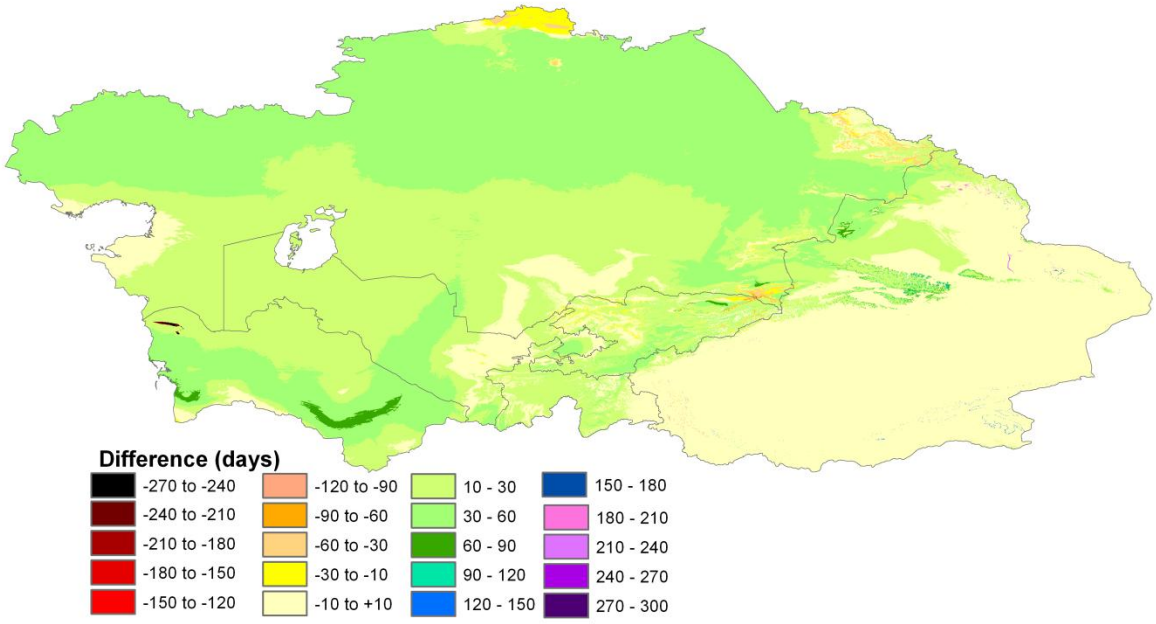

Figure 31. Projections of changes in the total moisture- and temperature-limited growing period for the period 2010-2040 scenario A1b compared to 1960-1990

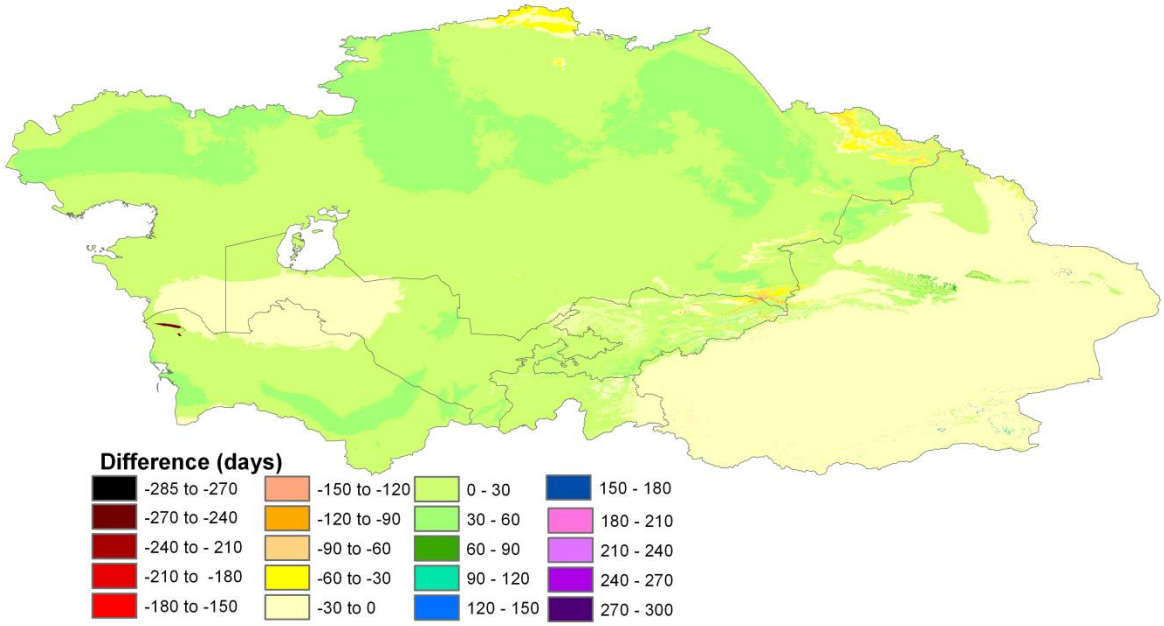

Figure 32. Projections of changes in the total moisture- and temperature-limited growing period for the period 2010-2040 scenario A2 compared to 1960-1990

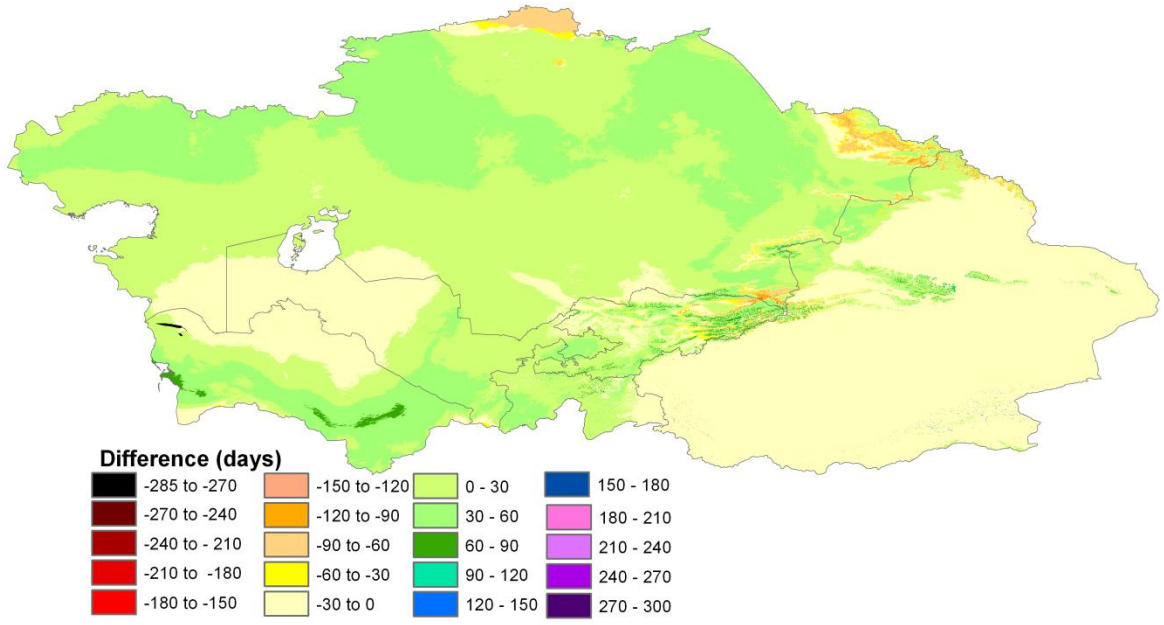

Figure 33. Projections of changes in the total moisture- and temperature-limited growing period for the period 2040-2070 scenario A1b compared to 1960-1990

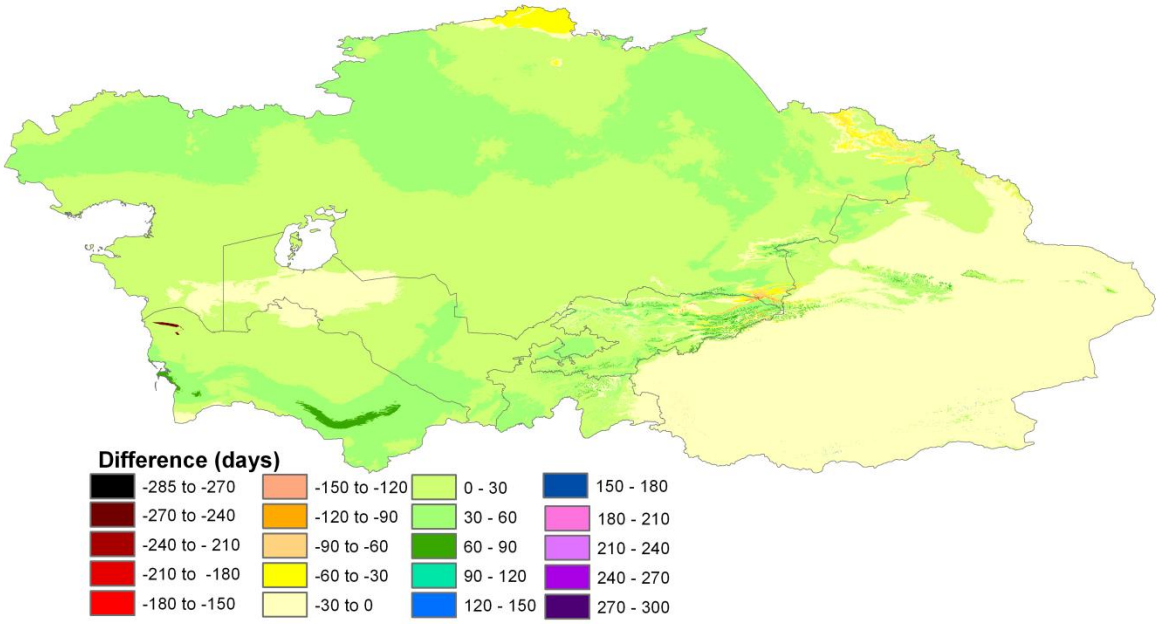

Figure 34. Projections of changes in the total moisture- and temperature-limited growing period for the period 2040-2070 scenario A2 compared to 1960-1990

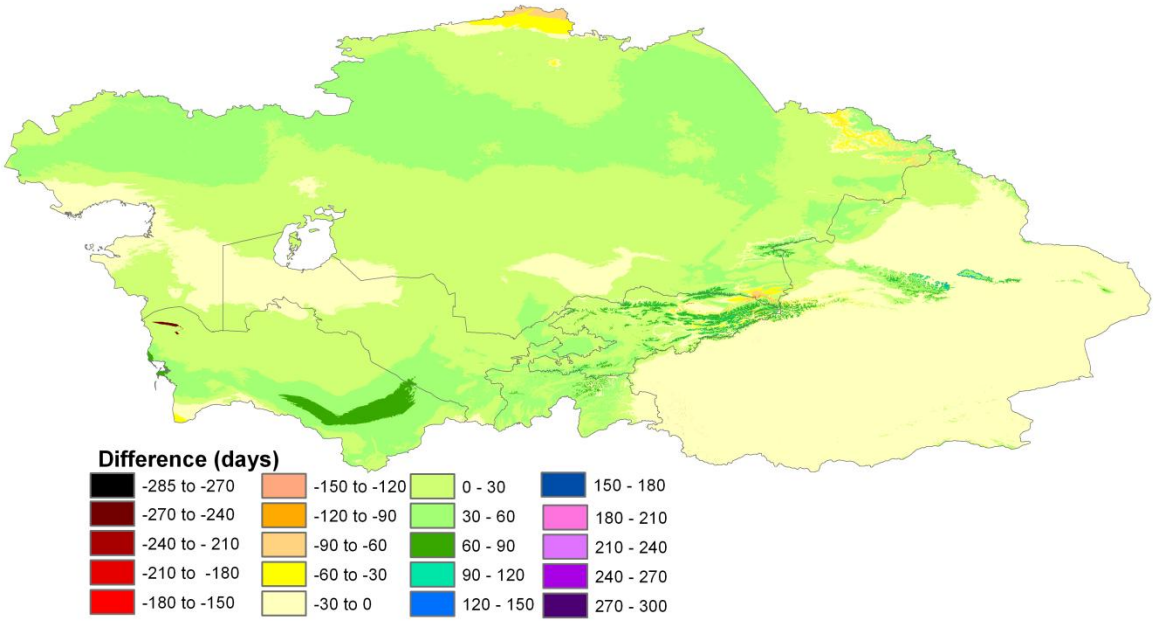

Figure 35. Projections of changes in the total moisture- and temperature-limited growing period for the period 2070-2100 scenario A1b compared to 1960-1990

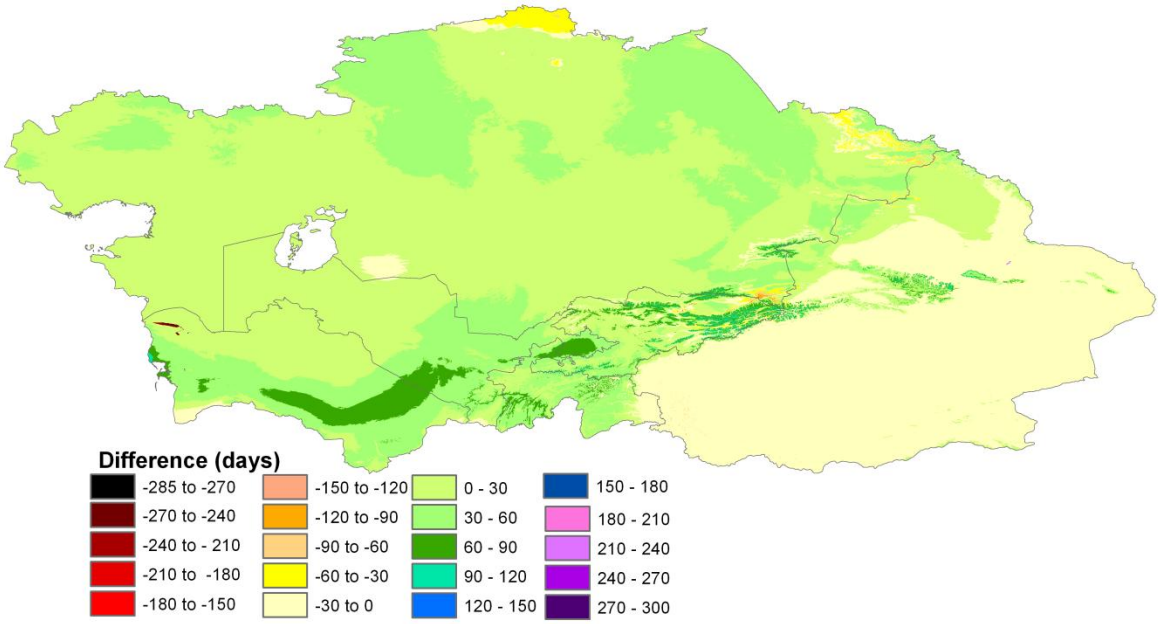

Figure 36. Projections of changes in the total moisture- and temperature-limited growing period for the period 2070-2100 scenario A2 compared to 1960-1990

Usually the total moisture-limited growing period is composed of two separate periods throughout the year when water availability does not constrain the productivity of adapted crops, and the temperature-limited growing period of a single period. As the moisture- and temperature-limited growing periods may not necessarily overlap, conditions may exist in which either one of the two are adequate for crop productivity, but not necessarily both. Therefore the total moisture- and temperature-limited growing period may consist of several sub-periods.

In the period 2010-2040 the projections indicate large increases in the areas with *increasing* moisture-limited growing period in Uzbekistan and Turkmenistan, and that in Kazakhstan, Kyrgyzstan and Tajikistan large increases are expected in the areas with *decreasing* moisture-limited growing periods. During this period the effects of global warming on the temperature-limited growing period are not very noticeable in the lowlands, but they are already having an impact in the mountain areas of all regions. In the mountain areas the decline in the growing period is attributed to larger areas with increased potential evapo-transpiration due to the rising temperature. However, the combined effect of changes in the moisture- and temperature-limited growing period appears already in the period 2010-2040 a positive one, with an increase in the total growing period in all regions, except in Xingjiang, which remains mostly stable.

During the periods 2040-2070 and 2070-2100 these trends develop further. Virtually the entire region experiences an increase in the temperature-limited growing period from 2040-2070. The moisture-limited growing period declines further in the mountain countries. Ultimately, in most of the region the moisture-and temperature-limited growing period is projected to increase significantly by 2070-2100 compared to the current climate.

3.2.3. Changes in climatic zones

The spatial changes in the climatic zones are visualized for the three time horizons 2010-2040, 2040-2070 and 2070-2100 and the two selected emission scenarios A1b and A2 in Figures 37-42 and are summarized in Tables 35-40 of Annex 3.

The projections based on the multi-model ensemble anticipate over the next 100 years a gradual increase in the area that changes from one to Köppen climatic zone to another. As with the previous climatic variables, little difference is noticed between the estimates based on the A1b or A2 emission scenarios.
Up to 2010-2040 the climatic zones are projected to remain more or less stable. The changes in temperature and moisture are not large enough to cause a geographical shift in the climatic zones. This picture changes during 2040-2070 in Kyrgyzstan where a significant area is projected to change towards a wetter climate and less seasonally concentrated precipitation. In the period 2070-2100 the trend towards a wetter climate in Kyrgyzstan is projected to extend over a somewhat larger area. By that time 20% of Kazakhstan is projected to evolve into a drier climate type with precipitation more concentrated in winter.

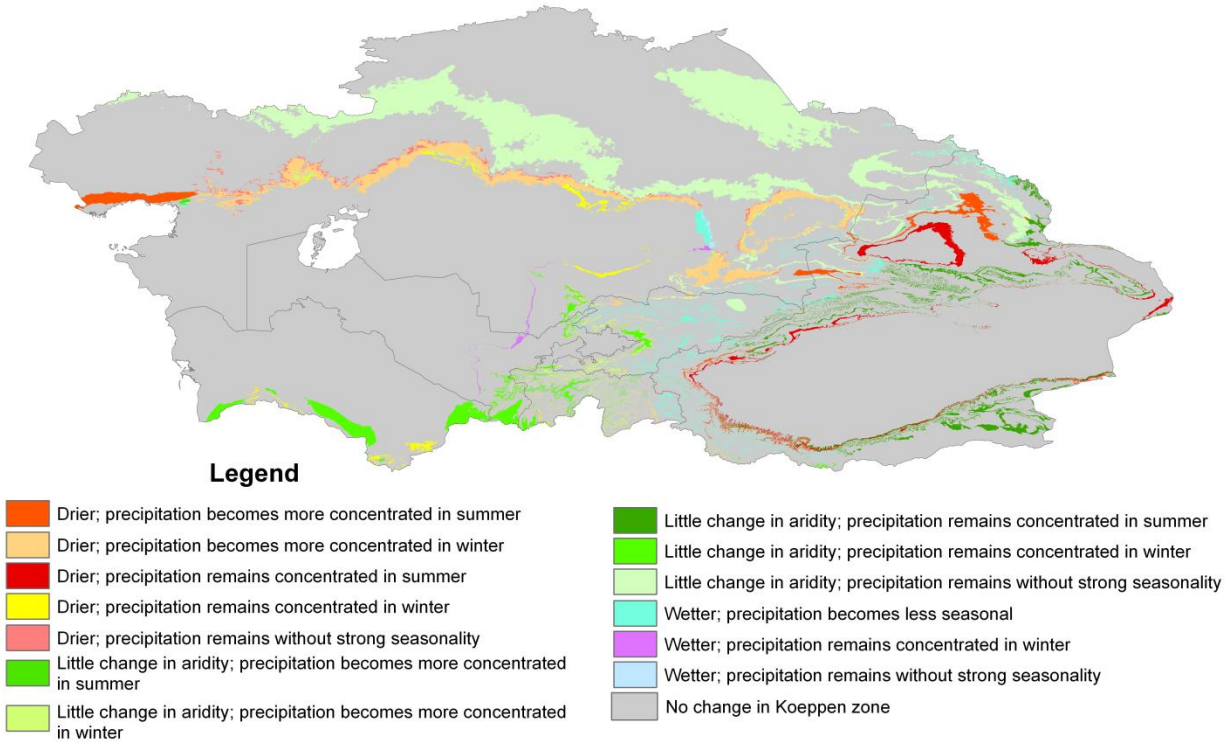

Figure 37. Projections of changes in the Köppen climatic zones for the period 2010-2040 scenario A1b compared to 1960-1990

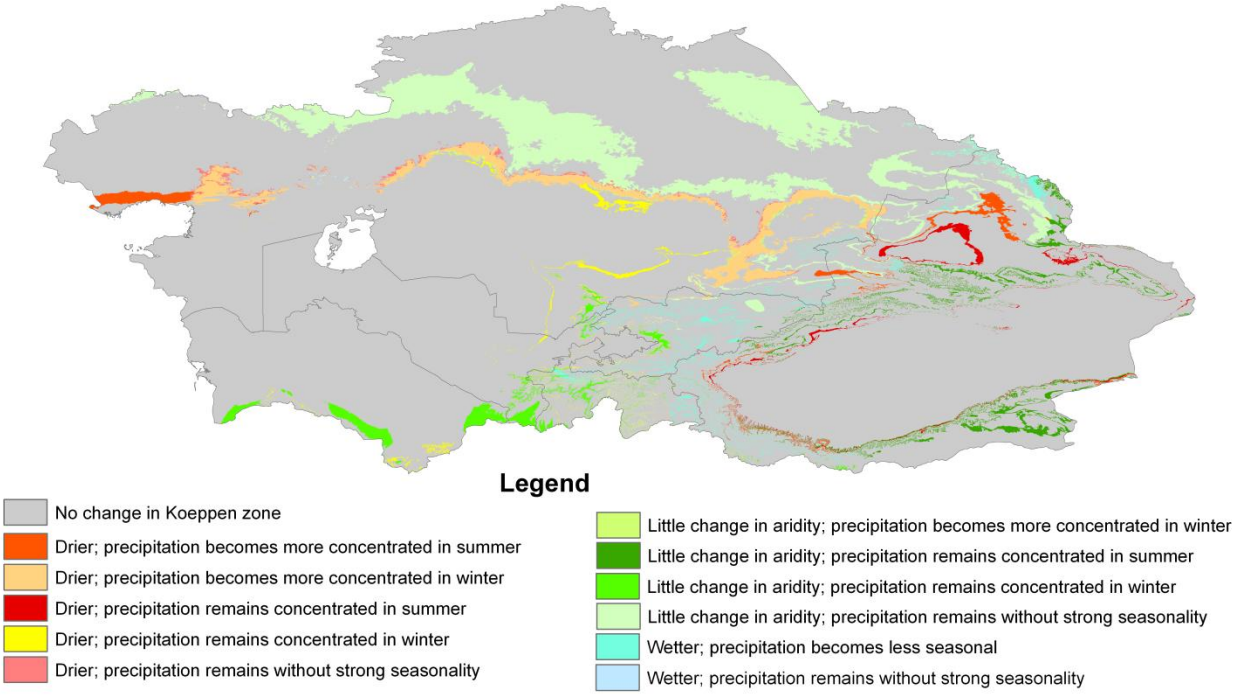

Figure 38. Projections of changes in the Köppen climatic zones for the period 2010-2040 scenario A2 compared to 1960-1990

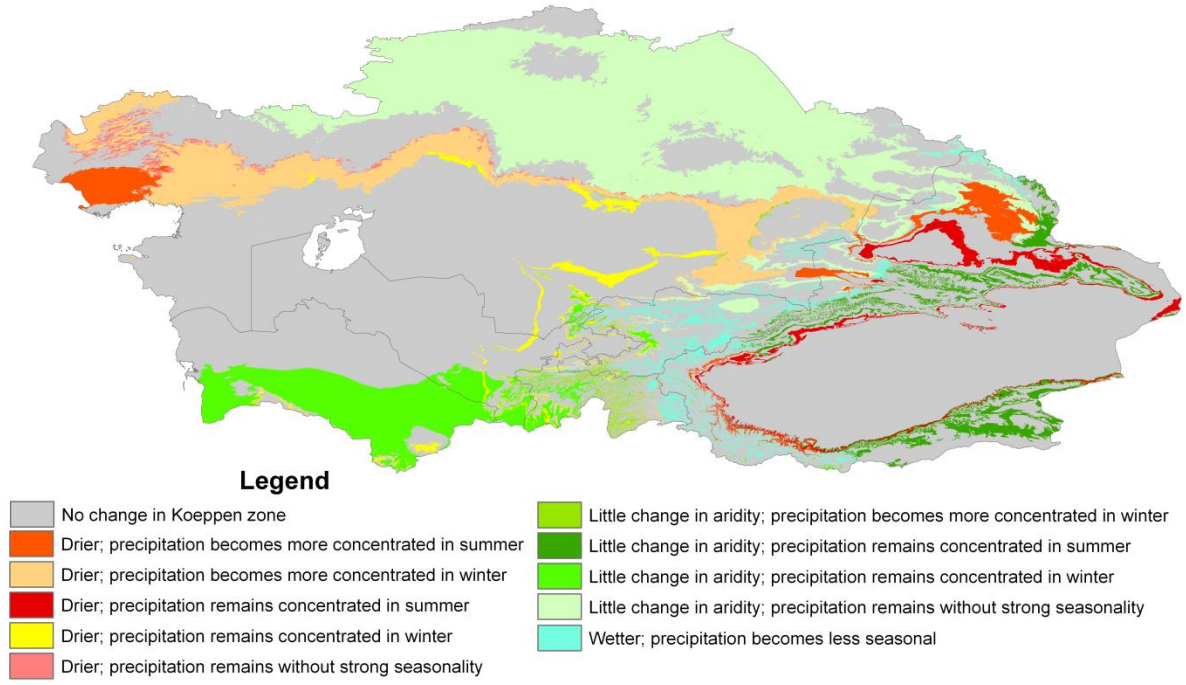

Figure 39. Projections of changes in the Köppen climatic zones for the period 2040-2070 scenario A1b compared to 1960-1990

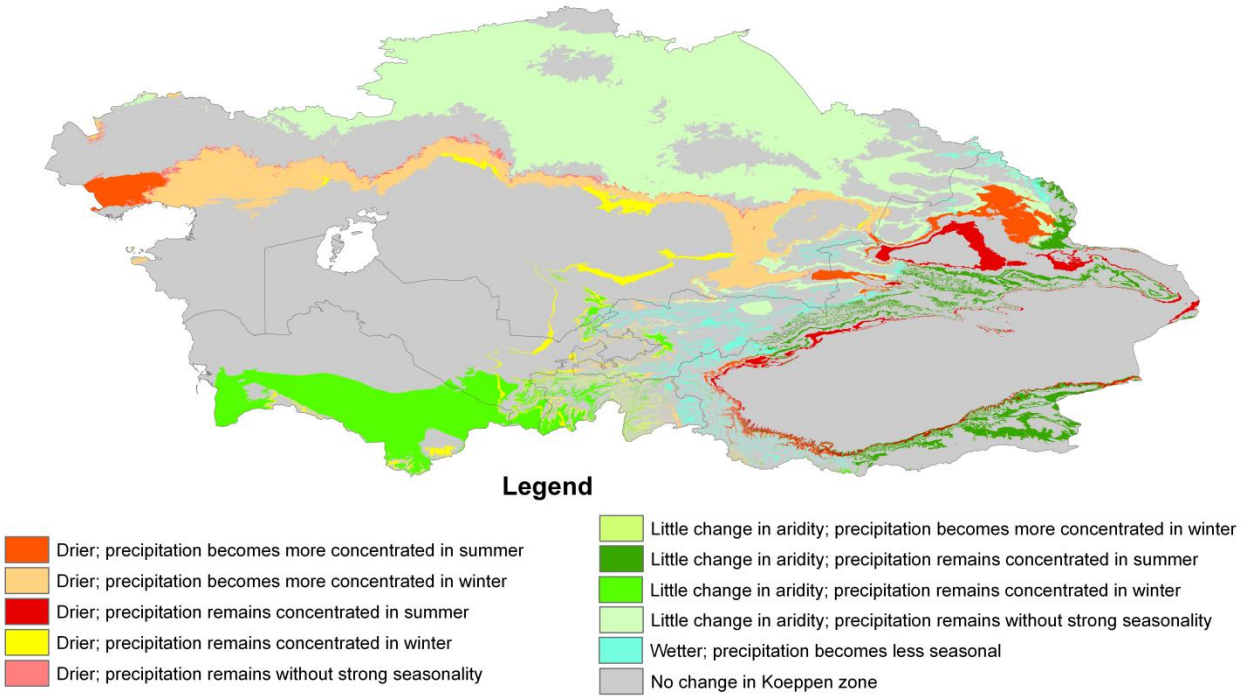

Figure 40. Projections of changes in the Köppen climatic zones for the period 2040-2070 scenario A2 compared to 1960-1990

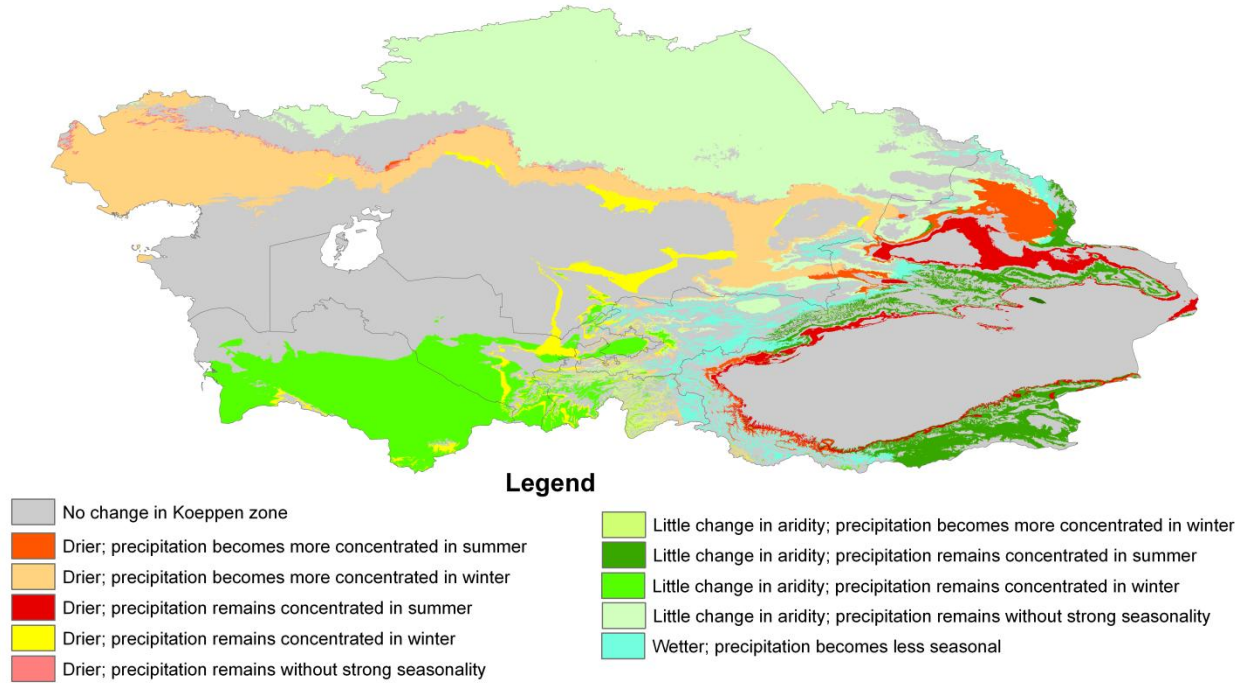

Figure 41. Projections of changes in the Köppen climatic zones for the period 2070-2100 scenario A1b compared to 1960-1990

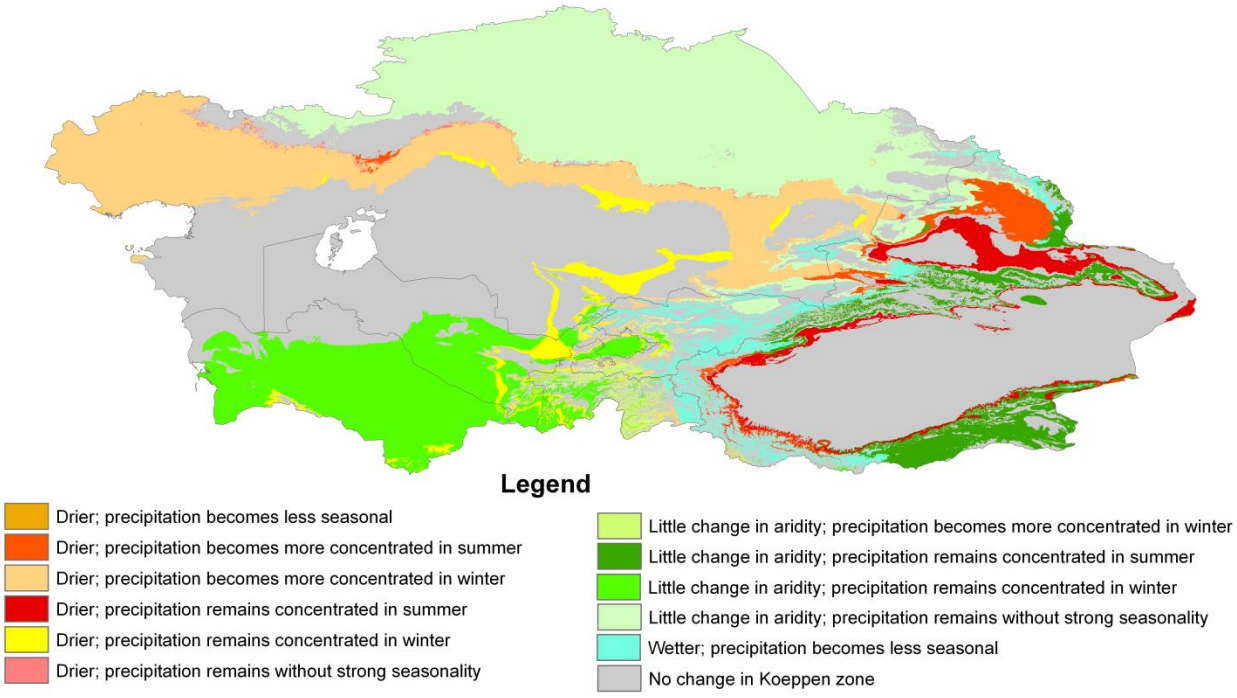

Figure 42. Projections of changes in the Köppen climatic zones for the period 2070-2100 scenario A2 compared to 1960-1990

3.3. Mapping drought and precipitation variability

The annual Standardized Precipitation Index maps for the period 1901-2007 are available on CD. Samples for some agricultural years are included as Annex 4. The full summary of the annual composition of SPI classes for each country and year is given in Annex 8.

The SPI analysis results for the period 1901-2007 indicates that in most years a strong tendency exists towards near-normal conditions. Droughts covering the entire region are rare. However, the region is so huge and varied in precipitation patterns that in most years in different parts of the region conditions of normality, drought and above-normal precipitation can co-exist.

Simple linear regression models were fitted to the 107-year time series of annual precipitation of each 0.5x0.5 degree grid cell by the least-squares method. From these models, the following trend surfaces have been derived and mapped:

- average absolute change of annual precipitation in mm per year (Fig. 43a);
- average relative change of annual precipitation in % per decade (Fig. 43b)
- correlation between annual precipitation and time (Fig. 43c);
- t-significance level of the linear time trend of precipitation (two-sided t-test) (Fig.43d).

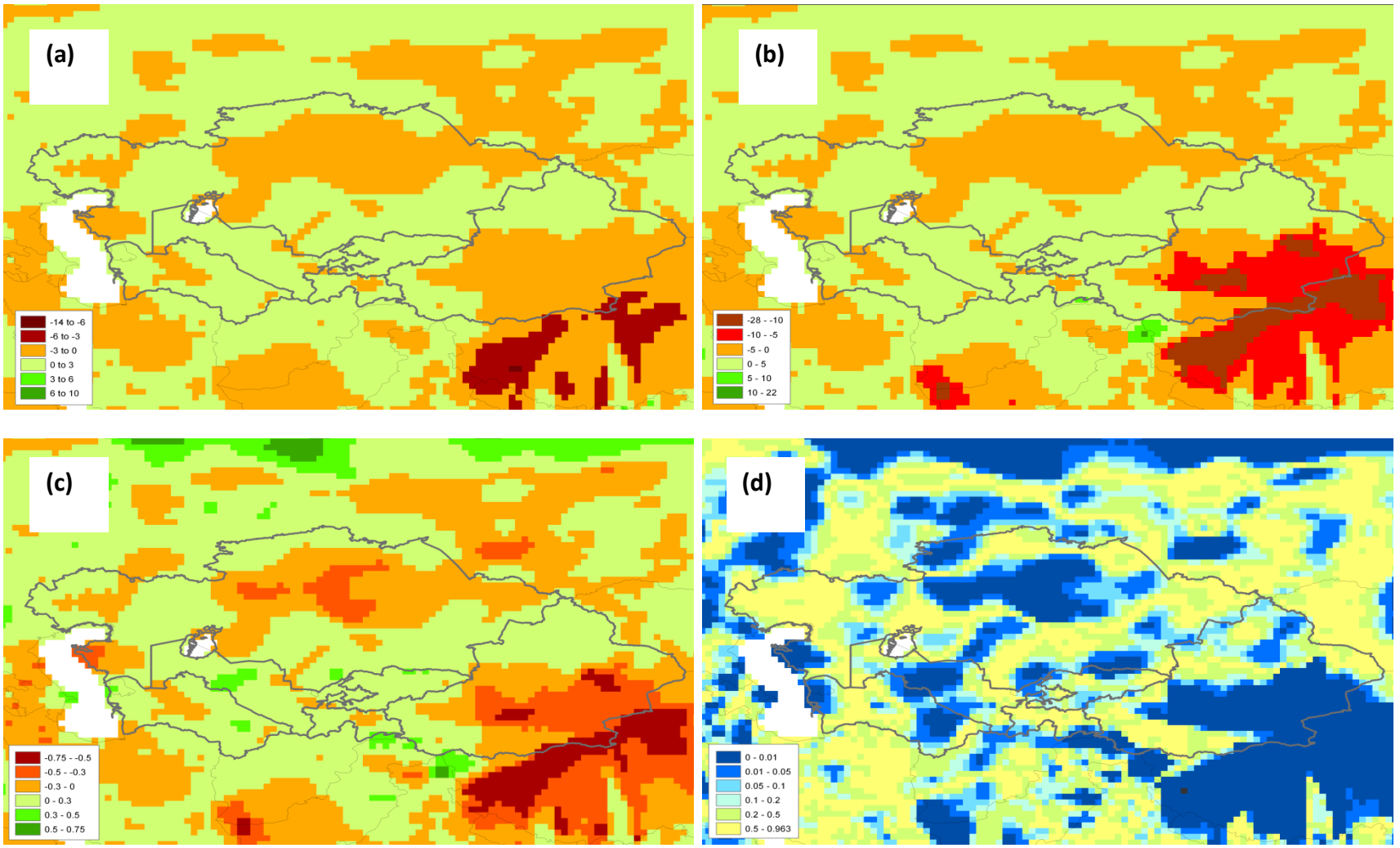

Figure 43. Annual precipitation trends 1901-2007 in and around the project area. (a) Absolute change of trend precipitation (in mm/year). (b) Relative change of trend precipitation (in % per 10 years). (c) Correlation coefficient of the trend precipitation. (d) Significance level of the trend (0-1). Data source: Schneider et al. 2008

These characteristics of the precipitation trends are also summarized on a country/region basis in Tables 7-10.

Table 7. Precipitation trend 1901-2007: absolute change in precipitation[13]

Change class (mm/year)	% in country/region					
	Kazakhstan	Uzbekistan	Turkmenist	Kyrgyzstan	Tajikistan	Xingjiang
-14 to -6	0	0	0	0	0	0
-6 to -3	0	0	0	0	0	1
-3 to 0	46	8	20	5	18	61
0 to 3	54	92	80	95	82	38
3 to 6	0	0	0	0	0	0
6 to 10	0	0	0	0	0	0

Table 8. Precipitation trend 1901-2007: relative change in precipitation

Change class (% /10 years)	% in country/region					
	Kazakhstan	Uzbekistan	Turkmenist	Kyrgyzstan	Tajikistan	Xingjiang
-28 - -10	0	0	0	0	0	8
-10 - -5	0	0	0	0	0	25
-5 - 0	46	8	20	5	18	28
0 - 5	54	92	80	95	82	38
5 - 10	0	0	0	0	0	0
10 - 22	0	0	0	0	0	0

Table 9. Precipitation trend 1901-2007: trend correlation coefficients

Correlation coeff.	% in country/region					
	Kazakhstan	Uzbekistan	Turkmenist	Kyrgyzstan	Tajikistan	Xingjiang
-0.75 - -0.5	0	0	0	0	0	7
-0.5 - -0.3	7	0	0	0	0	25
-0.3 - 0	39	8	20	5	18	30
0 - 0.3	53	83	77	94	80	38
0.3 - 0.5	0	9	3	1	2	0
0.5 - 0.75	0	0	0	0	0	0

[13] A magenta color fill indicates a particular class occupies at least 10% of the applicable geographical entity

Table 10. Precipitation trend 1901-2007: significance of the trend

Signifi-cance level	% in country/region					
	Kazakhstan	Uzbekistan	Turkmenist	Kyrgyzstan	Tajikistan	Xingjiang
0 - 0.01	16	15	15	8	4	38
0.01 - 0.05	15	22	20	8	13	9
0.05 - 0.1	10	11	9	14	14	7
0.1 - 0.2	9	13	10	25	7	10
0.2 - 0.5	20	23	21	26	16	19
0.5 - 0.97	30	16	25	19	46	17

In summary, the analysis of the GPCC precipitation dataset indicates that in the 20th century most of Central Asia experienced an increase in precipitation. The main exceptions occur in Kazakhstan, with only about 50% of the country showing a modest increase in the trend precipitation, and Xinjiang Province with about one third. Viewed over short periods of time these changes are small and largely masked by the large inter-annual precipitation variability. However small the changes, they are very substantial when cumulated over a century. On the other hand, correlation coefficients are low (-0.3 to +0.3) in >90% of the region and the significance of the trend is low (>0.05) in most of the region.
Thus, whereas the simple linear regression proves to be an adequate model to demonstrate the trend of precipitation and drought in this and other regions of the world, the picture that emerges is not as clear-cut and uniform as in the case of the Mediterranean Zone, where in spite of the high year-to-year variability, a clear and often highly significant negative trend was evidenced by the highly significant t-probabilities (De Pauw et al., 2011).

4. SYNTHESIS AND CONCLUSIONS

The projections of climate change provided in this study are entirely based on spatially downscaled coarse-resolution GCM models. The downscaling method is based on super-imposing coarse-resolution climate change projections on top of high-resolution current climate surfaces through spatial interpolation methods in a GIS environment. The advantages of the downscaling methodology are its ability to make optimal use of GIS-implemented optimal spatial interpolation methods, its ease of use, applicability to either global or regional circulation models, if available, and use of current climate as a guide for downscaling future climates.

The precipitation projections of individual GCM models show major differences whereas the projections for temperature changes are more consistent, with all models anticipating a significant warming (2-5°C) over the entire area by the end of the 21st century.

To minimize possible divergences by selecting one model or another, a multi-model ensemble approach was adopted in which the output from 7 major GCM models was averaged for two greenhouse gas emission scenarios, A1b (currently held to be an optimistic one) and A2 (a probably realistic one), and three time horizons, a near future (2010-2040), an intermediate future (2040-2070) and a far future (2070-2100). The multi-ensemble modeling approach has been used to assess changes in key climatic variables: precipitation, aridity, growing periods and climatic zones.

In all change themes evaluated in our study, little difference was observed between the outcomes from the A1b or A2 scenarios, making these outcomes relatively insensitive to the scenario used.

The projections based on the downscaled multi-model ensemble indicate for most of the region a modest increase in precipitation. As indicated by the study of precipitation variability during the 20th century, this trend towards increasing precipitation does not go counter with the precipitation trend of the past and grows stronger with time.
The trend towards higher precipitation could easily be countered by higher evapo-transpiration losses as a result of the increased temperatures. However, up to 2040-2070 no clear trend is anticipated, with about half of the region projected to experience a slight increase in aridity (0-10 points) and another half a slight decrease (0-10 points). For the period 2070-2100 a large increase is projected in the area affected by a slight increase in aridity (0-10 points), particularly in Kazakhstan, Uzbekistan, and Turkmenistan.

The overall effect of the changes in precipitation and temperature is expected to be positive on the growing period. Not much change is projected in the period 2010-2040 for the thermal growing period in the regions dominated by lowlands (Kazakhstan, Uzbekistan, Turkmenistan and Xingjiang). However, from 2040-2070 onward the increase in the thermal growing period is expected to be pronounced throughout the entire region. As for the moisture-limited growing period, up to 2040-2070 an increase is projected in most of Uzbekistan and Turkmenistan and a decline in the other areas. During the period 2040-2070 the moisture-limited growing period is expected to decline in most of the region.
In summary, the overall balance between changes in the thermal growing period and the moisture-limited growing period is expected to be positive by the end of the 21st century and most of the region is projected to witness an increase in the temperature- and moisture-limited growing period.

Until the end of the 21st century a gradual but significant increase is projected in the share of the region that changes from one Köppen climatic zone to another. The most significant changes are expected in mountainous areas as these are most sensitive to the impact of temperature rise. This may lead to wetter climate types in Kyrgyzstan, whereas a significant part of Kazakhstan is expected to evolve in a drier climate type with precipitation more concentrated in winter.

In our study we have focused on the application of relatively simple models on spatially downscaled climate change projections to draw conclusions about the general trends of climate change for different timelines and emission scenarios, without being crop-specific. In a companion study for the same project, Sommer et al. (2012) have modeled the potential impact of these changes on the main varieties of wheat. Their approach has been to process the high-resolution dataset of temperature and precipitation, generated through the methods explained in our report, at the level of the research sites for which experimental crop growth and yield data were available, using a sophisticated crop growth and potential yield simulation model (CROPSYST[14]). Despite their use of different methods and focus for assessing climate change impact, the two studies complement each other and come, at their own spatial scales, to similar overall conclusions, foremost that the impact of climatic change in Central Asia is projected to be *mostly positive*. The main reason for this is that the short-duration thermal growing period, which prevails in most of the region, is projected to become longer, opening new possibilities for growing adapted and higher-yielding crop varieties, and that this thermal effect will more than compensate for any drying effect as a result of the higher temperatures.

Sommer et al. (2012) have applied in their study a weather generator to generate daily precipitation, temperature and radiation, the key meteorological variables for running the CropSyst model, therefore the effect of short-term weather variability is built into their impact assessment. However, one of the major consequences of climate change will be changes in the frequency distribution of extreme events (drought, floods, frosts and heat waves). To assess the future impact of extreme events on crop productivity is certainly a hot topic for a follow-up study.

The results of both studies indicate that under the current projections of climate change impact, the implementation of improved land, water and crop management practices for drylands already recommended for *present* climatic conditions, is the most sensible way forward to adapt to climate change.

[14] Stockle, C.O., Donatelli, M., Nelson, R. 2003. CropSyst, a cropping systems simulation model. Eur. J. Agron. 18, 289–307.

REFERENCES

Abdullaev, I., Manthrithilake, H., Kazbekov, J., 2006. Water security in Central Asia: troubled future or pragmatic partnership? Paper 11, International Conference "The last drop?" Water, Security and Sustainable Development in Central Eurasia, 1-2 December 2006, Institute of Social Studies (ISS), the Hague, Netherlands.

Allen, R.G., Pereira, L.S., Raes, D., and Smith, M., 1998. Crop evapotranspiration. Guidelines for computing crop water requirements. FAO Irrigation and Drainage Paper 56, 300 pp., FAO, Rome

BCM, 2009. BCM Model Component – Atmospheric model: Description. Retrieved from http://www.bcm.uib.no/model/component.php?id=1 the 11.10.2009

CIA, 2009. The World Factbook 2009. Washington, DC: Central Intelligence Agency. Retrieved from https://www.cia.gov/library/publications/the-world-factbook/index.html the 20.11.2009

Choisnel, E., de Villele, O., and Lacroze, F., 1992. Une approche uniformisée du calcul de l'évapotranspiration potentielle pour l'ensemble des pays de la Communauté Européenne. Centre Commun de Recherche, Commission des Communautés Européennes, EUR 14223, 178 pp.

Christensen, J.H., B. Hewitson, A. Busuioc, A. Chen, X. Gao, I. Held, R. Jones, R.K. Kolli, W.-T. Kwon, R. Laprise, V. Magaña Rueda, L. Mearns, C.G. Menéndez, J. Räisänen, A. Rinke, A. Sarr and P. Whetton, 2007: Regional Climate Projections. In: Climate Change 2007: The Physical Science Basis. Contribution of Working Group I to the Fourth Assessment Report of the Intergovernmental Panel on Climate Change [Solomon, S., D. Qin, M. Manning, Z. Chen, M. Marquis, K.B. Averyt, M. Tignor and H.L. Miller (eds.)]. Cambridge University Press, Cambridge, United Kingdom and New York, NY, USA

CMIP 2007. Climate Model Documentation, References, and Links. Retrieved from http://www-pcmdi.llnl.gov/ipcc/model_documentation/ipcc_model_documentation.php , the 10.11.2009. Last update 17.07.2007

Debaveye, J., 1985. Soil survey technical documents. Vol.2: Handbook for data interpretation. Soil Survey and Assessment Project. Department of Development Cooperation, Min. Foreign Trade and Foreign Affairs, Belgium

De Pauw, E. 2008. Climatic and Soil Datasets for the ICARDA Wheat Genetic Resource Collections of the Eurasia Region. Explanatory Notes. ICARDA GIS Unit Technical Note

De Pauw, E. and Göbel, W. 2011. Climate change in drylands: from assessment methods to adaptation strategies. In J.L. Araus and G.A. Slafer (Eds.). Crop Stress Management & Global Climate Change. CABI Climate Change Series 2, pp. 15-36.

Doorenbos, J., and Pruitt, W.O., 1984. Guidelines for predicting crop water requirements. FAO Irrigation and Drainage Paper 24, FAO, Rome

Edwards, D. C., and McKee, T. B., 1997. Characteristics of 20th century drought in the United States at multiple time scales. Climo Report 97-2, Dept. of Atmos. Sci., CSU, Fort Collins, CO, May, 155 pp.

FAO. 2001. FAOCLIM, a CD-ROM with world-wide agroclimatic data, version 2. Environment and Natural Resources Service (SDRN) Working Paper No.5, Food and Agriculure Organization of the United Nations, Rome, Italy

Gordon, H. B. et al. 2002. The CSIRO Mk3 Climate System Model – Technical paper. CSIRO Atmospheric Research, Australia, 2002. Available on http://www.cmar.csiro.au/e-print/open/gordon_2002a.pdf

ICARDA, 2009. Adaptation to climate change in Central Asia and the People's Republic of China – Background Paper. 27th of February 2009.

IPCC. 2007: Regional Climate Projections. In: Climate Change 2007: The Physical Science Basis. Contribution of Working Group I to the Fourth Assessment Report of the Intergovernmental Panel on Climate Change Cambridge University Press, Cambridge, United Kingdom and New York, NY, USA.

IPCC, 2007: Summary for Policymakers. In: Climate Change 2007: The Physical Science Basis. Contribution of Working Group I to the Fourth Assessment Report of the Intergovernmental Panel on Climate Change [Solomon, S., D. Qin, M. Manning, Z. Chen, M. Marquis, K.B. Averyt, M.Tignor and H.L. Miller (eds.)]. Cambridge University Press, Cambridge, United Kingdom and New York, NY, USA.

IPCC. 2007: Regional Climate Projections. In: Climate Change 2007: The Physical Science Basis. Contribution of Working Group I to the Fourth Assessment Report of the Intergovernmental Panel on Climate Change Cambridge University Press, Cambridge, United Kingdom and New York, NY, USA.

Köppen, W., and Geiger, H., 1928. Handbuch der Klimatkunde. Berlin, Germany

McFarlane, N.A. , J.F. Scinocca, M.Lazare, R. Harvey, D. Verseghy, J. Li 2005. CCCMA Internal Report: The CCCma Third Generation Atmospheric General Circulation Model (AGCM3). Canadian Centre for Climate Modelling and Analysis, University of Victoria. Available on http://www.cccma.ec.gc.ca/papers/jscinocca/AGCM3_report.pdf

McKee, Thomas B., Doesken, Nolan J., and Kleist, J., 1993. The relationship of drought frequency and duration of time scales. Eighth Conference on Applied Climatology, 17-22 January 1993, Anaheim, California.

Schneider, U., Fuchs, T., Meyer-Christoffer, A., and Rudolf, B., 2008. Global Precipitation Analysis Products of the GPCC. Global Precipitation Climatology Centre (GPCC), DWD, Internet publication, 1-12.

R. Sommer, R., Glazirina M. and Yuldashev T. 2012. Assessing the vulnerability of selected agro-ecosystems in Central Asia to threats resulting from climate change –production and productivity of wheat. Report of sub-component 3 of the ADB funded project on "Adaptation to Climate Change in Central Asia and the People's Republic of China". ICARDA, 127 pp.

UNESCO, 1979. Map of the world distribution of arid regions. Map at scale 1:25,000,000 with explanatory note. United Nations Educational, Scientific and Cultural Organization, Paris, 54 pp. ISBN 92-3-101484-6

ANNEX 1. CLIMATE CHANGE ATTRIBUTE MAPS (on CD)

1. Central Asia and Xingjiang Province (China) Agroclimatic zones 10_40_A1b
2. Central Asia and Xingjiang Province (China) Agroclimatic zones 10_40_A2
3. Central Asia and Xingjiang Province (China) Agroclimatic zones 40_70_A1b
4. Central Asia and Xingjiang Province (China) Agroclimatic zones 40_70_A2
5. Central Asia and Xingjiang Province (China) Agroclimatic zones 70_100_A1b
6. Central Asia and Xingjiang Province (China) Agroclimatic zones 70_100_A2
7. Central Asia and Xingjiang Province (China) Agroclimatic zones Current
8. Central Asia and Xingjiang Province (China) Annual aridity index 10_40_A1b
9. Central Asia and Xingjiang Province (China) Annual aridity index 10_40_A2
10. Central Asia and Xingjiang Province (China) Annual aridity index 40_70_A1b
11. Central Asia and Xingjiang Province (China) Annual aridity index 40_70_A2
12. Central Asia and Xingjiang Province (China) Annual aridity index 70_100_A1b
13. Central Asia and Xingjiang Province (China) Annual aridity index 70_100_A2
14. Central Asia and Xingjiang Province (China) Annual aridity index current
15. Central Asia and Xingjiang Province (China) Annual Potential Evapo-transpiration 10_40_A1b
16. Central Asia and Xingjiang Province (China) Annual Potential Evapo-transpiration 10_40_A2
17. Central Asia and Xingjiang Province (China) Annual Potential Evapo-transpiration 40_70_A1b
18. Central Asia and Xingjiang Province (China) Annual Potential Evapo-transpiration 40_70_A2
19. Central Asia and Xingjiang Province (China) Annual Potential Evapo-transpiration 70_100_A1b
20. Central Asia and Xingjiang Province (China) Annual Potential Evapo-transpiration 70_100_A2
21. Central Asia and Xingjiang Province (China) Annual Potential Evapo-transpiration current
22. Central Asia and Xingjiang Province (China) Climatic zones according to the Köppen system 10_40_A1b
23. Central Asia and Xingjiang Province (China) Climatic zones according to the Köppen system 10_40_A2
24. Central Asia and Xingjiang Province (China) Climatic zones according to the Köppen system 40_70_A1b
25. Central Asia and Xingjiang Province (China) Climatic zones according to the Köppen system 40_70_A2
26. Central Asia and Xingjiang Province (China) Climatic zones according to the Köppen system 70_100_A1b
27. Central Asia and Xingjiang Province (China) Climatic zones according to the Köppen system 70_100_A2
28. Central Asia and Xingjiang Province (China) Climatic zones according to the Köppen system under current conditions
29. Central Asia and Xingjiang Province (China) monthly Potential Evapo-transpiration 10_40_A1b_A0
30. Central Asia and Xingjiang Province (China) monthly Potential Evapo-transpiration 10_40_A2_A0
31. Central Asia and Xingjiang Province (China) monthly Potential Evapo-transpiration 40_70_A1b_A0
32. Central Asia and Xingjiang Province (China) monthly Potential Evapo-transpiration 40_70_A2_A0
33. Central Asia and Xingjiang Province (China) monthly Potential Evapo-transpiration 70_100_A1b_A0
34. Central Asia and Xingjiang Province (China) monthly Potential Evapo-transpiration 70_100_A2_A0
35. Central Asia and Xingjiang Province (China) Annual maximum temperature 10_40_A1b
36. Central Asia and Xingjiang Province (China) Annual maximum temperature 10_40_A2
37. Central Asia and Xingjiang Province (China) Annual maximum temperature 40_70_A1b
38. Central Asia and Xingjiang Province (China) Annual maximum temperature 40_70_A2

39. Central Asia and Xingjiang Province (China) Annual maximum temperature 70_100_A1b
40. Central Asia and Xingjiang Province (China) Annual maximum temperature 70_100_A2
41. Central Asia and Xingjiang Province (China) Annual maximum temperature Current
42. Central Asia and Xingjiang Province (China) Annual mean precipitation 10_40_A1b
43. Central Asia and Xingjiang Province (China) Annual mean precipitation 10_40_A2
44. Central Asia and Xingjiang Province (China) Annual mean precipitation 40_70_A1b
45. Central Asia and Xingjiang Province (China) Annual mean precipitation 40_70_A2
46. Central Asia and Xingjiang Province (China) Annual mean precipitation 70_100_A1b
47. Central Asia and Xingjiang Province (China) Annual mean precipitation 70_100_A2
48. Central Asia and Xingjiang Province (China) Annual mean precipitation Current
49. Central Asia and Xingjiang Province (China) Annual mean temperature Current
50. Central Asia and Xingjiang Province (China) Annual mean temperature 10_40_A1b
51. Central Asia and Xingjiang Province (China) Annual mean temperature 10_40_A2
52. Central Asia and Xingjiang Province (China) Annual mean temperature 40_70_A1b
53. Central Asia and Xingjiang Province (China) Annual mean temperature 40_70_A2
54. Central Asia and Xingjiang Province (China) Annual mean temperature 70_100_A1b
55. Central Asia and Xingjiang Province (China) Annual mean temperature 70_100_A2
56. Central Asia and Xingjiang Province (China) Annual minimum temperature 10_40_A1b
57. Central Asia and Xingjiang Province (China) Annual minimum temperature 10_40_A2
58. Central Asia and Xingjiang Province (China) Annual minimum temperature 40_70_A1b
59. Central Asia and Xingjiang Province (China) Annual minimum temperature 40_70_A2
60. Central Asia and Xingjiang Province (China) Annual minimum temperature 70_100_A1b
61. Central Asia and Xingjiang Province (China) Annual minimum temperature 70_100_A2
62. Central Asia and Xingjiang Province (China) Annual minimum temperature Current
63. Central Asia and Xingjiang Province (China) Changes in the Potential Evapo-transpiration from current conditions to 2010-2040 scenario A1b
64. Central Asia and Xingjiang Province (China) Changes in the Potential Evapo-transpiration from current conditions to 2010-2040 scenario A2
65. Central Asia and Xingjiang Province (China) Changes in the Potential Evapo-transpiration from current conditions to 2040-2070 scenario A1b
66. Central Asia and Xingjiang Province (China) Changes in the Potential Evapo-transpiration from current conditions to 2040-2070 scenario A2
67. Central Asia and Xingjiang Province (China) Changes in the Potential Evapo-transpiration from current conditions to 2070-2100 scenario A1b
68. Central Asia and Xingjiang Province (China) Changes in the Potential Evapo-transpiration from current conditions to 2070-2100 scenario A2
69. Central Asia and Xingjiang Province (China) Changes in the Annual maximum temperature from current conditions to 2010-2040 scenario A1b
70. Central Asia and Xingjiang Province (China) Changes in the Annual maximum temperature from current conditions to 2010-2040 scenario A2
71. Central Asia and Xingjiang Province (China) Changes in the Annual maximum temperature from current conditions to 2040-2070 scenario A1b
72. Central Asia and Xingjiang Province (China) Changes in the Annual maximum temperature from current conditions to 2040-2070 scenario A2
73. Central Asia and Xingjiang Province (China) Changes in the Annual maximum temperature from current conditions to 2070-2100 scenario A1b
74. Central Asia and Xingjiang Province (China) Changes in the Annual maximum temperature from current conditions to 2070-2100 scenario A2

75. Central Asia and Xingjiang Province (China) Changes in the Annual minimum temperature from current conditions to 2010-2040 scenario A1b
76. Central Asia and Xingjiang Province (China) Changes in the Annual minimum temperature from current conditions to 2010-2040 scenario A2
77. Central Asia and Xingjiang Province (China) Changes in the Annual minimum temperature from current conditions to 2040-2070 scenario A1b
78. Central Asia and Xingjiang Province (China) Changes in the Annual minimum temperature from current conditions to 2040-2070 scenario A2
79. Central Asia and Xingjiang Province (China) Changes in the Annual minimum temperature from current conditions to 2070-2100 scenario A1b
80. Central Asia and Xingjiang Province (China) Changes in the Annual minimum temperature from current conditions to 2070-2100 scenario A2
81. Central Asia and Xingjiang Province (China) Changes in the Annual mean temperature from current conditions to 2010-2040 scenario A1b
82. Central Asia and Xingjiang Province (China) Changes in the Annual mean temperature from current conditions to 2010-2040 scenario A2
83. Central Asia and Xingjiang Province (China) Changes in the Annual mean temperature from current conditions to 2040-2070 scenario A1b
84. Central Asia and Xingjiang Province (China) Changes in the Annual mean temperature from current conditions to 2040-2070 scenario A2
85. Central Asia and Xingjiang Province (China) Changes in the Annual mean temperature from current conditions to 2070-2100 scenario A1b
86. Central Asia and Xingjiang Province (China) Changes in the Annual mean temperature from current conditions to 2070-2100 scenario A2
87. Projections of absolute changes in annual precipitation 2010-2040 scenario A1b compared to 1960-1990
88. Projections of absolute changes in annual precipitation 2010-2040 scenario A2 compared to 1960-1990
89. Projections of absolute changes in annual precipitation 2040-2070 scenario A1b compared to 1960-1990
90. Projections of absolute changes in annual precipitation 2040-2070 scenario A2 compared to 1960-1990
91. Projections of absolute changes in annual precipitation 2070-2100 scenario A1b compared to 1960-1990
92. Projections of absolute changes in annual precipitation 2070-2100 scenario A2 compared to 1960-1990
93. Projections of changes in aridity index points for the period 2010-2040 scenario A1b compared to 1960-1990
94. Projections of changes in aridity index points for the period 2010-2040 scenario A2 compared to 1960-1990
95. Projections of changes in aridity index points for the period 2040-2070 scenario A1b compared to 1960-1990
96. Projections of changes in aridity index points for the period 2040-2070 scenario A2 compared to 1960-1990
97. Projections of changes in aridity index points for the period 2070-2100 scenario A1b compared to 1960-1990
98. Projections of changes in aridity index points for the period 2070-2100 scenario A2 compared to 1960-1990

99. Projections of changes in the total moisture-limited growing period for the period 2010-2040 scenario A1b compared to 1960-1990
100. Projections of changes in the total moisture-limited growing period for the period 2010-2040 scenario A2 compared to 1960-1990
101. Projections of changes in the total moisture-limited growing period for the period 2040-2070 scenario A1b compared to 1960-1990
102. Projections of changes in the total moisture-limited growing period for the period 2040-2070 scenario A2 compared to 1960-1990
103. Projections of changes in the total moisture-limited growing period for the period 2070-2100 scenario A1b compared to 1960-1990
104. Projections of changes in the total moisture-limited growing period for the period 2070-2100 scenario A1b compared to 1960-1990
105. Projections of changes in the total temperature-limited growing period for the period 2010-2040 scenario A1b compared to 1960-1990
106. Projections of changes in the total temperature-limited growing period for the period 2010-2040 scenario A2 compared to 1960-1990
107. Projections of changes in the total temperature-limited growing period for the period 2040-2070 scenario A1b compared to 1960-1990
108. Projections of changes in the total temperature-limited growing period for the period 2040-2070 scenario A2 compared to 1960-1990
109. Projections of changes in the total temperature-limited growing period for the period 2070-2100 scenario A1b compared to 1960-1990
110. Projections of changes in the total temperature-limited growing period for the period 2070-2100 scenario A2 compared to 1960-1990
111. Projections of changes in the total moisture- and temperature-limited growing period for the period 2010-2040 scenario A1b compared to 1960-1990
112. Projections of changes in the total moisture- and temperature-limited growing period for the period 2010-2040 scenario A2 compared to 1960-1990
113. Projections of changes in the total moisture- and temperature-limited growing period for the period 2040-2070 scenario A1b compared to 1960-1990
114. Projections of changes in the total moisture- and temperature-limited growing period for the period 2040-2070 scenario A2 compared to 1960-1990
115. Projections of changes in the total moisture- and temperature-limited growing period for the period 2070-2100 scenario A1b compared to 1960-1990
116. Projections of changes in the total moisture- and temperature-limited growing period for the period 2070-2100 scenario A2 compared to 1960-1990

Notes on abbreviations:

10_40_A1b: Future 2010-2040, GHG-emission scenario A1b
10_40_A2: Future 2010-2040, GHG-emission scenario A2
40_70_A1b: Future 2040-2070, GHG-emission scenario A1b
40_70_A2: Future 2040-2070, GHG-emission scenario A2
70_100_A1b: Future 2070-2100, GHG-emission scenario A1b
70_100_A2: Future 2070-2100, GHG-emission scenario A2

ANNEX 2. CATEGORIES OF THE KÖPPEN CLASSIFICATION SYSTEM

Despite a misleading simplicity of criteria, programming the Köppen classification system has been fairly complex. A problem was that not all category boundary conditions, set out in the description of the system, are well defined or lead to mutually exclusive results. For this reason additional boundary thresholds, and even new categories, had to be created to meet climatic conditions that were not anticipated by the Köppen system, while retaining the overall logic of the system.

With the criteria and thresholds specified in the next section, it is possible to define the Köppen climate classes up to four levels deep. Whereas the criteria and thresholds for the upper levels of the classification are standard in the literature, they vary for the lower levels. As a basis for programming the classification we used the guidelines in Debaveye (1985).

Climatic data needed

As mentioned before, the Köppen classification system requires only monthly temperature and precipitation averages. These are provided to CLIMAP in the form of 12 monthly grids. From the monthly averages the following values are calculated:

- Mean annual temperature ($Temp_{year}$)
- Mean temperature of the coldest month of the year ($Temp_{coldest}$)
- Mean temperature of the warmest month of the year ($Temp_{warmest}$)
- Annual precipitation total ($Prec_{year}$)
- Precipitation of the wettest month of the year ($Prec_{WetYr}$)
- Precipitation of the wettest month in summer ($Prec_{WetSum}$)
- Precipitation of the wettest month in winter ($Prec_{WetWin}$)
- Precipitation of the driest month in year ($Prec_{DryYr}$)
- Precipitation of the driest month in summer ($Prec_{DrySum}$)
- Precipitation of the driest month in winter ($Prec_{DryWin}$)

Derived classification criteria and categories

Rainfall distribution categories

- Equal
- Summer rain
- Winter rain

Type of drought categories

- Winter drought
- Summer drought
- No dry season

Summer type categories

- hot summer
- warm summer
- cool summer

Temperature regime categories for the B climate

- hot B climate
- cool B climate
- cold B climate

Criteria and category tests

Rainfall distribution

There is no definition in Köppen's system for an 'equal' rainfall distribution. However, it had to be introduced because in many tropical areas climatic conditions are such that the categories 'summer rain' or 'winter rain' do not exist or are meaningless. In our program we assume that the rainfall distribution is 'equal' if it is *neither 'summer rain' nor 'winter rain'.* To avoid that a very small difference in precipitation between either part of the year creates an artifact, a condition is imposed that the difference in precipitation should be substantial, at least 20%.

'equal distribution':

- $Prec_{May\text{-}Sep} < 1.2 * Prec_{Nov\text{-}Mar}$ **or** $Prec_{Nov\text{-}Mar} < 1.2 * Prec_{May\text{-}Sep}$ **(1)**

'winter rain':

- if N. Hemisphere: $Prec_{Nov\text{-}Mar} \geq 1.2 * Prec_{May\text{-}Sep}$ **(2a)**
- if S. Hemisphere: $Prec_{May\text{-}Sep} \geq 1.2 * Prec_{Nov\text{-}Mar}$ **(2b)**

'summer rain':

- if N. Hemisphere: $Prec_{May\text{-}Sep} \geq 1.2 * Prec_{Nov\text{-}Mar}$ **(3a)**
- if S. Hemisphere: $Prec_{Nov\text{-}Mar} \geq 1.2 * Prec_{May\text{-}Sep}$ **(3b)**

Major climatic groups and rainfall distribution

- If $Prec_{year} > 20* (Temp_{year} +7)$: climate (*A* or *C* or *D*) with equal rainfall distribution **(4)**
- if $Prec_{year} \leq 20* (Temp_{year} +7)$: climate *B* with equal rainfall distribution **(5)**
    - if $Prec_{year} < 10* (Temp_{year} +7)$: climate *BW* with equal rainfall distribution **(6)**
    - if $Prec_{year} \geq 10* (Temp_{year} +7)$: climate *BS* with equal rainfall distribution **(7)**
- If $Prec_{year} > 20* (Temp_{year} +14)$: climate (*A* or *C* or *D*) with summer rain **(8)**
- if $Prec_{year} \leq 20* (Temp_{year} +14)$: climate *B* with summer rain **(9)**
    - if $Prec_{year} < 10* (Temp_{year} +14)$: climate *BW* with summer rain **(10)**
    - if $Prec_{year} \geq 10* (Temp_{year} +14)$: climate *BS* with summer rain **(11)**
- If $Prec_{year} > 20* Temp_{year}$: climate (*A* or *C* or *D*) with winter rain **(12)**
- if $Prec_{year} \leq 20* Temp_{year}$: climate *B* with winter rain **(13)**
    - if $Prec_{year} < 10* Temp_{year}$: climate *BW* with winter rain **(14)**
    - if $Prec_{year} \geq 10* Temp_{year}$: climate *BS* with winter rain **(15)**

Both tests are needed later for the unequivocal identification of the climate class.

Thermal regime B climate

'hot B climate': $Temp_{year} \geq 18°C$ **(16)**
'cool B climate': $Temp_{year} < 18°C$ and $Temp_{warmest} \geq 18°C$ **(17)**
'cold B climate': $Temp_{year} < 18°C$ and $Temp_{warmest} < 18°C$ **(18)**

Drought in climates C,D:

'winter drought': **(19)**

- if N. Hemisphere: $Precip_{wettest\ Jun\text{-}Aug} > 10^* Prec_{driest\ Dec\text{-}Feb}$
- if S. Hemisphere: $Precip_{wettest\ Dec\text{-}Feb} > 10^* Prec_{driest\ Jun\text{-}Aug}$

'summer drought': **(20)**

- if N. Hemisphere: $Precip_{wettest\ Dec\text{-}Feb} > 3^* Prec_{driest\ Jun\text{-}Aug}$
- if S. Hemisphere: $Precip_{wettest\ Jun\text{-}Aug} > 3^* Prec_{driest\ Dec\text{-}Feb}$

'no dry season': neither winter drought nor summer drought **(21)**

Summer Type in C,D climates:

'hot summer': $Temp_{warmest} \geq 22°C$ **(22)**

'warm summer': $Temp_{warmest} < 22°C$ and (no.of months with Tmean>10°C) ≥ 4 **(23)**

'cool summer': $Temp_{warmest} < 22°C$ and (no.of months with Tmean>10°C) <4
and $Temp_{coldest} > -38°C$ **(24)**

Classification on the basis of above criteria

A-climates

- If $Temp_{coldest} > 18°C$ and one of the following options are true:
  - **(1)** and **(4)**
  - **(2)** and **(8)**
  - **(3)** and **(12)**

subdivisions of A-climates:

Af:

- $Temp_{coldest} \geq 18°C$ and $Prec_{DryYr} \geq 60$ mm

Am:

- $Temp_{coldest} \geq 18°C$ and $Prec_{DryYr} < 60$ mm and $Prec_{year} > 1000$ mm and $Prec_{DriestYr} \geq 100 - 0.04^* Prec_{year}$

Aw:

- $Temp_{coldest} \geq 18°C$ and $Prec_{DryYr} < 60$ mm and $Prec_{year} < 2500$ mm and $Prec_{DriestYr} < 100 - 0.04^* Prec_{year}$ and **(2)**

As:

- $Temp_{coldest} \geq 18°C$ and $Prec_{DryYr} < 60$ mm and $Prec_{year} < 2500$ mm and $Prec_{DriestYr} < 100 - 0.04^* Prec_{year}$ and **(3)**

B-climates

- If one of the following options is true:
  - **(1)** and **(5)**
  - **(2)** and **(9)**
  - **(3)** and **(13**)

Subdivision of B-climates:

BS:

- if one of the following options is true:

- **(1)** and **(7) :** *BS0*[15]
- **(2)** and **(11):** *BSw*
- **(3)** and **(15):** *BSs*

BS0:

BS0h: **+ (16***)*
BS0k: **+ (17)**
BS0k': **+ (18)**

BSw:

BSwh: **+ (16***)*
BSwk: **+ (17)**
BSwk': **+ (18)**

BSs:

BSsh: **+ (16***)*
BSsk: **+ (17)**
BSsk': **+ (18)**

BW:

- if one of the following options is true:
  - **(1)** and **(6):** *BW0*[16]
  - **(2)** and **(10):** *BWw*
  - **(3)** and **(14):** *BWs*

BW0:

BW0h: **+ (16***)*
BW0k: **+ (17)**
BW0k': **+ (18)**

BWw:

BWwh: **+ (16***)*
BWwk: **+ (17)**
BWwk': **+ (18)**

BWs:

BWsh: **+ (16***)*
BWsk: **+ (17)**
BWsk': **+ (18)**

C-climates

- If (not B-climate) and $Temp_{coldest} \leq 18°C$ and $Temp_{coldest} \geq -3°C$

Subdivision of C-climates:

Cw: **+(19)**

- *Cwa*: **+ (22)**

[15] A new category, not in the original classification, to cover transitional BS climates in which neither winter or summer drought occurs

[16] A new category, not in the original classification. In hyper-arid areas where it rarely rains, a distinction between summer or winter drought is meaningless. To capture this concept of 'ultra-aridity', this new category has been established.

- *Cwb*: **+ (23)**
- *Cwc*: **+ (24)**

Cs: **+(20)**

- *Csa*: **+ (22)**
- *Csb*: **+ (23)**
- *Csc*: **+ (24)**

Cf: **+(21)**

- *Cfa*: **+ (22)**
- *Cfb*: **+ (23)**
- *Cfc*: **+ (24)**

D-climates

- If (not B-climate) and $Temp_{warmest}$ >10°C and $Temp_{coldest}$ <-3°C

Subdivision of D-climates:

Df: **+ (21)**

- *Dfa*: **+ (22)**
- *Dfb*: **+ (23)**
- *Dfc*: **+ (24)**

Dw: **+ (19)**

- *Dwa*: **+ (22)**
- *Dwb*: **+ (23)**
- *Dwc*: **+ (24)**

Ds[17]: **+ (20)**

- *Dsa*: **+ (22)**
- *Dsb*: **+ (23)**
- *Dsc*: **+ (24)**

E-climates

- If not B-climate and $Temp_{warmest}$ (≤ 10°C and >0°C) and $Temp_{coldest}$ < -3°C

F-climates

$Temp_{warmest}$ ≤ 0°C

[17] A new category, not in the original classification, to account for subarctic climates with humid winters

ANNEX 3. SUMMARY TABLES OF PROJECTED CLIMATIC CHANGES[18]

A3.1. CHANGES IN ARIDITY

Table 11. Projected changes in aridity between recent climate (1960-1990) and 2010-2040 scenario A1b-25

Change Class	Kazakhstan	Uzbekistan	Turkmenist	Kyrgyzstan	Tajikistan	Xingjiang
-20 to -10	1	0	0	1	1	0
-10 to 0	55	41	56	55	43	70
0 to 10	43	58	44	31	25	29
10 to 20	0	0	0	10	10	1
20 to 30	0	0	0	1	6	0
30 to 50	0	0	0	1	7	0
50 to 70	0	0	0	1	4	0
70 to 100	0	0	0	0	3	0

Table 12. Projected changes in aridity between recent climate (1960-1990) and 2010-2040 scenario A2

Change Class	Kazakhstan	Uzbekistan	Turkmenist	Kyrgyzstan	Tajikistan	Xingjiang
-20 to -10	1	0	0	1	1	0
-10 to 0	56	24	18	54	41	68
0 to 10	43	76	82	31	24	31
10 to 20	0	0	0	10	11	1
20 to 30	0	0	0	1	6	0
30 to 50	0	0	0	1	7	0
50 to 70	0	0	0	1	4	0
70 to 100	0	0	0	0	4	0
> 100	0	0	0	0	1	0

Table 13. Projected changes in aridity between recent climate (1960-1990) and 2040-2070 scenario A1b-25

Change Class	Kazakhstan	Uzbekistan	Turkmenist	Kyrgyzstan	Tajikistan	Xingjiang
-20 to -10	1	0	0	0	1	0
-10 to 0	58	44	35	53	44	64
0 to 10	41	56	65	32	26	35
10 to 20	0	0	0	10	9	1
20 to 30	0	0	0	1	6	0
30 to 50	0	0	0	1	6	0
50 to 70	0	0	0	1	4	0
70 to 100	0	0	0	0	3	0

[18] A magenta color fill indicates a particular class occupies at least 10% of the applicable geographical entity

Table 14. Projected changes in aridity between recent climate (1960-1990) and 2040-2070 scenario A2

Change Class	Kazakhstan	Uzbekistan	Turkmenist	Kyrgyzstan	Tajikistan	Xingjiang
-20 to -10	1	0	0	0	1	0
-10 to 0	51	38	38	48	43	54
0 to 10	48	62	62	32	23	44
10 to 20	0	0	0	15	11	1
20 to 30	0	0	0	2	6	0
30 to 50	0	0	0	1	7	0
50 to 70	0	0	0	1	4	0
70 to 100	0	0	0	0	4	0
> 100	0	0	0	0	1	0

Table 15. Projected changes in aridity between recent climate (1960-1990) and 2070-2100 scenario A1b

Change Class	Kazakhstan	Uzbekistan	Turkmenist	Kyrgyzstan	Tajikistan	Xingjiang
-50 to -30	0	0	0	0	1	0
-30 to -20	0	0	0	1	1	0
-20 to -10	2	1	0	13	8	0
-10 to 0	87	93	79	64	45	65
0 to 10	11	6	21	19	27	34
10 to 20	0	0	0	1	8	1
20 to 30	0	0	0	1	4	0
30 to 50	0	0	0	1	4	0
50 to 70	0	0	0	0	1	0

Table 16. Projected changes in aridity between recent climate (1960-1990) and 2070-2100 scenario A2

Change Class	Kazakhstan	Uzbekistan	Turkmenist	Kyrgyzstan	Tajikistan	Xingjiang
-20 to -10	0	0	0	1	1	0
-10 to 0	61	52	39	42	43	39
0 to 10	38	48	61	35	21	58
10 to 20	0	0	0	18	12	2
20 to 30	0	0	0	2	6	0
30 to 50	0	0	0	1	7	0
50 to 70	0	0	0	1	4	0
70 to 100	0	0	0	0	4	0
> 100	0	0	0	0	1	0

A3.2. CHANGES IN GROWING PERIODS

Table 17. Projected changes in the total moisture-limited growing period between recent climate (1960-1990) and 2010-2040 scenario A1b

Change (days)	Kazakhstan	Uzbekistan	Turkmenist	Kyrgyzstan	Tajikistan	Xingjiang
-180 - -150	1	0	0	1	0	1
-150 - -120	5	0	0	12	4	3
-120 - -90	22	0	0	11	24	5
-90 - -60	33	0	0	9	8	6
-60 - -30	11	0	0	9	7	8
-30 - -10	7	9	2	13	14	4
-10 - 10	13	20	12	26	37	54
10 - 30	6	23	14	10	6	7
30 - 60	2	46	48	4	0	8
60 - 90	0	1	19	2	0	3
90 - 120	0	0	5	1	0	1
120 - 150	0	0	0	1	0	0
150 - 180	0	0	0	1	0	0
Decrease	**79**	**9**	**2**	**55**	**56**	**27**
Stable	**13**	**20**	**12**	**26**	**37**	**54**
Increase	**8**	**70**	**86**	**19**	**6**	**19**

Table 18. Projected changes in the total moisture-limited growing period between recent climate (1960-1990) and 2010-2040 scenario A2

Change (days)	Kazakhstan	Uzbekistan	Turkmenist	Kyrgyzstan	Tajikistan	Xingjiang
-180 - -150	1	0	0	1	3	0
-150 - -120	2	0	0	5	4	1
-120 - -90	7	0	0	7	3	2
-90 - -60	36	0	0	15	16	7
-60 - -30	18	0	0	11	9	13
-30 - -10	7	1	1	18	7	6
-10 - 10	14	27	24	30	51	55
10 - 30	13	50	28	5	4	5
30 - 60	0	21	40	4	1	8
60 - 90	0	0	4	2	0	2
90 - 120	0	0	3	2	0	0
120 - 150	0	0	0	1	0	0
Decrease	**73**	**1**	**1**	**57**	**43**	**30**
Stable	**14**	**27**	**24**	**30**	**51**	**55**
Increase	**14**	**71**	**75**	**14**	**5**	**15**

Table 19. Projected changes in the total moisture-limited growing period between recent climate (1960-1990) and 2040-2070 scenario A1b

Change (days)	Kazakhstan	Uzbekistan	Turkmenist	Kyrgyzstan	Tajikistan	Xingjiang
-180 - -150	1	0	0	0	5	0
-150 - -120	2	0	0	5	2	1
-120 - -90	3	0	0	9	11	2
-90 - -60	36	0	0	14	9	5
-60 - -30	18	0	0	12	10	13
-30 - -10	9	3	7	28	16	6
-10 - 10	23	42	23	21	43	55
10 - 30	6	54	46	3	3	5
30 - 60	0	0	18	4	1	9
60 - 90	0	0	4	2	0	2
90 - 120	0	0	1	2	0	0
Decrease	**70**	**3**	**8**	**68**	**53**	**28**
Stable	**23**	**42**	**23**	**21**	**43**	**55**
Increase	**6**	**54**	**70**	**11**	**4**	**17**

Table 20. Projected changes in the total moisture-limited growing period between recent climate (1960-1990) and 2040-2070 scenario A2

Change (days)	Kazakhstan	Uzbekistan	Turkmenist	Kyrgyzstan	Tajikistan	Xingjiang
-180 - -150	1	0	0	0	3	0
-150 - -120	2	0	0	4	2	1
-120 - -90	4	0	0	7	4	2
-90 - -60	36	0	0	15	16	6
-60 - -30	17	0	0	12	11	14
-30 - -10	9	1	3	27	10	6
-10 - 10	20	30	24	24	49	56
10 - 30	9	61	37	4	4	6
30 - 60	0	7	30	4	1	7
60 - 90	0	0	4	2	0	2
90 - 120	0	0	2	2	0	0
Decrease	**70**	**2**	**3**	**65**	**46**	**29**
Stable	**20**	**30**	**24**	**24**	**49**	**56**
Increase	**10**	**68**	**73**	**11**	**5**	**15**

Table 21. Projected changes in the total moisture-limited growing period between recent climate (1960-1990) and 2070-2100 scenario A1b

Change (days)	Kazakhstan	Uzbekistan	Turkmenist	Kyrgyzstan	Tajikistan	Xingjiang
-180 - -150	1	0	0	0	0	0
-150 - -120	1	0	0	4	2	1
-120 - -90	12	0	0	10	15	6
-90 - -60	28	0	0	13	12	6
-60 - -30	26	4	3	19	13	8
-30 - -10	22	25	18	33	38	6
-10 - 10	10	62	28	14	18	59
10 - 30	1	9	40	3	1	9
30 - 60	0	0	6	2	1	4
60 - 90	0	0	4	2	0	2
Decrease	**89**	**29**	**21**	**79**	**80**	**27**
Stable	**10**	**62**	**28**	**14**	**18**	**59**
Increase	**1**	**9**	**51**	**7**	**2**	**15**

Table 22. Projected changes in the total moisture-limited growing period between recent climate (1960-1990) and 2070-2100 scenario A2

Change (days)	Kazakhstan	Uzbekistan	Turkmenist	Kyrgyzstan	Tajikistan	Xingjiang
-180 - -150	1	0	0	0	2	0
-150 - -120	1	0	0	1	1	1
-120 - -90	3	0	0	7	12	2
-90 - -60	19	0	0	13	9	5
-60 - -30	29	1	0	26	9	7
-30 - -10	12	11	15	29	44	6
-10 - 10	33	72	34	13	18	62
10 - 30	2	16	42	3	2	11
30 - 60	0	0	7	4	2	3
60 - 90	0	0	3	2	1	2
90 - 120	0	0	0	2	0	1
Decrease	**66**	**13**	**15**	**77**	**77**	**21**
Stable	**33**	**72**	**34**	**13**	**18**	**62**
Increase	**2**	**16**	**51**	**11**	**5**	**16**

Table 23. Projected changes in the total temperature-limited growing period between recent climate (1960-1990) and 2010-2040 scenario A1b

Change	Kazakhstan	Uzbekistan	Turkmenist	Kyrgyzstan	Tajikistan	Xingjiang
0 - 10	96	73	60	15	9	76
10 - 30	4	26	40	79	85	23
30 - 60	0	1	0	6	7	2
Stable	**96**	**73**	**60**	**15**	**9**	**76**
Increase	**4**	**27**	**40**	**85**	**91**	**24**

Table 24. Projected changes in the total temperature-limited growing period between recent climate (1960-1990) and 2010-2040 scenario A2

Change	Kazakhstan	Uzbekistan	Turkmenist	Kyrgyzstan	Tajikistan	Xingjiang
0 - 10	95	70	57	11	9	78
10 - 30	5	29	42	83	86	21
30 - 60	0	1	0	6	5	2
Stable	**95**	**70**	**57**	**11**	**9**	**78**
Increase	**5**	**30**	**43**	**89**	**91**	**22**

Table 25. Projected changes in the total temperature-limited growing period between recent climate (1960-1990) and 2040-2070 scenario A1b

Change	Kazakhstan	Uzbekistan	Turkmenist	Kyrgyzstan	Tajikistan	Xingjiang
0 - 10	0	0	2	1	4	1
10 - 30	99	88	59	47	23	86
30 - 60	1	12	39	46	68	12
60 - 90	0	0	0	6	5	1
Stable	**0**	**0**	**2**	**1**	**4**	**1**
Increase	**100**	**100**	**98**	**99**	**96**	**99**

Table 26. Projected changes in the total temperature-limited growing period between recent climate (1960-1990) and 2040-2070 scenario A2

Change	Kazakhstan	Uzbekistan	Turkmenist	Kyrgyzstan	Tajikistan	Xingjiang
0 - 10	0	0	2	2	5	1
10 - 30	100	90	64	50	28	87
30 - 60	0	9	34	44	63	11
60 - 90	0	0	0	5	4	1
Stable	**0**	**0**	**2**	**2**	**5**	**1**
Increase	**100**	**100**	**98**	**98**	**95**	**99**

Table 27. Projected changes in the total temperature-limited growing period between recent climate (1960-1990) and 2070-2100 scenario A1b

Change	Kazakhstan	Uzbekistan	Turkmenist	Kyrgyzstan	Tajikistan	Xingjiang
0 - 10	0	0	2	0	2	0
10 - 30	94	56	24	5	0	74
30 - 60	6	42	71	71	70	20
60 - 90	0	2	3	19	25	5
90 - 120	0	0	0	4	2	1
Stable	0	0	2	0	2	0
Increase	100	100	98	100	98	100

Table 28. Projected changes in the total temperature-limited growing period between recent climate (1960-1990) and 2070-2100 scenario A2

Change	Kazakhstan	Uzbekistan	Turkmenist	Kyrgyzstan	Tajikistan	Xingjiang
0 - 10	0	0	2	0	2	0
10 - 30	82	15	2	1	0	60
30 - 60	17	74	79	68	53	32
60 - 90	0	10	18	24	41	7
90 - 120	0	0	0	6	4	1
Stable	0	0	2	0	2	0
Increase	100	100	98	100	98	100

Table 29. Projected changes in the total moisture- and temperature-limited growing period between recent climate (1960-1990) and 2010-2040 scenario A1b

Change (days)	Kazakhstan	Uzbekistan	Turkmenist	Kyrgyzstan	Tajikistan	Xingjiang
-60 - -30	1	0	0	1	0	0
-30 - -10	1	0	0	4	0	0
-10 - 10	6	14	4	24	32	84
10 - 30	36	66	47	51	60	10
30 - 60	56	20	45	20	8	4
60 - 90	0	0	4	0	0	0
% Decrease	**2**	**0**	**0**	**5**	**0**	**0**
% Stable	**6**	**14**	**4**	**24**	**32**	**84**
% Increase	**92**	**86**	**96**	**71**	**68**	**16**

Table 30. Projected changes in the total moisture- and temperature-limited growing period between recent climate (1960-1990) and 2010-2040 scenario A2

Change (days)	Kazakhstan	Uzbekistan	Turkmenist	Kyrgyzstan	Tajikistan	Xingjiang
-90 - -60	0	0	0	1	0	0
-60 - -30	1	0	0	1	0	0
-30 - -10	1	0	0	5	0	0
-10 - 10	8	46	36	37	31	91
10 - 30	59	48	48	45	65	6
30 - 60	29	5	16	10	4	2
Decrease	**3**	**0**	**0**	**8**	**0**	**1**
Stable	**8**	**46**	**36**	**37**	**31**	**91**
Increase	**89**	**53**	**64**	**55**	**69**	**8**

Table 31. Projected changes in the total moisture- and temperature-limited growing period between recent climate (1960-1990) and 2040-2070 scenario A1b

Change (days)	Kazakhstan	Uzbekistan	Turkmenist	Kyrgyzstan	Tajikistan	Xingjiang
-90 - -60	0	0	0	1	0	0
-60 - -30	2	0	0	2	0	0
-30 - -10	1	0	0	4	0	0
-10 - 10	6	48	29	32	18	90
10 - 30	57	37	30	32	54	5
30 - 60	34	15	38	23	26	3
60 - 90	0	0	3	6	1	0
Decrease	**3**	**0**	**0**	**7**	**0**	**1**
Stable	**6**	**48**	**29**	**32**	**18**	**90**
Increase	**91**	**51**	**71**	**61**	**82**	**9**

Table 32. Projected changes in the total moisture- and temperature-limited growing period between recent climate (1960-1990) and 2040-2070 scenario A2

Change (days)	Kazakhstan	Uzbekistan	Turkmenist	Kyrgyzstan	Tajikistan	Xingjiang
-90 - -60	0	0	0	1	0	0
-60 - -30	1	0	0	2	0	0
-30 - -10	1	0	0	3	0	0
-10 - 10	5	43	23	30	19	91
10 - 30	55	38	35	31	51	5
30 - 60	36	19	38	29	29	2
60 - 90	0	0	3	5	1	0
Decrease	**3**	**0**	**0**	**6**	**0**	**1**
Stable	**5**	**43**	**23**	**30**	**19**	**91**
Increase	**92**	**57**	**76**	**64**	**81**	**8**

Table 33. Projected changes in the total moisture- and temperature-limited growing period between recent climate (1960-1990) and 2070-2100 scenario A1b

Change (days)	Kazakhstan	Uzbekistan	Turkmenist	Kyrgyzstan	Tajikistan	Xingjiang
-90 - -60	0	0	0	1	0	0
-60 - -30	1	0	0	2	0	0
-30 - -10	1	0	1	4	0	0
-10 - 10	21	54	29	24	15	91
10 - 30	40	27	29	31	36	4
30 - 60	36	18	32	23	46	3
60 - 90	0	0	8	12	2	1
90 - 120	0	0	0	3	0	0
Decrease	**3**	**0**	**2**	**7**	**0**	**1**
Stable	**21**	**54**	**29**	**24**	**15**	**91**
Increase	**76**	**46**	**69**	**69**	**85**	**8**

Table 34. Projected changes in the total moisture- and temperature-limited growing period between recent climate (1960-1990) and 2070-2100 scenario A2

Change (days)	Kazakhstan	Uzbekistan	Turkmenist	Kyrgyzstan	Tajikistan	Xingjiang
-90 - -60	0	0	0	1	0	0
-60 - -30	1	0	0	2	0	0
-30 - -10	1	0	0	3	0	0
-10 - 10	6	40	9	22	13	89
10 - 30	64	22	35	29	23	6
30 - 60	27	31	41	24	54	4
60 - 90	0	7	13	14	9	1
90 - 120	0	0	0	5	0	0
Decrease	**2**	**0**	**1**	**6**	**0**	**1**
Stable	**6**	**40**	**9**	**22**	**13**	**89**
Increase	**92**	**60**	**90**	**72**	**87**	**11**

A3.3. CHANGES IN CLIMATIC ZONES

Table 35. Projected changes in the Köppen climatic zones between recent climate (1960-1990) and 2010-2040 scenario A1b

Aridity and precipitation pattern change	Kazakhstan	Uzbekistan	Turkmenist	Kyrgyzstan	Tajikistan	Xingjiang
Drier; precipitation becomes more concentrated in summer	1	0	0	0	0	2
Drier; precipitation becomes more concentrated in winter	4	0	0	1	1	0
Drier; precipitation remains concentrated in summer	0	0	0	0	0	2
Drier; precipitation remains concentrated in winter	0	0	1	0	1	0
Drier; precipitation remains without strong seasonality	1	0	0	0	0	0
Wetter; precipitation becomes less seasonal	0	0	0	7	2	1
Little change in aridity; precipitation becomes more concentrated in winter	0	0	0	3	5	0
Little change in aridity; precipitation remains concentrated in summer	0	0	0	0	0	4
Little change in aridity; precipitation remains concentrated in winter	0	2	6	2	7	0
Little change in aridity; precipitation remains without strong seasonality	13	0	0	2	0	2
No change in Koeppen zone	81	97	93	84	84	89

Table 36. Projected changes in the Köppen climatic zones between recent climate (1960-1990) and 2010-2040 scenario A2

Aridity and precipitation pattern change	Kazakhstan	Uzbekistan	Turkmenist	Kyrgyzstan	Tajikistan	Xingjiang
Drier; precipitation becomes more concentrated in summer	1	0	0	0	0	1
Drier; precipitation becomes more concentrated in winter	4	0	0	1	0	0
Drier; precipitation remains concentrated in summer	0	0	0	0	0	1
Drier; precipitation remains concentrated in winter	1	0	1	0	1	0
Drier; precipitation remains without strong seasonality	1	0	0	0	0	0
Wetter; precipitation becomes less seasonal	0	0	0	7	3	1
Little change in aridity; precipitation becomes more concentrated in winter	0	0	0	1	4	0
Little change in aridity; precipitation remains concentrated in summer	0	0	0	0	0	4
Little change in aridity; precipitation remains concentrated in winter	0	2	6	2	6	0
Little change in aridity; precipitation remains without strong seasonality	13	0	0	2	0	2
No change in Koeppen zone	81	97	94	86	85	90

Table 37. Projected changes in the Köppen climatic zones between recent climate (1960-1990) and 2040-2070 scenario A1b

Aridity and precipitation pattern change	Kazakhstan	Uzbekistan	Turkmenist	Kyrgyzstan	Tajikistan	Xingjiang
Drier; precipitation becomes more concentrated in summer	2	0	0	0	0	4
Drier; precipitation becomes more concentrated in winter	11	0	0	2	1	0
Drier; precipitation remains concentrated in summer	0	0	0	0	0	5
Drier; precipitation remains concentrated in winter	1	2	1	1	5	0
Drier; precipitation remains without strong seasonality	1	0	0	0	0	0
Wetter; precipitation becomes less seasonal	0	0	0	17	6	2
Little change in aridity; precipitation becomes more concentrated in winter	0	0	0	2	10	0
Little change in aridity; precipitation remains concentrated in summer	0	0	0	1	0	8
Little change in aridity; precipitation remains concentrated in winter	0	9	47	2	16	0
Little change in aridity; precipitation remains without strong seasonality	33	0	0	7	0	3
No change in Koeppen zone	51	89	51	68	62	78

Table 38. Projected changes in the Köppen climatic zones between recent climate (1960-1990) and 2040-2070 scenario A2

Aridity and precipitation pattern change	Kazakhstan	Uzbekistan	Turkmenist	Kyrgyzstan	Tajikistan	Xingjiang
Drier; precipitation becomes more concentrated in summer	1	0	0	0	0	4
Drier; precipitation becomes more concentrated in winter	9	0	0	3	2	0
Drier; precipitation remains concentrated in summer	0	0	0	0	0	4
Drier; precipitation remains concentrated in winter	1	2	1	1	5	0
Drier; precipitation remains without strong seasonality	1	0	0	0	0	0
Wetter; precipitation becomes less seasonal	0	0	0	16	4	2
Little change in aridity; precipitation becomes more concentrated in winter	0	0	0	2	9	0
Little change in aridity; precipitation remains concentrated in summer	0	0	0	1	0	7
Little change in aridity; precipitation remains concentrated in winter	0	8	45	2	15	0
Little change in aridity; precipitation remains without strong seasonality	32	0	0	5	0	3
No change in Koeppen zone	54	89	54	71	65	80

Table 39. Projected changes in the Köppen climatic zones between recent climate (1960-1990) and 2070-2100 scenario A1b

Aridity and precipitation pattern change	Kazakhstan	Uzbekistan	Turkmenist	Kyrgyzstan	Tajikistan	Xingjiang
Drier; precipitation becomes more concentrated in summer	0	0	0	0	0	5
Drier; precipitation becomes more concentrated in winter	19	0	0	4	3	0
Drier; precipitation remains concentrated in summer	0	0	0	0	0	7
Drier; precipitation remains concentrated in winter	2	5	2	2	8	0
Drier; precipitation remains without strong seasonality	1	0	0	0	0	0
Wetter; precipitation becomes less seasonal	0	0	0	23	7	4
Little change in aridity; precipitation becomes more concentrated in winter	0	0	0	5	14	0
Little change in aridity; precipitation remains concentrated in summer	0	0	0	1	0	12
Little change in aridity; precipitation remains concentrated in winter	0	24	67	2	21	0
Little change in aridity; precipitation remains without strong seasonality	38	0	0	8	0	3
No change in Koeppen zone	40	70	31	55	47	68

Table 40. Projected changes in the Köppen climatic zones between recent climate (1960-1990) and 2070-2100 scenario A2

Aridity and precipitation pattern change	Kazakhstan	Uzbekistan	Turkmenist	Kyrgyzstan	Tajikistan	Xingjiang
Drier; precipitation becomes more concentrated in summer	0	0	0	0	0	6
Drier; precipitation becomes more concentrated in winter	22	0	0	5	4	1
Drier; precipitation remains concentrated in summer	0	0	0	0	0	8
Drier; precipitation remains concentrated in winter	2	6	2	2	10	0
Wetter; precipitation becomes less seasonal	0	0	0	25	8	5
Little change in aridity; precipitation becomes more concentrated in winter	0	0	0	4	16	0
Little change in aridity; precipitation remains concentrated in summer	0	0	0	1	0	13
Little change in aridity; precipitation remains concentrated in winter	0	34	77	2	23	0
Little change in aridity; precipitation remains without strong seasonality	37	0	0	9	0	3
No change in Koeppen zone	37	59	21	50	40	65

ANNEX 4- MAPS OF THE ANNUAL STANDARDIZED PRECIPITATION INDEX (PERIOD 1901-2007)

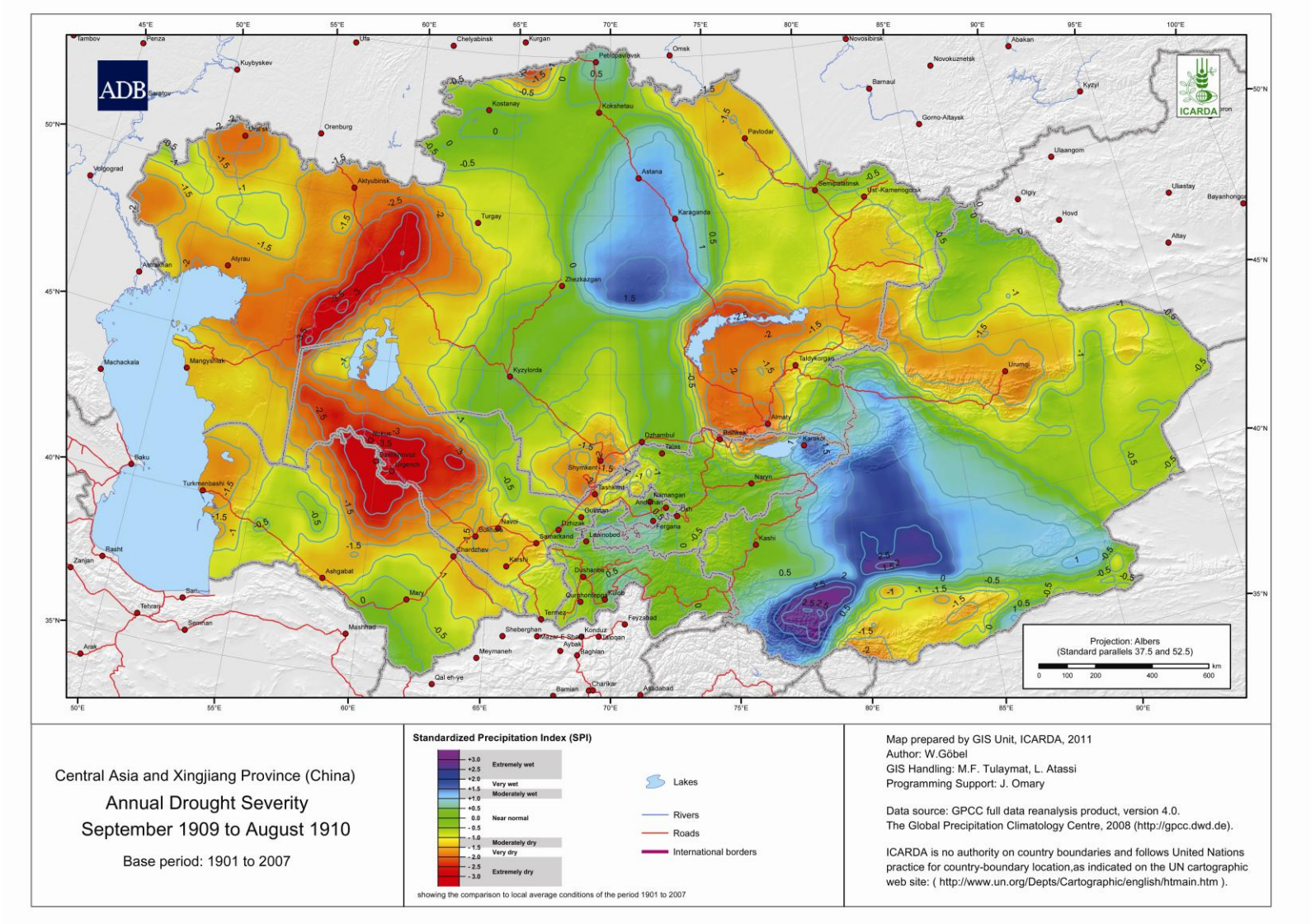

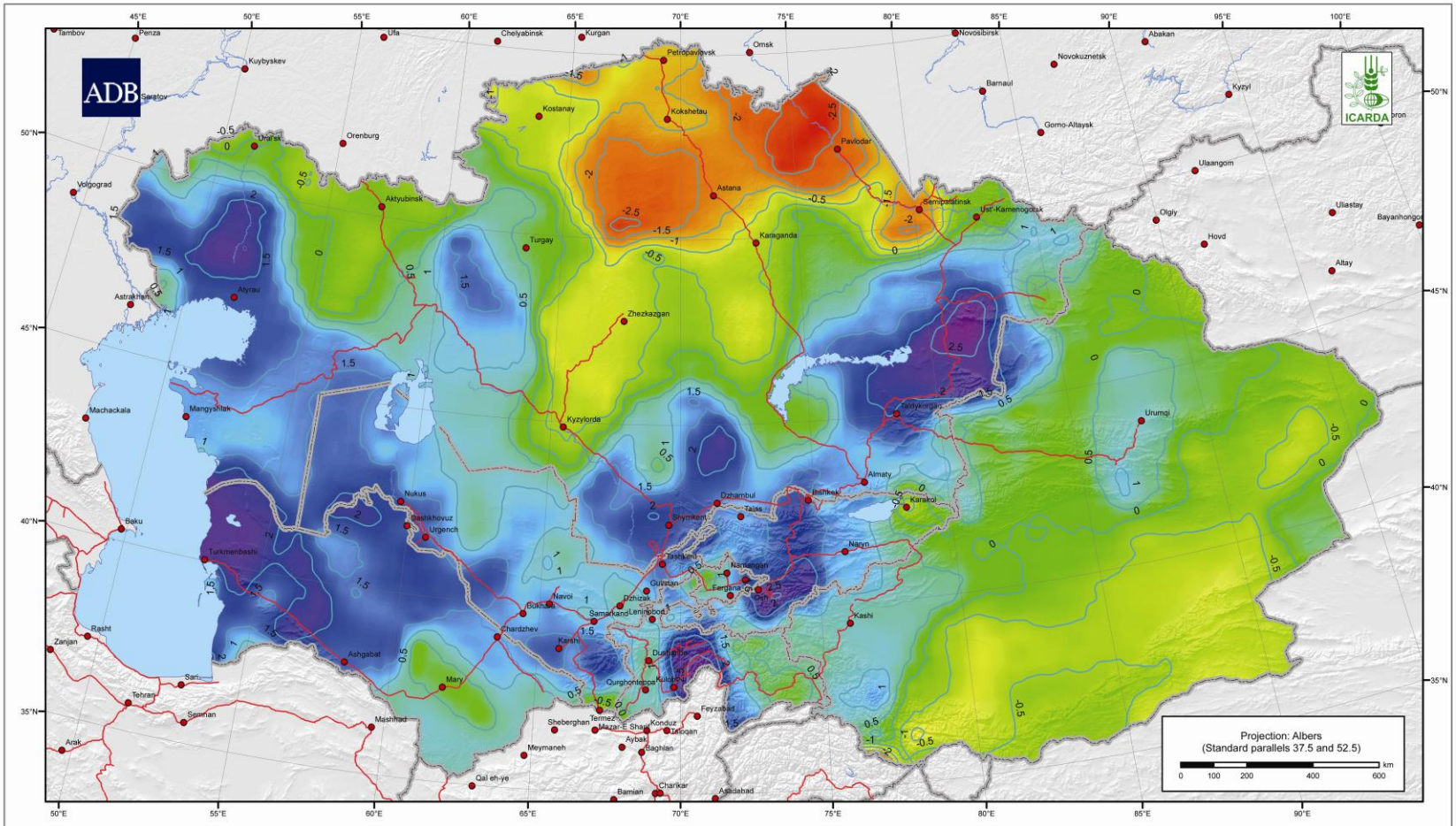

Central Asia and Xingjiang Province (China)

Annual Drought Severity
September 1951 to August 1952

Base period: 1901 to 2007

Standardized Precipitation Index (SPI)

+3.0	Extremely wet
+2.5	
+2.0	Very wet
+1.5	Moderately wet
+1.0	
+0.5	
0.0	Near normal
-0.5	
-1.0	
-1.5	Moderately dry
-2.0	Very dry
-2.5	
-3.0	Extremely dry

showing the comparison to local average conditions of the period 1901 to 2007

Lakes
Rivers
Roads
International borders

Map prepared by GIS Unit, ICARDA, 2011
Author: W.Göbel
GIS Handling: M.F. Tulaymat, L. Atassi
Programming Support: J. Omary

Data source: GPCC full data reanalysis product, version 4.0.
The Global Precipitation Climatology Centre, 2008 (http://gpcc.dwd.de).

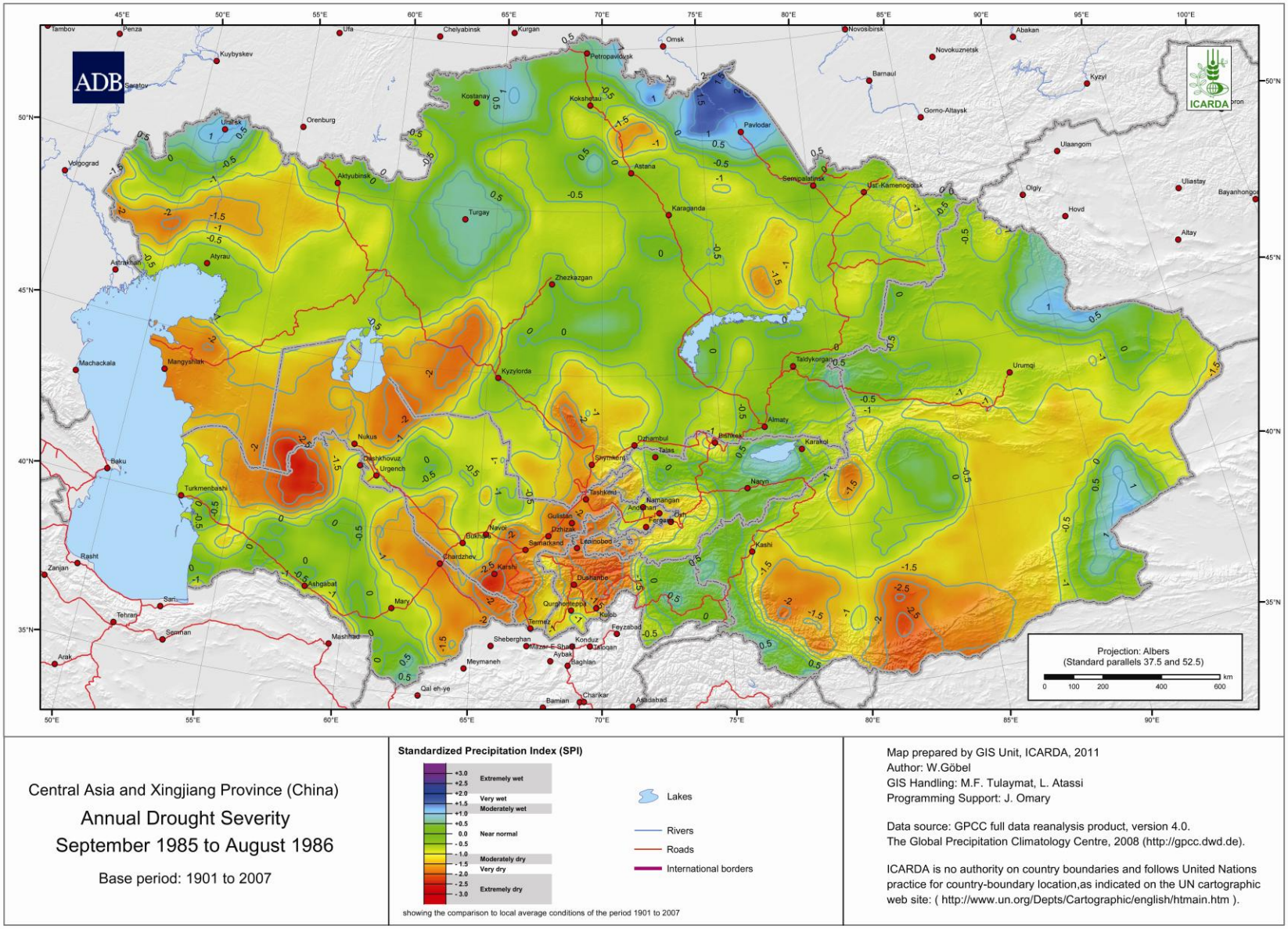

Central Asia and Xingjiang Province (China)

Annual Drought Severity

September 1985 to August 1986

Base period: 1901 to 2007

Map prepared by GIS Unit, ICARDA, 2011
Author: W.Göbel
GIS Handling: M.F. Tulaymat, L. Atassi
Programming Support: J. Omary

Data source: GPCC full data reanalysis product, version 4.0.
The Global Precipitation Climatology Centre, 2008 (http://gpcc.dwd.de).

ICARDA is no authority on country boundaries and follows United Nations practice for country-boundary location,as indicated on the UN cartographic web site: (http://www.un.org/Depts/Cartographic/english/htmain.htm).

ANNEX 5. STANDARDIZED PRECIPITATION INDEX SUMMARIES BY COUNTRY AND YEAR

Table 41. Distribution of the annual SPI in Kazakhstan

SPI Classes	Extreme -ly dry	Very dry	Modera-tely dry	Near normal	Modera-tely wet	Very Wet	Extreme-ly wet
1902	0.0%	0.7%	2.8%	77.8%	7.2%	3.2%	8.1%
1903			0.5%	65.5%	14.9%	11.7%	7.3%
1904	0.1%	3.2%	8.4%	86.0%	2.2%	0.1%	
1905	0.0%	0.2%	1.8%	55.9%	20.1%	15.1%	6.7%
1906		2.1%	6.2%	81.4%	7.4%	2.9%	0.0%
1907	0.0%	0.4%	1.2%	83.0%	13.2%	1.9%	0.1%
1908		0.0%	4.2%	47.2%	19.9%	17.4%	11.2%
1909	0.6%	2.4%	6.3%	86.3%	4.3%	0.1%	
1910	11.1%	13.9%	22.4%	45.8%	5.7%	1.1%	
1911	3.1%	8.7%	16.3%	56.8%	8.3%	6.1%	0.6%
1912	0.1%	0.7%	1.9%	67.5%	12.6%	7.6%	9.6%
1913	1.8%	7.5%	16.5%	68.9%	4.9%	0.4%	0.0%
1914			0.3%	50.5%	22.6%	18.1%	8.4%
1915	0.1%	0.4%	0.7%	59.7%	24.1%	12.5%	2.4%
1916	1.1%	1.0%	5.6%	74.5%	8.8%	7.3%	1.6%
1917	10.3%	8.7%	17.1%	59.8%	4.0%	0.1%	
1918	9.3%	10.3%	24.9%	49.2%	4.6%	1.6%	
1919	2.1%	5.0%	7.8%	62.5%	16.1%	3.6%	2.9%
1920	3.9%	11.8%	22.8%	61.3%	0.0%	0.0%	0.0%
1921	3.1%	4.4%	9.9%	63.8%	2.3%	4.8%	11.6%
1922		0.2%	2.2%	76.9%	13.2%	4.6%	2.9%
1923	3.0%	1.4%	8.5%	83.1%	3.9%	0.1%	
1924	0.0%	0.2%	2.6%	74.1%	20.3%	2.8%	
1925	3.4%	6.4%	16.1%	65.7%	7.2%	1.2%	
1926			4.0%	65.8%	20.5%	7.2%	2.4%
1927	13.7%	10.1%	13.4%	61.8%	1.1%		
1928		0.0%	0.2%	37.0%	21.9%	14.5%	26.3%
1929	7.4%	16.0%	21.3%	53.6%	1.6%	0.1%	
1930	11.4%	10.7%	10.9%	51.5%	4.8%	2.7%	7.8%
1931	0.5%	1.2%	5.4%	87.6%	5.0%	0.2%	
1932	0.7%	6.4%	10.4%	73.5%	6.9%	2.1%	
1933	2.5%	5.6%	11.8%	76.6%	1.6%	1.4%	0.4%
1934		0.5%	4.4%	75.7%	14.2%	4.3%	0.9%
1935	0.0%	3.1%	17.7%	76.7%	1.9%	0.5%	
1936	14.3%	11.4%	14.5%	59.6%	0.1%	0.0%	
1937	0.5%	10.7%	19.5%	65.0%	4.3%	0.0%	

1938	3.7%	9.6%	12.3%	64.2%	5.9%	3.4%	0.9%
1939	7.9%	8.3%	14.2%	67.4%	2.1%		
1940	4.2%	6.1%	16.8%	68.5%	2.2%	1.8%	0.4%
1941			0.4%	60.4%	20.3%	15.6%	3.3%
1942			0.6%	87.1%	9.9%	2.4%	0.0%
1943	0.0%	1.2%	12.3%	85.6%	0.8%	0.0%	
1944	15.0%	16.7%	20.9%	46.2%	1.2%		
1945	3.7%	7.3%	11.8%	75.1%	1.9%	0.2%	0.0%
1946		0.1%	2.0%	66.9%	15.1%	13.0%	3.0%
1947		0.0%	1.0%	71.6%	10.6%	9.9%	6.9%
1948	0.0%	2.5%	13.6%	78.7%	2.8%	2.3%	0.0%
1949	0.1%	4.3%	6.8%	60.0%	16.4%	6.4%	6.0%
1950	0.4%	3.7%	14.6%	76.5%	3.0%	1.6%	0.2%
1951	24.6%	26.1%	28.8%	20.4%			
1952	6.8%	5.9%	5.4%	47.9%	17.0%	11.7%	5.2%
1953			0.6%	91.5%	5.3%	2.5%	0.0%
1954			0.2%	69.5%	19.7%	5.8%	4.8%
1955	11.2%	22.7%	21.3%	44.7%			
1956		0.5%	5.7%	92.7%	1.1%		
1957	1.2%	4.7%	7.2%	80.2%	6.5%	0.1%	
1958	0.3%	0.3%	0.5%	27.3%	21.9%	31.0%	18.7%
1959	0.4%	1.2%	2.4%	80.7%	12.5%	2.7%	0.0%
1960			0.2%	68.1%	22.4%	7.9%	1.4%
1961	0.2%	2.9%	9.1%	81.9%	5.4%	0.4%	
1962		0.2%	4.1%	87.7%	6.7%	1.2%	0.1%
1963	0.7%	0.9%	1.3%	86.9%	9.2%	0.9%	0.1%
1964				47.2%	26.2%	13.5%	13.1%
1965	0.2%	12.6%	19.9%	64.7%	1.1%	0.4%	1.0%
1966			0.8%	59.9%	25.0%	10.5%	3.6%
1967	1.2%	4.3%	6.9%	83.7%	3.7%	0.2%	
1968	1.6%	4.3%	10.6%	80.5%	2.3%	0.7%	
1969	0.0%	0.4%	4.9%	74.8%	13.0%	4.5%	2.4%
1970		0.0%	2.6%	86.1%	9.3%	1.7%	0.3%
1971	1.5%	3.0%	9.2%	70.7%	11.4%	4.1%	
1972	3.2%	2.2%	5.8%	75.6%	6.1%	5.9%	1.1%
1973		0.0%	3.1%	84.0%	11.0%	1.7%	
1974	12.7%	6.5%	7.4%	65.9%	6.7%	0.8%	
1975	23.7%	25.5%	26.2%	24.5%			
1976	0.1%	2.7%	16.6%	78.6%	1.9%		
1977	0.1%	1.7%	9.4%	84.4%	4.4%		
1978			1.7%	84.8%	7.2%	3.6%	2.6%
1979		0.9%	3.4%	74.1%	19.2%	2.0%	0.3%
1980			1.4%	91.8%	5.6%	0.9%	0.2%
1981		2.3%	4.2%	45.7%	13.0%	12.2%	22.6%

1982	0.9%	3.5%	12.7%	78.6%	3.8%	0.4%	
1983	0.0%	0.9%	2.9%	91.6%	3.4%	1.0%	0.2%
1984	2.0%	6.9%	19.9%	69.1%	1.5%	0.4%	0.1%
1985	1.1%	1.6%	6.9%	80.5%	7.6%	2.1%	0.1%
1986	1.1%	7.7%	11.3%	76.6%	2.1%	1.2%	0.0%
1987			0.2%	75.0%	17.8%	6.7%	0.3%
1988	0.0%	0.4%	1.7%	69.2%	15.3%	7.9%	5.4%
1989	0.1%	1.5%	7.8%	83.2%	6.3%	0.3%	0.7%
1990			2.9%	72.3%	13.4%	7.3%	4.1%
1991	3.9%	6.1%	16.3%	63.2%	3.2%	2.5%	4.7%
1992	0.2%	2.2%	3.8%	84.1%	4.1%	2.8%	2.7%
1993		0.2%	1.3%	51.1%	28.8%	13.8%	4.8%
1994	3.4%	3.5%	9.2%	71.8%	6.8%	2.6%	2.6%
1995	1.6%	8.7%	23.1%	64.9%	1.6%	0.1%	0.0%
1996	10.7%	12.6%	19.8%	56.9%	0.0%		
1997	4.0%	7.8%	12.8%	62.1%	7.5%	2.5%	3.2%
1998	3.3%	8.1%	13.4%	70.8%	3.6%	0.7%	0.0%
1999	2.3%	6.5%	14.5%	67.4%	5.6%	2.0%	1.6%
2000	1.2%	3.9%	9.9%	67.0%	9.6%	7.5%	1.0%
2001	3.9%	4.1%	4.9%	70.8%	13.8%	2.1%	0.5%
2002				57.6%	16.4%	14.5%	11.4%
2003	0.1%	0.9%	6.8%	53.2%	21.1%	11.4%	6.5%
2004	2.5%	3.8%	6.8%	78.3%	6.2%	2.4%	0.1%
2005	0.0%	0.9%	2.3%	81.1%	12.4%	3.2%	0.0%
2006	1.2%	7.4%	18.0%	73.3%			
2007			0.3%	82.1%	12.3%	4.8%	0.4%

Table 42. Distribution of the annual SPI in Kyrgyzstan

SPI Classes	Extreme -ly dry	Very dry	Modera-tely dry	Near normal	Modera-tely wet	Very Wet	Extreme-ly wet
1902				26.3%	32.8%	20.7%	20.1%
1903				48.3%	39.2%	10.8%	1.6%
1904		0.0%	7.3%	92.7%			
1905				93.7%	4.4%	1.9%	
1906			5.0%	95.0%			
1907			0.7%	91.3%	7.7%	0.2%	
1908	0.2%	0.5%	1.3%	68.9%	15.5%	8.7%	4.9%
1909			1.6%	98.4%			
1910	1.3%	2.7%	5.6%	81.2%	7.5%	1.7%	
1911	2.2%	11.8%	22.1%	63.9%			
1912	21.1%	8.7%	7.0%	63.0%	0.3%		
1913		1.9%	13.4%	84.6%			
1914		4.2%	11.9%	83.8%			
1915			0.7%	97.5%	1.6%	0.2%	
1916	9.1%	41.0%	24.4%	25.6%			
1917	90.2%	7.8%	2.0%				
1918	43.3%	43.1%	10.5%	3.1%			
1919	10.2%	11.6%	10.6%	67.6%			
1920		0.7%	10.2%	82.5%	6.2%	0.3%	
1921			0.5%	35.7%	24.2%	16.3%	23.2%
1922		1.0%	2.7%	93.5%	2.8%		
1923				100.0%	0.0%		
1924			1.1%	91.8%	7.1%	0.0%	
1925		10.3%	15.0%	74.7%			
1926		3.6%	20.0%	76.4%			
1927	32.2%	42.6%	17.5%	7.7%			
1928				59.7%	10.1%	13.0%	17.1%
1929				100.0%			
1930		2.7%	25.9%	71.4%			
1931			1.0%	86.2%	11.3%	1.5%	
1932		0.7%	22.0%	77.3%			
1933	1.0%	5.8%	16.8%	76.4%			
1934				30.2%	58.0%	10.9%	0.9%
1935	0.0%	1.7%	9.0%	89.4%			
1936				80.1%	17.1%	2.8%	
1937			1.6%	98.4%			
1938	2.3%	6.7%	28.8%	61.8%	0.4%		
1939	1.3%	18.5%	38.9%	41.4%			
1940			1.7%	96.3%	2.1%		
1941				97.9%	2.1%		

1942				74.0%	25.2%	0.8%	
1943		9.7%	12.5%	74.6%	3.2%		
1944	3.2%	9.7%	28.3%	58.7%			
1945				80.1%	14.8%	5.1%	
1946			0.1%	94.6%	5.2%	0.1%	
1947	7.7%	21.2%	20.3%	50.6%	0.2%		
1948		0.7%	5.7%	93.1%	0.5%		
1949				57.1%	28.9%	14.1%	0.0%
1950		1.2%	16.4%	81.4%	0.9%		
1951		5.5%	8.4%	86.1%			
1952				20.9%	41.7%	28.1%	9.3%
1953				77.8%	15.5%	6.7%	
1954				13.7%	20.7%	25.8%	39.8%
1955			12.3%	85.3%	2.2%	0.2%	
1956				70.8%	14.8%	13.2%	1.2%
1957		0.0%	5.2%	94.7%	0.0%		
1958				34.8%	27.7%	30.5%	7.0%
1959				79.4%	16.4%	4.2%	
1960			2.8%	84.3%	12.2%	0.7%	
1961	3.8%	12.3%	25.3%	58.6%			
1962	1.4%	2.9%	14.7%	81.0%			
1963				92.4%	7.6%		
1964				59.4%	37.1%	3.5%	
1965	3.3%	17.9%	27.7%	51.1%			
1966		0.1%	1.0%	54.3%	42.2%	2.4%	
1967	0.4%	1.6%	2.3%	84.1%	9.1%	2.4%	
1968	1.3%	1.0%	7.3%	87.3%	2.8%	0.4%	
1969				26.9%	15.5%	15.0%	42.6%
1970		0.0%	0.6%	75.9%	20.7%	2.8%	
1971	0.2%	9.2%	24.0%	66.6%			
1972			1.4%	97.8%	0.8%	0.1%	
1973		0.6%	4.9%	87.5%	7.1%		
1974	7.4%	12.1%	18.2%	59.5%	2.7%	0.1%	
1975	12.5%	25.5%	31.5%	30.2%	0.3%		
1976		4.6%	16.1%	79.3%			
1977			14.2%	85.8%			
1978			0.9%	88.4%	9.5%	1.2%	
1979			0.9%	67.0%	23.9%	8.2%	
1980			0.2%	99.8%			
1981				42.8%	31.8%	21.0%	4.3%
1982	13.7%	9.6%	26.2%	49.0%	1.5%		
1983	1.5%	1.8%	2.5%	94.2%			
1984		3.0%	35.7%	61.2%	0.0%		
1985			0.3%	95.7%	4.0%		

1986	0.9%	5.1%	16.1%	77.9%			
1987				20.3%	33.1%	32.4%	14.2%
1988				38.2%	30.3%	25.5%	6.0%
1989	0.0%	5.7%	21.4%	72.9%			
1990			0.3%	85.2%	14.0%	0.5%	
1991		0.7%	5.3%	92.1%	1.9%		
1992	2.7%	3.2%	2.9%	84.2%	6.2%	0.8%	
1993			0.0%	70.1%	26.6%	3.3%	
1994	0.9%	2.1%	6.1%	80.6%	9.1%	1.2%	
1995	13.5%	11.2%	14.1%	61.2%	0.1%		
1996	1.9%	5.1%	12.2%	72.7%	5.9%	1.9%	0.2%
1997	12.9%	4.8%	17.4%	63.8%	1.1%		
1998				56.7%	9.6%	21.3%	12.4%
1999		0.1%	2.7%	62.7%	21.4%	12.6%	0.5%
2000	1.1%	1.6%	11.3%	83.2%	2.9%		
2001		0.2%	1.8%	85.9%	9.3%	2.8%	
2002				53.5%	15.0%	12.3%	19.3%
2003				26.7%	36.4%	34.4%	2.5%
2004				78.9%	19.2%	1.9%	
2005				65.3%	29.7%	4.5%	0.5%
2006	1.2%	1.9%	27.0%	70.0%			
2007	3.4%	1.8%	11.4%	74.1%	9.3%		

Table 43. Distribution of the annual SPI in Tajikistan

SPI Classes	Extreme-ly dry	Very dry	Modera-tely dry	Near normal	Modera-tely wet	Very Wet	Extreme-ly wet
1902		6.8%	19.6%	72.5%	1.0%	0.0%	
1903				26.4%	45.5%	27.4%	0.5%
1904	11.9%	6.8%	11.2%	70.1%			
1905			1.4%	98.5%			
1906				91.4%	8.5%	0.0%	
1907	7.2%	10.4%	13.6%	68.7%			
1908		0.1%	0.5%	90.6%	8.8%		
1909			14.4%	85.5%			
1910			0.0%	99.9%			
1911	10.2%	24.6%	14.5%	40.6%	4.3%	2.7%	3.0%
1912	7.2%	9.3%	9.5%	74.0%			
1913	0.2%	2.0%	13.5%	83.3%	0.8%		
1914	2.6%	11.2%	14.7%	71.4%			
1915				99.5%	0.4%		
1916	18.0%	19.8%	17.0%	45.1%			
1917	63.1%	22.5%	9.9%	4.4%			
1918	6.0%	17.9%	23.9%	52.0%			
1919			1.7%	97.9%	0.3%		
1920			3.1%	96.8%			
1921				35.6%	17.9%	18.3%	28.1%
1922				99.8%	0.2%		
1923				99.7%	0.2%		
1924			2.5%	97.4%			
1925				99.9%			
1926	1.2%	2.7%	7.3%	88.7%			
1927	0.9%	15.9%	31.1%	45.4%	6.6%		
1928				97.7%	2.2%		
1929				99.9%			
1930		0.1%	10.3%	70.1%	11.9%	7.4%	0.0%
1931				80.8%	19.1%	0.1%	
1932			0.6%	97.5%	1.8%		
1933			5.7%	94.2%			
1934				68.1%	12.3%	16.4%	3.1%
1935			0.2%	99.8%			
1936			5.0%	84.4%	10.5%		
1937		0.3%	10.0%	89.6%			
1938			4.2%	95.7%			
1939		0.5%	7.6%	91.8%			
1940		0.3%	16.8%	82.8%			
1941				96.9%	2.9%	0.1%	

1942				72.1%	22.0%	5.8%	
1943				99.8%	0.2%		
1944		0.5%	10.4%	89.1%			
1945				83.2%	14.0%	2.6%	
1946		0.9%	12.8%	67.4%	18.4%	0.4%	
1947	7.7%	5.2%	26.8%	60.2%			
1948		1.2%	6.2%	62.5%	16.7%	13.3%	
1949				52.1%	16.0%	15.3%	16.6%
1950	4.6%	5.9%	14.3%	75.1%			
1951			0.2%	99.7%			
1952				54.7%	22.3%	10.8%	12.1%
1953				66.6%	21.2%	12.0%	
1954				28.0%	22.4%	26.1%	23.4%
1955			0.8%	97.6%	1.5%		
1956			0.4%	95.6%	4.0%		
1957		0.0%	5.3%	91.0%	3.6%		
1958				35.0%	30.8%	19.2%	14.9%
1959				76.7%	8.6%	8.8%	5.8%
1960			6.5%	82.8%	10.3%	0.3%	
1961		2.6%	30.5%	66.8%			
1962	1.8%	2.9%	8.6%	85.8%	0.8%		
1963				82.7%	15.4%	1.9%	
1964				55.8%	15.3%	9.1%	19.6%
1965	2.4%	1.9%	13.7%	77.4%	4.5%	0.0%	
1966			4.5%	83.5%	7.7%	4.2%	
1967	3.9%	4.1%	4.9%	76.4%	10.6%		
1968	3.9%	2.3%	3.7%	60.6%	28.2%	0.8%	0.4%
1969				16.5%	12.0%	8.2%	63.3%
1970			8.0%	91.9%			
1971	39.3%	18.7%	24.5%	17.5%			
1972			0.5%	97.6%	1.8%		
1973			6.4%	92.5%	1.0%		
1974	18.4%	24.1%	19.5%	37.8%			
1975	4.0%	14.2%	16.2%	65.5%			
1976			20.6%	57.1%	5.5%	9.2%	7.6%
1977	9.1%	17.2%	23.8%	49.8%			
1978			3.1%	74.9%	10.5%	11.0%	0.4%
1979			2.8%	71.0%	22.1%	4.0%	
1980			5.2%	94.7%			
1981				97.5%	2.3%	0.1%	
1982		0.1%	8.6%	91.2%			
1983				96.9%	3.0%		
1984	5.0%	4.9%	6.8%	83.2%			
1985			0.2%	99.0%	0.7%		

1986	14.8%	19.9%	17.3%	48.0%			
1987				27.0%	29.3%	9.5%	34.1%
1988				52.2%	23.4%	13.2%	11.2%
1989		0.4%	16.5%	82.9%			
1990				88.5%	11.4%		
1991			7.4%	79.1%	6.8%	5.4%	1.2%
1992			1.5%	58.1%	17.8%	15.0%	7.6%
1993			7.5%	55.1%	26.7%	10.5%	
1994	13.6%	3.8%	3.4%	71.0%	6.5%	1.7%	
1995	16.1%	5.4%	9.5%	62.1%	3.1%	2.5%	1.3%
1996				81.3%	3.4%	2.9%	12.3%
1997	2.0%	0.9%	8.5%	76.7%	4.9%	4.2%	2.7%
1998				14.8%	44.1%	31.1%	9.9%
1999			1.3%	80.3%	2.3%	2.2%	13.8%
2000	12.4%	32.3%	28.8%	26.5%			
2001	41.8%	11.1%	8.8%	38.1%	0.0%		
2002		0.8%	7.2%	72.9%	10.0%	6.4%	2.6%
2003			1.0%	45.0%	10.8%	15.0%	28.2%
2004			0.1%	71.6%	18.2%	4.6%	5.4%
2005				26.3%	47.6%	18.9%	7.1%
2006	1.9%	3.5%	11.5%	81.6%	1.4%		
2007	7.3%	8.1%	21.2%	63.3%	0.0%		

Table 44. Distribution of the annual SPI in Turkmenistan

SPI Classes	Extreme-ly dry	Very dry	Modera-tely dry	Near normal	Modera-tely wet	Very Wet	Extreme-ly wet
1902	6.3%	2.6%	9.1%	81.9%			
1903			0.1%	79.8%	19.7%	0.4%	
1904		13.0%	19.0%	67.9%	0.0%		
1905	0.1%	14.5%	11.5%	73.8%			
1906			6.0%	52.7%	35.2%	6.0%	
1907				81.1%	18.8%		
1908		1.8%	16.5%	74.9%	6.8%		
1909			6.2%	81.6%	7.3%	5.0%	
1910	14.4%	11.3%	31.7%	42.6%			
1911		0.1%	7.7%	76.8%	13.2%	2.2%	
1912	16.4%	22.8%	25.7%	34.5%	0.5%		
1913			5.4%	94.6%			
1914				99.2%	0.8%		
1915				40.2%	35.3%	17.9%	6.6%
1916		0.0%	6.9%	88.2%	2.9%	1.9%	
1917	63.6%	17.5%	14.6%	4.3%			
1918		0.1%	3.8%	96.0%			
1919		11.0%	50.0%	38.9%			
1920			0.7%	65.4%	24.2%	7.8%	1.8%
1921			12.9%	87.0%			
1922				84.2%	14.4%	1.3%	
1923			2.5%	61.7%	21.2%	14.6%	
1924				85.6%	14.3%		
1925	2.8%	9.4%	21.5%	66.3%			
1926				69.1%	24.0%	6.9%	
1927	17.6%	26.4%	29.2%	26.8%			
1928			5.4%	67.2%	8.3%	10.1%	9.0%
1929	4.1%	10.1%	21.7%	64.0%			
1930	0.0%	0.5%	7.8%	91.6%			
1931		0.0%	1.4%	94.9%	3.6%		
1932				64.5%	29.1%	6.4%	
1933			0.2%	74.3%	25.5%	0.0%	
1934			2.3%	80.4%	15.3%	1.9%	
1935	2.8%	8.9%	10.4%	77.9%			
1936	0.3%	5.5%	5.3%	88.8%			
1937	7.7%	19.7%	34.2%	38.3%			
1938	5.9%	7.0%	17.3%	69.6%	0.1%		
1939	0.1%	0.2%	0.9%	86.2%	12.5%	0.1%	
1940		0.1%	6.3%	70.7%	12.2%	10.2%	0.5%
1941				85.7%	11.1%	3.2%	

1942			4.0%	90.6%	5.3%		
1943		0.0%	1.8%	70.4%	19.0%	6.6%	2.2%
1944	2.8%	19.8%	21.8%	55.6%			
1945	0.5%	9.9%	5.1%	84.3%			
1946		0.3%	1.4%	96.9%	1.4%		
1947		9.7%	15.9%	74.3%			
1948	0.6%	11.5%	21.3%	66.5%			
1949			2.1%	75.5%	22.4%		
1950		10.8%	12.7%	74.4%	2.0%		
1951	0.9%	11.7%	52.6%	34.7%			
1952				25.0%	16.1%	39.1%	19.8%
1953	0.0%	0.1%	0.3%	98.7%	0.7%		
1954			0.0%	38.4%	28.2%	33.0%	0.3%
1955	0.3%	1.2%	9.9%	88.5%	0.1%		
1956				87.8%	12.1%		
1957		0.5%	12.2%	84.5%	2.7%		
1958		0.7%	5.2%	84.6%	8.9%	0.5%	
1959				42.2%	32.1%	25.4%	0.2%
1960		0.5%	18.7%	78.0%	2.5%	0.3%	
1961	17.8%	7.3%	19.2%	51.3%	3.5%	0.9%	
1962		0.2%	8.9%	83.5%	7.1%	0.3%	
1963			2.7%	86.1%	10.6%	0.6%	0.0%
1964				65.4%	29.3%	5.3%	0.0%
1965	0.0%	2.1%	15.0%	80.9%	1.9%	0.1%	
1966		1.4%	4.2%	40.8%	35.7%	16.5%	1.3%
1967		0.1%	9.5%	90.2%	0.1%		
1968				95.8%	4.0%	0.1%	
1969				1.2%	4.7%	38.6%	55.5%
1970			2.5%	78.2%	13.8%	5.0%	0.4%
1971	4.6%	5.5%	25.0%	64.9%			
1972				68.5%	21.8%	8.7%	0.9%
1973			0.1%	85.0%	14.9%		
1974	0.1%	0.3%	0.9%	79.3%	9.3%	7.7%	2.4%
1975	3.7%	13.4%	49.2%	33.5%			
1976		0.1%	0.6%	70.1%	8.3%	8.4%	12.5%
1977	2.1%	3.5%	17.8%	76.5%	0.1%		
1978			0.4%	41.6%	22.4%	14.6%	20.9%
1979				66.6%	26.4%	7.0%	
1980		1.6%	4.2%	67.5%	26.0%	0.7%	
1981				12.5%	18.6%	31.5%	37.4%
1982	1.0%	6.1%	17.8%	50.2%	16.3%	7.0%	1.7%
1983	4.5%	2.5%	10.7%	75.4%	6.6%	0.3%	
1984	1.3%	3.2%	15.1%	80.4%			
1985	1.1%	4.9%	9.4%	80.2%	3.2%	1.3%	

1986	7.9%	21.8%	16.0%	54.3%			
1987		0.0%	1.8%	75.0%	20.0%	3.2%	
1988				45.6%	33.0%	18.0%	3.4%
1989	4.8%	7.7%	13.2%	67.0%	7.4%		
1990			3.6%	88.1%	8.2%	0.1%	
1991		0.2%	0.5%	64.1%	19.6%	10.4%	5.2%
1992	2.3%	0.9%	1.6%	75.4%	16.6%	3.1%	0.1%
1993	2.8%	1.1%	1.3%	86.2%	8.1%	0.4%	
1994			5.8%	71.9%	7.3%	6.9%	8.0%
1995	4.6%	13.3%	22.3%	58.7%	1.0%		
1996	4.7%	11.7%	24.9%	58.6%			
1997	7.5%	4.9%	11.2%	70.2%	2.5%	1.2%	2.4%
1998	0.0%	1.2%	2.2%	47.9%	14.1%	24.3%	10.3%
1999	13.8%	19.8%	19.6%	46.9%			
2000	8.4%	17.2%	19.6%	54.8%			
2001	3.5%	21.0%	16.5%	58.8%	0.1%		
2002	0.0%	0.2%	0.4%	72.6%	12.6%	6.2%	7.9%
2003				22.9%	59.5%	16.8%	0.7%
2004			2.3%	83.7%	12.3%	1.6%	
2005			0.1%	83.2%	7.6%	4.3%	4.7%
2006	5.4%	9.8%	17.5%	67.1%	0.1%		
2007			2.9%	96.9%	0.1%		

Table 45. Distribution of the annual SPI in Uzbekistan

SPI Classes	Extreme-ly dry	Very dry	Modera-tely dry	Near normal	Modera-tely wet	Very Wet	Extreme-ly wet
1902		2.1%	7.4%	86.3%	1.2%	1.5%	1.4%
1903				62.5%	27.4%	10.1%	
1904		6.0%	12.0%	82.0%			
1905	0.6%	3.8%	4.9%	86.2%	3.7%	0.8%	
1906				50.5%	44.0%	5.5%	
1907				90.0%	10.0%		
1908		11.4%	20.5%	54.9%	10.7%	2.4%	
1909		1.6%	16.3%	81.3%	0.6%	0.2%	
1910	33.6%	13.0%	22.2%	31.1%			
1911	0.5%	3.3%	16.9%	56.5%	5.7%	4.8%	12.2%
1912	29.0%	12.5%	13.3%	42.7%	2.6%	0.0%	
1913	0.1%	1.1%	40.9%	50.7%	5.8%	1.5%	
1914	2.4%	5.1%	5.3%	69.5%	12.4%	3.6%	1.7%
1915			0.3%	61.7%	22.0%	16.0%	
1916	1.5%	2.8%	8.0%	86.3%	1.3%	0.2%	
1917	56.8%	30.7%	11.8%	0.7%			
1918	0.3%	11.4%	17.5%	70.5%	0.3%		
1919	0.7%	1.4%	5.5%	80.8%	5.8%	4.1%	1.7%
1920		0.1%	5.3%	93.7%	0.6%	0.2%	0.0%
1921			0.2%	89.9%	1.5%	3.5%	4.9%
1922				99.6%	0.4%		
1923				92.9%	6.9%	0.2%	
1924				93.3%	6.6%	0.0%	
1925		2.0%	6.2%	91.8%	0.0%		
1926		2.1%	3.1%	85.7%	8.3%	0.8%	
1927	6.9%	20.3%	25.1%	47.7%			
1928	0.2%	16.1%	14.0%	65.2%	2.1%	1.7%	0.7%
1929	0.0%	0.5%	5.9%	93.0%	0.6%		
1930	6.5%	27.1%	23.4%	43.0%			
1931				94.7%	5.2%	0.1%	
1932			0.0%	64.9%	13.2%	21.9%	
1933			0.4%	76.5%	10.5%	8.9%	3.7%
1934			0.1%	76.5%	13.2%	9.6%	0.7%
1935		0.2%	3.3%	96.6%			
1936	1.9%	3.0%	15.6%	78.4%	1.1%		
1937	0.4%	4.8%	29.0%	65.9%			
1938		0.2%	6.4%	93.3%	0.1%		
1939		0.5%	7.2%	88.7%	3.5%		
1940			5.0%	53.5%	20.1%	12.6%	8.8%
1941				87.8%	7.4%	3.8%	1.0%

1942		1.5%	9.7%	78.5%	8.8%	1.6%	
1943		1.0%	9.7%	80.9%	5.6%	2.8%	
1944	1.7%	8.3%	46.4%	43.5%			
1945			0.7%	86.7%	9.9%	2.7%	
1946		5.9%	12.7%	81.4%			
1947	0.0%	2.2%	19.2%	78.5%			
1948	0.0%	8.4%	21.7%	69.9%	0.0%		
1949				68.3%	29.8%	2.0%	
1950	7.3%	6.3%	36.3%	50.1%			
1951	13.1%	17.0%	35.1%	34.8%			
1952				24.3%	43.8%	31.3%	0.6%
1953	0.1%	0.7%	5.4%	92.3%	1.4%		
1954				33.8%	23.5%	30.8%	11.9%
1955	2.9%	15.6%	37.2%	44.3%			
1956			0.6%	87.9%	9.1%	2.4%	
1957		1.2%	15.3%	83.5%			
1958				51.2%	27.4%	20.8%	0.6%
1959				84.4%	15.0%	0.5%	
1960		0.6%	12.4%	78.2%	7.2%	1.5%	
1961	4.9%	8.8%	28.5%	57.8%			
1962	0.3%	2.5%	3.7%	66.9%	19.3%	7.4%	
1963			2.3%	75.2%	8.8%	6.7%	7.0%
1964				67.1%	26.1%	6.1%	0.6%
1965	2.5%	6.2%	19.3%	72.0%	0.0%		
1966		0.0%	6.1%	83.4%	10.2%	0.2%	
1967			3.5%	89.7%	6.8%		
1968			6.9%	92.3%	0.8%	0.0%	
1969				22.4%	18.8%	17.1%	41.7%
1970				89.0%	9.1%	1.9%	
1971	14.0%	13.0%	26.4%	46.7%			
1972			0.3%	87.1%	11.8%	0.8%	
1973				92.3%	6.8%	0.9%	
1974	0.6%	3.1%	6.5%	89.8%			
1975	21.3%	18.8%	41.1%	18.8%			
1976			0.1%	97.8%	1.9%	0.1%	
1977		1.0%	15.7%	83.2%			
1978				41.8%	25.8%	13.0%	19.4%
1979			1.5%	58.8%	32.8%	6.5%	0.4%
1980		0.3%	1.0%	91.9%	6.8%		
1981				30.7%	10.5%	9.7%	49.0%
1982	0.6%	3.6%	17.6%	74.4%	3.2%	0.5%	
1983			1.3%	88.6%	4.2%	3.7%	2.2%
1984	0.0%	6.5%	10.2%	77.2%	4.7%	1.3%	
1985		0.6%	1.3%	93.7%	4.3%	0.2%	

1986	12.6%	31.1%	24.3%	31.9%			
1987				48.1%	33.6%	16.7%	1.6%
1988				82.8%	11.1%	6.0%	0.0%
1989	0.4%	1.7%	15.3%	64.0%	18.6%		
1990			0.7%	97.1%	2.1%	0.1%	
1991			0.0%	46.7%	26.8%	21.6%	4.9%
1992				56.8%	27.9%	14.2%	1.0%
1993				58.4%	31.0%	10.5%	
1994				76.1%	16.3%	6.6%	1.0%
1995		0.1%	2.0%	97.9%			
1996	13.1%	20.9%	27.8%	38.3%			
1997		0.0%	2.5%	92.1%	5.4%		
1998			0.0%	31.3%	28.1%	28.5%	12.1%
1999	0.5%	3.5%	31.2%	64.6%	0.1%		
2000	3.1%	9.3%	27.0%	60.6%			
2001	6.9%	15.9%	29.6%	47.5%			
2002				22.2%	33.2%	27.9%	16.7%
2003				38.1%	32.9%	22.6%	6.5%
2004			1.0%	75.7%	11.8%	11.1%	0.4%
2005		0.2%	4.5%	59.1%	34.9%	1.2%	
2006	1.8%	3.9%	22.3%	70.5%	1.5%		
2007	0.1%	0.3%	3.0%	93.8%	2.8%		

Table 46. Distribution of the annual SPI in Xinjiang

SPI Classes	Extreme-ly dry	Very dry	Modera-tely dry	Near normal	Modera-tely wet	Very Wet	Extreme-ly wet
1902			0.0%	30.4%	20.2%	10.0%	39.3%
1903				14.8%	42.8%	29.1%	13.4%
1904		0.1%	0.3%	73.8%	10.2%	14.4%	1.2%
1905		0.3%	1.3%	78.9%	18.5%	0.9%	0.0%
1906			5.8%	77.1%	10.9%	2.6%	3.6%
1907	0.4%	1.4%	1.7%	70.3%	21.4%	4.3%	0.5%
1908	0.2%	0.3%	0.4%	47.6%	28.0%	14.1%	9.4%
1909			2.0%	67.7%	17.4%	11.5%	1.3%
1910	0.0%	5.9%	12.7%	58.0%	12.1%	7.2%	4.0%
1911	5.0%	3.7%	3.5%	54.1%	16.9%	16.0%	0.8%
1912	32.1%	8.6%	7.4%	37.8%	10.2%	3.8%	0.0%
1913		1.2%	1.9%	67.8%	16.6%	12.2%	0.2%
1914	0.3%	2.0%	3.8%	91.0%	1.3%	0.6%	1.0%
1915	2.8%	9.9%	7.2%	71.0%	7.7%	1.4%	0.0%
1916	2.5%	8.6%	9.9%	75.6%	3.1%	0.2%	
1917	11.0%	5.8%	6.4%	75.2%	0.9%	0.4%	0.2%
1918	24.3%	13.0%	29.2%	30.5%	0.6%	0.6%	1.8%
1919	1.9%	3.2%	10.6%	39.2%	3.4%	5.6%	36.0%
1920		0.5%	14.3%	58.5%	19.3%	3.5%	3.9%
1921				22.9%	19.7%	25.5%	31.9%
1922	21.0%	6.4%	7.6%	60.1%	4.3%	0.5%	0.1%
1923	30.0%	7.6%	9.2%	31.9%	16.3%	4.2%	0.8%
1924			7.4%	86.6%	4.5%	1.4%	0.0%
1925	0.0%	4.1%	8.8%	85.3%	0.5%	0.2%	1.0%
1926	2.6%	3.4%	1.4%	68.8%	15.4%	8.3%	0.0%
1927	0.3%	1.5%	2.3%	86.8%	8.4%	0.7%	
1928	1.5%	0.8%	0.9%	11.3%	6.7%	25.6%	53.1%
1929		0.1%	0.9%	76.2%	21.3%	0.7%	0.8%
1930			0.6%	37.9%	22.6%	18.6%	20.2%
1931			0.0%	72.3%	22.4%	4.2%	1.0%
1932		1.0%	9.8%	81.3%	6.3%	1.0%	0.8%
1933	2.7%	9.2%	27.2%	50.5%	1.0%	0.8%	8.6%
1934	0.1%	0.8%	2.3%	45.9%	39.8%	10.6%	0.4%
1935	0.1%	3.1%	5.5%	87.7%	3.0%	0.3%	0.3%
1936		0.1%	1.5%	96.6%	1.0%	0.5%	0.4%
1937			0.1%	94.7%	5.2%		
1938		0.3%	3.1%	93.3%	3.3%	0.0%	
1939	7.2%	9.2%	12.1%	71.4%			
1940	1.4%	0.5%	4.7%	78.9%	13.4%	1.1%	
1941		0.1%	0.3%	79.2%	19.2%	1.2%	

1942				48.0%	15.6%	16.3%	20.1%
1943	0.7%	3.1%	4.8%	57.8%	6.6%	8.6%	18.3%
1944	17.0%	16.1%	11.8%	54.8%	0.3%		
1945	4.8%	2.8%	4.3%	82.4%	4.9%	0.7%	
1946	0.0%	1.0%	1.8%	69.0%	20.7%	6.2%	1.2%
1947	2.7%	2.4%	5.3%	78.9%	4.8%	2.3%	3.6%
1948	0.5%	15.1%	14.9%	62.9%	6.0%	0.5%	0.0%
1949				95.0%	4.3%	0.6%	0.0%
1950	9.6%	12.8%	12.8%	59.6%	4.7%	0.4%	0.0%
1951		1.7%	6.1%	92.1%			
1952	0.0%	0.1%	0.2%	95.7%	3.0%	0.9%	0.1%
1953			3.2%	94.2%	1.3%	0.4%	0.8%
1954		0.8%	5.9%	86.5%	4.9%	1.7%	0.1%
1955			1.0%	97.7%	1.2%		
1956		8.0%	21.0%	69.6%	1.3%	0.1%	0.0%
1957	0.9%	14.3%	23.1%	60.5%	1.1%	0.0%	
1958		0.0%	2.9%	69.3%	19.1%	8.0%	0.7%
1959		1.3%	20.6%	71.6%	4.6%	1.8%	0.0%
1960	0.1%	5.7%	17.0%	70.9%	4.3%	1.9%	
1961	0.3%	14.3%	29.4%	54.8%	1.2%		
1962	5.8%	12.9%	26.4%	54.9%	0.0%		
1963		3.5%	14.8%	80.8%	0.9%	0.0%	
1964	0.4%	0.8%	3.9%	92.3%	2.5%	0.0%	
1965		6.8%	25.3%	67.8%	0.1%		
1966		1.6%	17.1%	77.5%	3.3%	0.5%	
1967			6.4%	92.2%	1.4%		
1968	1.4%	9.5%	21.6%	65.7%	0.8%	0.3%	0.6%
1969		0.8%	8.6%	78.8%	7.9%	1.7%	2.1%
1970	0.0%	1.6%	8.2%	88.0%	1.8%	0.3%	
1971	0.2%	2.7%	8.3%	86.4%	2.4%		
1972			2.7%	80.1%	6.4%	6.4%	4.4%
1973	0.9%	1.6%	9.9%	84.8%	2.2%	0.6%	
1974	3.2%	8.7%	12.8%	72.1%	2.6%	0.6%	0.1%
1975	1.0%	10.2%	29.9%	57.9%	0.3%	0.7%	0.1%
1976		1.1%	8.7%	89.5%	0.6%		
1977	0.9%	3.4%	8.9%	86.6%	0.1%		
1978			8.9%	91.1%			
1979		2.4%	13.7%	82.3%	1.5%		
1980	9.9%	9.7%	17.3%	62.1%	0.9%		
1981			0.4%	86.4%	11.3%	1.0%	0.9%
1982	0.7%	2.1%	5.5%	88.4%	3.2%	0.1%	
1983		1.1%	6.9%	90.4%	1.4%	0.1%	
1984	4.8%	1.9%	10.9%	73.4%	8.4%	0.6%	
1985	4.9%	6.7%	20.6%	65.8%	0.4%	0.6%	0.9%

1986	3.0%	8.0%	26.9%	60.5%	1.5%		
1987			0.2%	70.6%	17.3%	6.4%	5.4%
1988				68.1%	15.6%	14.7%	1.5%
1989		0.1%	5.8%	89.6%	3.2%	1.1%	0.2%
1990			0.1%	88.0%	7.5%	2.3%	2.2%
1991	0.0%	0.2%	3.3%	90.1%	5.9%	0.4%	
1992		0.0%	0.3%	89.5%	8.3%	1.8%	
1993	0.2%	1.1%	1.0%	69.5%	18.9%	7.9%	1.3%
1994	2.6%	3.6%	33.5%	55.4%	3.0%	1.6%	0.2%
1995	2.0%	1.3%	9.7%	86.7%	0.3%	0.0%	
1996	0.9%	0.5%	1.6%	63.3%	7.6%	11.5%	14.5%
1997	3.0%	2.2%	9.2%	85.5%	0.1%		
1998	0.0%	1.3%	4.7%	83.8%	8.0%	2.1%	
1999		0.3%	5.1%	87.6%	4.9%	2.0%	0.1%
2000		1.0%	3.9%	89.3%	2.2%	2.6%	0.9%
2001	0.8%	15.2%	16.1%	60.7%	3.3%	3.0%	0.9%
2002			0.0%	81.2%	12.2%	6.5%	0.1%
2003	0.1%	1.0%	1.0%	78.3%	10.9%	6.4%	2.3%
2004			3.4%	85.1%	10.0%	1.4%	0.0%
2005				66.8%	20.2%	10.1%	2.9%
2006			0.4%	98.2%	1.3%		
2007		0.2%	12.3%	74.9%	8.7%	3.8%	